PHOTOELECTRIC ACTION SPECTROSCOPY OF CHLOROPLAST BLACK LIPID MEMBRANE

Thesis for the Degree of M. S.

MICHIGAN STATE UNIVERSITY

SHILLING FENG

1971

ABSTRACT

PHOTOELECTRIC ACTION SPECTROSCOPY OF
CHLOROPLAST BLACK LIPID MEMBRANE

By

Shilling Feng

Bimolecular lipid membranes containing chloroplast pigments (chl-BLM) in aqueous solutions are currently considered to be the most realistic approach to the thylakoid membrane of chloroplasts both from morphological and functional points of view.

The present work can be summarized by the following three points:

(1) Physical and chemical properties of chl-BLM both in dark and in light: It was found that chl-BLM has a high dark resistance (10^6 ohm-cm^2) and capacitance (1 $\mu F/cm^2$). Ohm's law holds within certain transmembrane voltages (e.g., ± 32 mv, at KCl bulk phase, pH 5). Electrical voltage was generated across the membrane upon illumination. This photoinduced voltage was greatly modified either by introducing photomodifiers (for example, $FeCl_3$, DCMU, or DNP) or changing the pH of the bulk phase. A non-linear dependence of photovoltage on the intensity of incident light was observed.

(2) Mechanism of photovoltage generation in chl-BLM: The polarity of photovoltage is closely related to the dark transmembrane voltage. At high dark transmembrane voltage a biphasic waveform photoresponse was observed which can be analyzed into four components.

The proposed mechanism of photovoltage generation involved the generation and trapping of excitons, hole migration, oxidation of water, and proton migration.

(3) Photoredox action spectrum of chl-BLM: The term photoredox action spectrum is defined as open circuit light-generated voltage across chl-BLM versus wavelength of incident light. Three types of action spectrum of chl-BLM formed with fresh lipid solution were found at different times after the membrane formation. Among them only the one appearing latest followed the absorption spectrum of the same chl-BLM forming solution. The red band in the action spectrum showed a time dependent blue shift from 670 nm to 660 nm and then 655 nm. It is suspected that there exists a form of a pigment (probably chl a 670) which undergoes transformation both in dark and in light. One or more extra peaks were observed beyond 700 nm which may indicate the existence of pigment(s) absorbing far-red light.

PHOTOELECTRIC ACTION SPECTROSCOPY OF CHLOROPLAST BLACK LIPID MEMBRANE

by

Shilling Feng

A THESIS

Submitted to
Michigan State University
in partial fulfillment of the requirements
for the degree of

MASTER OF SCIENCE

Department of Biophysics

1971

To My Mother

ACKNOWLEDGMENTS

I acknowledge the help and encouragement of Professor H. T. Tien whose ideas and insight helped me throughout this course. I also thank him for his extreme patience during the course of my study.

Thanks are also due to Dr. S. Izawa and Dr. J. Huebnor for many precious suggestions and discussions. Thanks are extended to Dr. S. Sahu and Dr. B. Karvaly for the invaluable discussions. And I thank Dr. A. El-Bayoumi for suggesting to me that I take the advanced course in photosynthesis; it was really helpful and interesting.

Special thanks are given to the Department for providing such a friendly and stimulating environment in which this work was carried out.

I am deeply grateful to my eldest brother Mr. Feng Chinn for his constant inspiration to me.

Appreciation is extended to the National Institutes of Health for supporting this work with Grant GM-14971.

TABLE OF CONTENTS

LIST OF TABLES

LIST OF FIGURES

GLOSSARY

BLM	bimolecular (or bilayer or black) lipid membrane
BLM-I	photovoltaic action spectra taken from chl-BLM (less than one hour old) formed with fresh MFM
BLM-II	photoelectric action spectra taken from middle-aged chl-BLM formed with fresh MFM or young chl-BLM formed with aged MFM
BLM-III	photoelectric action spectra taken from aged chl-BLM formed with fresh or aged MFM
chl	chlorophyll or chloroplast
chl-BLM	bimolecular lipid membrane containing chloroplast pigments
C_m	dark membrane (chl-BLM) capacitance
CMU	3-(p-chlorophenyl)-1,1-dimethylurea
DCMU	3-(3,4-dichlorophenyl)-1,1-dimethylurea
DNP	2,4-dinitrophenol
E	peak ratio of red maximum peak height/blue maximum peak height (Data were taken from those action spectra which had been calibrated for constant incident energy.)
E_t	dark transmembrane voltage
MFM	membrane-forming material
PS-I and PS-II	photosystem I and photosystem II
photovoltage	voltage generated by light
Q	peak ratio of red maximum peak height/blue maximum peak height (Data were taken from those action spectra which had been calibrated for constant incident energy.)
R_m	dark chl-BLM resistance
Y	peak ratio of red maximum peak height/blue maximum peak height (Data were taken from those action spectra which had not been calibrated for constant incident energy.)

CHAPTER I

INTRODUCTION

Artificial bimolecular lipid membranes (BLM) were prepared for the first time by Mueller, Rudin, Tien, and Wescott (1962a). The physical, chemical, and biochemical investigations of these model membranes have opened new possibilities in membranology. Some of the basic features of the BLM are the following:

(1) These ultra-thin membranes have been proved both theoretically and experimentally to be of bimolecular structure (Goldup, Ohki and Danielli, 1970; Tien, 1971). The polar head of the lipid is oriented towards the aqueous phase and the long apolar hydrocarbon chains are randomly inserted inside the membrane. That is why they are usually termed bimolecular or bilayer lipid membranes (abbreviated as BLM),

(2) Because of the hydrophobic interior of the BLM, the resistance and capacitance are relatively high (10^6 - 10^8 ohm-cm^2; 0.5 - 1.0 μF/cm^2),

(3) The BLM is permeable to water and neutral lipophyllic molecules under certain circumstances. However, it is generally impermeable to ions such as Na^+, K^+ (Mueller and Rudin, 1969),

(4) They have relatively long stability in aqueous solutions,

(5) The BLM separating two aqueous phases shows a very close similarity to the bimolecular leaflet concept of natural membranes introduced by Gorter and Grendel (1925) and later modified by Davson and Danielli (1935),

(6) The properties of BLM are, in several respects, similar to those of biological membranes thus making them useful for the study of membrane-associated phenomena at the molecular level.

Owing to these and the advantage of simple and neat techniques, BLMs have been extensively investigated by many scientists. Within the past decade (1962-1971), much information has been accumulated including different chemical and physical properties and basic structure of BLM as well as technical improvement of membrane formation. A detailed review of the basic physiochemical properties of BLM and the techniques of membrane formation have been published by Tien and Diana (1968). A comparison of the different membrane models and the biological membranes has been made by Bangham (1968) and Castleden (1969). The biological aspects of the BLM have been generally reviewed by Thompson and Henn (1969) and the two most recent reviews have been published by Goldup et al (1970) and by Tien (1971).

Recently, intensive experimental investigations have begun in order to study such biological phenomena in which membrane structure is thought to be of fundamental importance. First of all, three outstanding examples should be mentioned: the problems of visual process using a modified BLM as noted by Kobamoto and Tien (1969, 1971); nerve excitation as noted by Mueller et al (1962b) and Mueller and Rudin (1968); and photosynthesis and related phenomena.

The aim of the present work is both experimental and theoretical investigations about the possible role of the membrane in the primary processes of photosynthesis. The importance of such studies lies (among

others) in the proof of the following hypothesis: Bassham and Calvin (1957) and Katz (1949) have suggested that a crystal-lattice (-like configuration) containing chlorophyll molecules and other compounds might be involved in the photosynthetic apparatus, and such an organized structure of light sensitive pigments might possess photoconductivity. By recognizing the similarity between BLM structure and the high degree of orderliness and lamellar organization of chloroplast pigments in nature, Tien (1968a) began to elaborate a method for forming BLM containing photosynthetic pigments and lipids. This lipid membrane constituted from chloroplast pigments in aqueous solution exhibits the photoelectric effect. On the basis of various available information the current picture of BLM containing chloroplast pigments can be considered as a structure having liquid crystalline-like and lamellar organization, i.e., as a model system for the photosynthetic thylakoid membrane of the chloroplast.

Therefore it is quite clear that studies on the mechanism of the conductivity and photoelectric processes of a chloroplast BLM (chl-BLM) can make some contribution to a better understanding of the primary processes of photosynthesis. Therefore, the photoelectric properties of chl-BLM were studied under various conditions.

CHAPTER II

LITERATURE REVIEW

General Concepts of Photosynthesis

Solar energy is the primary energy source of the world. Photosynthesis is the unique way to convert solar energy into useful form (i.e., chemical energy) in living systems. The process of photosynthesis is carried out in green oxygen-evolving plants and photosynthetic bacteria containing chloroplasts and chromatophores, respectively. Compositions of these photosynthetic organisms are pigments, lipids, and protein which are arranged in an orderly lamellar structure. The major functional component is chlorophyll a, which absorbs about 50% of the solar spectrum (wavelengths shorter than 700 nm). Actually, 60% of the absorbed solar energy is probably absorbed by the pigments, rather than wasted by various processes (e.g., reflection, inactive absorption, etc.). Throughout the process of photosynthesis more than half of the absorbed energy is wasted. Even under optimal conditions only 34% of absorbed solar energy can be transferred into effective chemical energy (Rabinowitch and Govindjee, 1969). Substantially, photosynthesis can be discussed on the basis of two chain processes: energy conversion and CO_2 fixation.

Energy conversion is that chain of processes in which solar energy is converted into the chemical energy of metastable high energy compounds (e.g., reduced pyridine nucleotides and adenosine triphosphate) through a series of electron transfer reactions and the so-called

non-cyclic coupled phosphorylation. This series of processes is usually called the primary processes of photosynthesis or photosynthetic apparatus.

In the second process of carbon dioxide fixation, atmospheric CO_2 incorporated by the plants is reduced and carbohydrates are formed through the Calvin cycle and related processes. These processes are supplied by the energy stored in the primary processes (ATP, NADPH).

Combining the above processes allows the overall reaction to be summarized in the following equation:

$$CO_2 + H_2O \xrightarrow[\text{green plant}]{\text{light}} O_2 + (CH_2O) \qquad (1)$$

The processes in CO_2 reduction have almost been worked out in sufficient detail. Rabinowitch and Govindjee (1969) and Kok (1965) treat the different aspects of these problems in detail. As far as the primary process is concerned, it has been extensively investigated for many years in various laboratories. However, very little information is available. This is probably due to the following reasons: the reaction rates of these processes are too fast (10^{-15} to 10^{-4} seconds); the intermediates are unstable (photosensitive); and they are very structure dependent. Therefore their direct (in vivo and in vitro) investigation is extremely difficult from a technical and experimental point of view.

Since it is such a complicated process and its ramifications cover so many areas, a complete review in a few pages is practically impossible. Here, attention is focused mainly on two topics: primary processes in photosynthesis and action spectra.

Introduction of Primary Processes in Photosynthesis

There are working hypotheses about the mechanism of primary processes in photosynthesis. Among these the most promising one is the existence of two photoacts, namely PS-I and PS-II, taking place in photosynthesis. Each photosynthesis unit (PSU) contains about 250 chlorophyll molecules, but only one of the chlorophyll a molecules (per photoact)--the so-called trapping center--is capable of converting the energy of its excited state into chemical energy. The remaining chlorophylls and all the accessory pigments transfer their energy to this particular trapping center. The trapping center in PS-I is known to be P_{700} (Kok, 1956). In PS-II, there is much evidence which indicates the existence of a trapping center different from P_{700}. However, there is at this time no way to identify it. It should be noted that Doring, Stiehl, and Witt (1967), and Doring, Bailey, Krentz, and Witt (1968) have suggested that the trapping center of PS-II might be P_{696}. The composition of these two photoacts is not the same at all in spite of their structural similarities. PS-I contains mainly accessory pigments and few chlorophyll a, whereas PS-II contains mainly chlorophyll a and few accessory pigments. Therefore, the maximum functional wavelength for PS-II is shorter than PS-I (below 680 nm). For a number of years much evidence has been found supporting the existence of a coupled function of two light reactions. It is believed that the metabolic energy transfer chain consists of coupled oxidation and reduction reactions. The most likely mechanisms by which the energy of an excited chl a molecule may be converted to chemical free energy is that the

excited chl a molecule donates an electron in the excited state to a neighboring molecule and then this electron-deficient chl a molecule accepts an electron from an adjacent donor molecule. It is believed that PS-I and PS-II are coupled in functioning. Excitation of PS-II results in transfer of an electron from +1 V to 0 V, thus creating a primary oxidant, namely X, and a primary reductant, namely Q^-. This strong primary oxidant, X, is capable of oxidizing water which leads to H^+ generation and O_2 evolution. The electron from the primary reductant, Q^-, is then tumbling down through the so-called electron-transfer chain effecting non-cyclic phosphorylation which is located between the two pigments assemblies. The terminal electron carrier cytochrom f or plastocyanin is thus reduced. The energy generated via this process is about 4 eVs, which is thought to be used in ATP formation. Photons absorbed by PS-I are transferred to P_{700}. This excited P_{700} donates an electron from a redox potential of 0.4 mv to -0.6 mv to an unidentified acceptor, namely Z. The reduced cyt-f or plastiquinone from PS-II will then be able to give up an electron to the oxidized P_{700}.

The primary reductant, Z, is assumed capable of reducing $NADP^+$ with the presence of H^+ and mediated by some enzyme and electron carriers. The over-all electron pathway and its intermediates can be easily visualized in the Z scheme (Boardman, 1968).

In case the absorbed quanta were not used by transfer to neighboring pigment molecules, two possible routes of deactivation of energy are possible: (i) dissipation as heat, and (ii) emission of light

(fluorescence). For an efficient photosynthesis, energy must be transferred to the trapping center in the order of 10^{-11} to 10^{-10} second (Boardman, 1968).

Investigations on the Action Spectra of Photosynthetic Organisms

Action spectra of the photosynthetic organism (e.g., intact leaf, chloroplast extraction, etc.) have been widely investigated by various means. Some important findings will be reviewed here. Action spectrum in photosynthesis is defined as a plot of the intensity of certain measurable quantities (e.g., CO_2 fixation, O_2 evolution, $NADP^+$ reduction, cytochrom-f reduction, photoelectricity, and luminescence, etc.) versus the wavelength of the incident or absorbed light, which produced this quantity.

Quantum Efficiency of the O_2 Evolution and CO_2 Fixation

Action spectra for the photosynthesis obtained by Emerson et al (1943, 1959) and by Tanada (1951) with green algae, red algae, and diatom, respectively, led to the conclusion that quanta absorbed by carotenoids are relatively more ineffective in bringing about photosynthesis than other pigments (chlorophyll a and b, phycobilins, etc.). The same conclusion was drawn by Englemann (1883-85) and Dutton et al (1940) (cited by Rabinowitch and Govindjee, 1969) on the basis of O_2 evolution. This hypothesis is proved to be true in most of the cases except in the red algae. Haxo and Blinks (1950) and Halldal (1969) found that the photosynthetic action spectra of green brown algae agree

with the absorption spectra for these algae. However, in the case of red algae, the action spectra for photosynthesis followed the absorption of light by the accessory pigment phycoerythrin, primarily, while chlorophyll a appeared practically inactive. In the higher plants, Emerson's hypothesis seems to be valid. By measuring the action spectra for CO_2 fixation of radish and corn leaves, Bulley, Nelson and Tregunna (1969) postulated that if the action spectrum is based on constant incident energy, the red region of the spectrum is more effective in the photosynthesis than either the green or blue one. On the other hand, if the comparison is made on the basis of a constant number of quanta absorbed in each region of the spectrum, the blue region becomes as effective or even slightly more effective than the red region.

Recent Investigations

The above hypothesis was deduced primarily from the similarity between the action spectrum and absorption spectrum. This similarity has been observed under various conditions with different techniques. Izawa, Itoh and Shibata (1963) studied the effect of monochromatic light on the rate of photoinduced shrinkage of intact chloroplasts extracted from fresh spinach leaves. Action spectra obtained in this way showed two major peaks, a minor peak, and a shoulder. In spite of the small peak around 720-740 nm, the action spectrum resembles the absorption spectrum of the same sample, whereas the action spectrum for corn leaf by Balegh and Biddulph (1970) has a higher red band (see Figure 1 and Table 1). Balegh and Biddulph thought this was due to the layer scattering at short wavelength rather than at the longer wavelength.

Figure 1--The photosynthetic action spectrum and absorption spectrum of bean leaf (after Balegh and Biddulph, 1970).

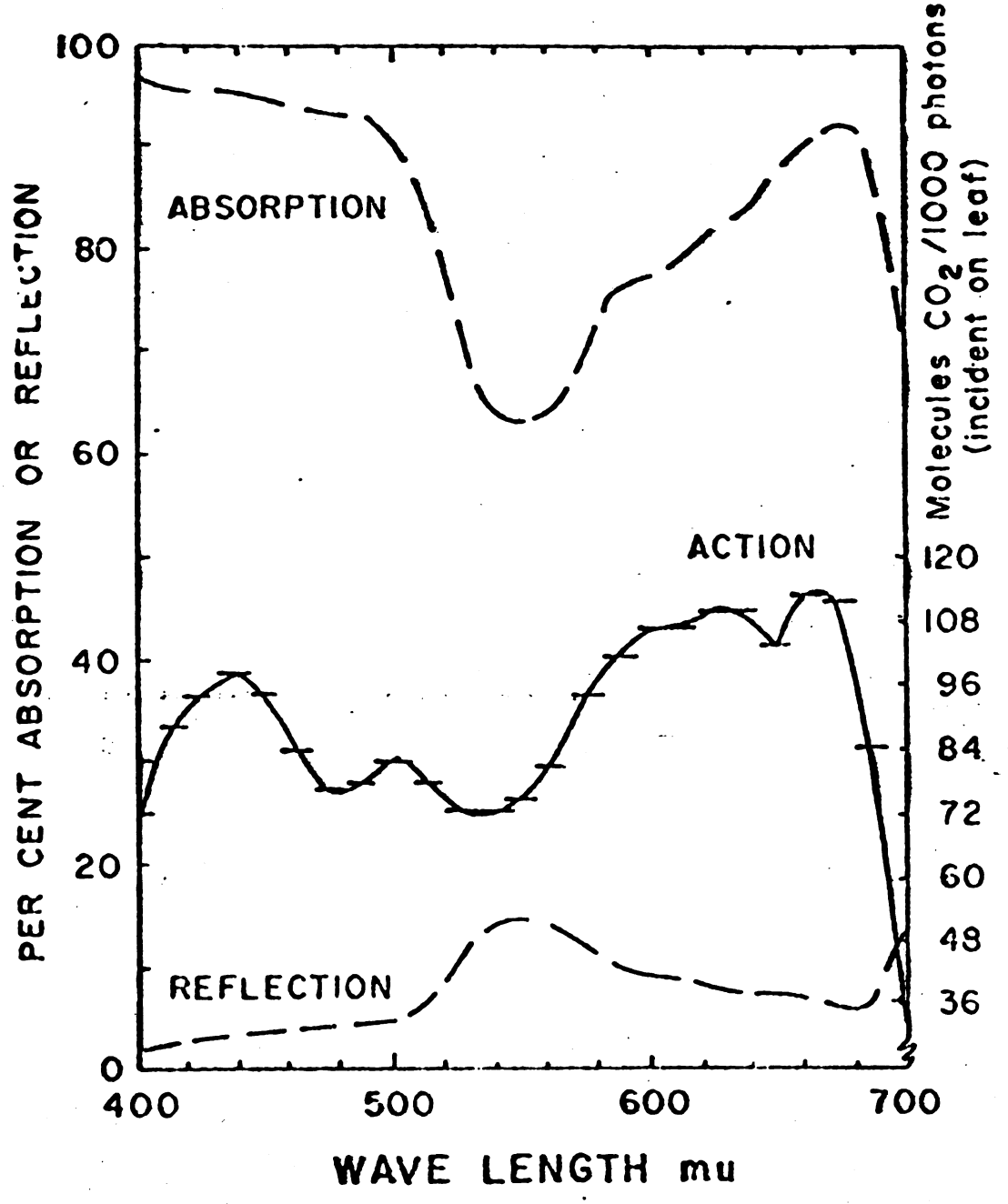
100
80
60
40
20
0
PER CENT ABSORPTION OR REFLECTION
ABSORPTION
ACTION
REFLECTION
120
108
96
84
72
60
48
36
Molecules CO_2/1000 photons (incident on leaf)
400
500
600
700
WAVE LENGTH mu

Table 1--Spectral characteristics of action and absorption spectra reported by various investigators.

Spectrum Types	Blue peak region (nm)			Red peak region (nm)			Peak beyond 700 nm	γ	System	Reference
	shoulder	minor peak	major peak	shoulder	minor peak	major peak				
Action Spectrum	490	no	435	no	no	680	720 ∿ 740	0.65	shrinkage of spinach chloroplast suspension	Izawa, Itoh, and Shibata (1963)
Absorption Spectrum	480	no	435	no	no	678	no	0.60	shrinkage of spinach chloroplast suspension	Izawa, Itoh, and Shibata (1963)
Action Spectrum	--	--	--	--	620	675, 650	--	--	photosynthetic O_2 evolution of wheat leaf	Egneus (1968)
Action Spectrum	400-500	no	no	no	no	670	--	1.5	photosynthetic CO_2 fixation of radish leaves	Bulley, Nelson, and Tregunna (1969)
Action Spectrum	no	500	437	600-612	620	670	--	1.2	CO_2 fixation of bean plant	Balegh and Biddulph (1970)

From many extensive investigations (summarized in Table 1) the following conclusions have generally been made:

(1) The two major bands around 675-680 nm might be attributed to the absorption of chlorophyll a.

(2) The minor peaks around 650 nm and 490 nm might be due to the absorption of chlorophyll b.

(3) The dip around 600 nm observed by Govindjee and Bazzaz (1967) and Rabinowitch and Govindjee (1969) is probably caused by a short wavelength component of a double absorption band belonging to an aggregated form of chlorophyll a (e.g., a dimer). The long wave component of this doublet may be responsible for the red drop above 680 nm (Rabinowitch, 1968). The other kind of interpretation offered by Lewis (1943) and Myers (1963) was that this dip might be due to absorption of chlorophyll b which is inactive in photosynthesis.

(4) As far as the dip in the blue region is concerned, both chlorophyll b and carotenoids are possibly responsible for it.

(5) The regular red drop in action spectra is related to the well-known Emerson effect (drop of photosynthesis quantum yield in red region and increase of photosynthesis effectiveness after illumination by short wavelength.

The position of the red peak in action spectra was found to have a relatively large deviation between different systems. For example, the red peak has been observed by Black et al (1962) and Izawa et al (1963) at 680 nm; by Jagendorf et al (1958) at 675 nm; by Rabinowitch et al

(1968) at 678 nm; by Kok and Hoch (1961) at 710 nm. The most interesting observation was the one demonstrated by Litvin and Ho (1967). From their research for action spectrum on Elodea leaf they found the following things: (i) An increase of light intensity resulted in a shift of maximum in action spectrum from 680 nm to 670 nm and 650 nm. (ii) Maximum of action spectrum for oxygen evolution also shifted from 700 mm to 680 mm and 670 mm with time. This changeable characteristic of the red peak position reminds us of the multiple forms of chlorophyll a (e.g., chl a 673 and chl a 683) in vivo (Govindjee and Rabinowitch, 1968). With this concept in mind, the discrepancy between the red peak position determined by different investigations seems not unexpectable.

Investigations on the Action Spectrum of PS-I or PS-II and the Demonstration of the Emerson Effect

From action spectra the individual or coupled functions of PS-I and PS-II are observable. Duysens, Amesz and Kamp (1961) obtained an action spectrum for cytochrome oxidations in DCMU-poisoned algae. This action spectrum showed peaks at 680 nm due to chlorophyll a, and at 560 nm due to phycoerthyrin. This is the first report of an action spectrum for PS-I alone. Horio and San Pietro (1964), by measuring the ferricyanide reduction in a normal Hill reaction, recorded the action spectrum with a peak at 660 nm for which the PS-II is supposedly responsible.

Similar investigations have also been carried out on the model system. Ludlow and Park (1969) using formaldehyde-fixed algae, measured

the activity of PS-I and PS-II individually. The algebraic sum of these two action spectra is generally in agreement with the absorption spectrum. The action spectrum determined by Mueller et al for the production of the fast absorption changes at 515 nm (PS-II) and 433 nm (PS-I) in chloroplast fragments, indicates that PS-II is activated by the light absorbed by chl b and chl a 670 nm, and that PS-I is activated by the light absorbed by chl a 683 and chl a 695 nm. From these investigations, pigments involved in each system are now identifiable. Currently it is believed that PS-I is enriched with chl a 685-690 nm, chl a 700-705 nm, and chl a 720 nm; while PS-II contains chl a 670 nm and chl b.

The Emerson enhancement may also be demonstrated from the investigation of action spectra. Kok and Hoch (1961) reported that photosynthetic action spectra of blue-green algae showed that quanta absorbed by chl a alone were much less effectively used than those absorbed by both chl a and phycocyanin. Litvin and Ho (1967), by measuring the action spectra of photosynthesis of higher plants, announced that they were able to demonstrate the Emerson enhancement. Later, Govindjee, Rabinowitch and Govindjee (1968) observed an enhancement only when a strong blue light, 480 nm, was added to far-red light. However, this is different from the work of Warburg, Krippahl and Schroeder reported in 1955, in which they demonstrated (by addition of a catalytic amount of blue light) the Emerson enhancement.

Model System Investigations

Two new working hypotheses, the possible crystalline structure of the lamellarly ordered chlorophyll and the probable nonenzymatic process

(non-specificity for different electron acceptors) in the primary mechanism of energy conversion and electron transfer, offer a great possibility for in vitro studies in the primary processes in photosynthesis. A few characteristics of these new concepts and some of the representative model systems are summarized below.

A monomolecular chlorophyll a layer on a cadmium sulfide film was investigated by Nelson (1957) as a model system for studying the primary processes of photosynthesis. Photoconductivity of two components was observed in which a fast rise was followed by a slow one. Both the absorption spectrum and the action spectrum of this chlorophyll monolayer were taken between 600 nm and 740 nm. The red band in both measurements fell at the same wavelength, 675 nm. In contrast, the position of the red absorption peak of the chlorophyll a component in solution is around 660 nm and that related to photosynthesis is around 680 nm. This substantial agreement of the peak of photosynthetic action spectra with the peak positions in the absorption and the photoelectric properties strongly support Katz's (1949) as well as Bassham's and Calvin's (1957) hypothesis, i.e., the photoexcitation of chlorophyll molecules followed by the generation of electrons and holes in the membrane (or lamellar). Similar photoconductivity was observed earlier on a chlorophyll sample compressed in the form of a disk by Eley (1948). Furthermore, Tweet, Gaines and Bellamy (1964) were able to observe fluorescence from chlorophyll molecules spread in monomolecular films on aqueous surfaces. The fluorescence emission of the chlorophyll a films was dependent on the concentration of chlorophyll a; an enhanced concentration quenching was pointed out. Although there

are several possibilities for the interpretation of the concentration quenching it seems very likely that the intermolecular energy migration due to the inductive resonance transfer mechanism might be responsible for it in the first place, which was suggested and experimentally investigated by Rabinowitch (1956) and Forster (1959). This migration will lead to fluorescence quenching if the excitation energy is trapped by a center which has a high probability for nonradiative transition to the ground state (e.g., a non-fluorescent dimer).

However, it should be noted that this interpretation based on such an energy transfer mechanism differs from that proposed by Katz as well as Bassham and Calvin. The mutual points between these proposals are the following:

(1) the photoexcitability of chlorophyll molecules, and

(2) the highly organized structure of chlorophyll molecules, providing a possibility of intermolecular transfer.

The other distinctive model system in the research of primary processes in photosynthesis which should be mentioned here is chloroplast pigments containing bimolecular lipid membrane (chl-BLM) in aqueous phase (Tien, 1968a and b). In membrane research, chl-BLMs are currently considered to be the most realistic model system from both morphological and functional points of view. The important similarities now being discovered between the chl-BLM synthesized membrane, and in vivo thylakoid membrane structures are the following:

(1) The thickness in both cases is around 60-90 Å.

(2) Unit membrane theory is proved to be true in BLM. In the thylakoid membrane there is a great possibility that this theory might hold also.

(3) The resistances of both membrane structures are quite high (10^6 ohms).

(4) Chlorophyll molecules are supposedly arranged in these membranes.

(5) Energy conversion is proposed to occur in these membranes.

(6) The environment of chl-BLM, aqueous phase, is closer to the physiological environment of the thylakoid membrane than the other model systems.

The early studies on this model system carried out by Tien (1968a and b) indicate that both photoconductivity and photovoltaic effects are possible in the chl-BLM. Tien (1968a and b) has concluded that the observed photoelectric phenomena are due to the charge separation. This hypothesis is based on the highly insulating character of the liquid hydrocarbon layer in the interior of the chl-BLM and on the high field strength due to the transmembrane potential (asymmetry, applied potential). In considering the fate of the separated electrons and holes, redox reactions at opposite sides of the chl-BLM should be the most likely processes. According to Tien's picture, the most probable reaction which can take place at the interfaces or biface in which the holes accumulate is the photolysis of water. The results in photocurrent studies indicate the appearance of a proton, which is one of the hypothetical products of the photolysis of water. Whether the water oxidation does indeed happen under the illumination of chl-BLM is not certain at the present time, because the data from experimental measurements indicate that both electronic and ionic charge carriers might contribute to the observed photoelectric phenomena.

Hesketh (1969) confirmed Tien's observations from the negative correlation between observed photoemf and temperature. In the following year, Van and Tien (1970) measured the temperature effect to the photoemf on chl-BLM. It has been reported that the thermoelectric behavior of chl-BLM has a temperature coefficient of about 6×10^{-2} mV per degree over the range of 15-40 °C. Therefore, it is certain that temperature effect in this kind of observation is negligible if the temperature condition is within the range of 15-40 °C. The charge generation and separation processes followed by redox reactions were once more confirmed by Tien and Verma (1970). By introducing modifiers such as Fe^{+3} into the aqueous solution, the photoresponse was dramatically enhanced. Similar results have also been reported by Trissl and Lauger (1970). In their case, membranes are formed from a mixture of lecithin and chlorophyll a.

The distance between porphyrin rings in BLM was calculated from the fluorescence measurement observed by Alamuti and Lauger (1970). Concerning the arrangement of chlorophyll molecules in BLM, it was tentatively proposed that the hydrophobic phytol chains were inserted between the hydrocarbon chain of the lipid solution and the plane of the porphyrin ring lying in the polar surface of the BLM (Ting, et al, 1968). This description is generally in agreement with the results of Tien and Diana (1967) deduced from surface tension measurement. The only exception is that the latter workers believed that the plane of the porphyrin ring is perpendicularly inserted between the polar groups of the lipid molecules of chl-BLM. Additional suggestions were made by

Cherry, Hsu and Chapmann (1971). By comparing the polarized and unpolarized absorption spectra of chl-BLM, it is inferred that there is some degree of orientation of porphyrin rings of chlorophyll molecules in the bilayer and at transition moments the red and blue bands must lie in different directions. To point out what actually occurs, further investigation is necessary.

CHAPTER III

EXPERIMENTAL

Experimental Detail and Materials and their Preparation

Extraction of Pigments

Chloroplast pigments used in the present investigations were prepared from fresh spinach leaves obtained from the local food market. The following procedure described by Tien et al (1968) was modified in order to obtain a suitable extract for BLM formation:

1. The spinach leaves were washed, the ribs and stalks removed, and then the leaves, free from ribs and stalks, were dried.
2. The dried leaves were chopped in a buffer solution (pH 7.5) consisting of 0.5 M/1 sucrose and 1 M/1 $KHCO_3$ in an electrical blender at relatively low speed for five minutes and high speed for three minutes.
3. The above products were filtered and the dark green filtrate was twice centrifuged (the condensates were discarded).
4. The residue was treated by petroleum ether-methanol (2:1 V/V) solution and after separating the aqueous and petroleum phases the petroleum ether was evaporated in an evaporator at 40 °C.
5. The dried residue (petroleum ether-soluble pigments and lipids fraction) was used for BLM-forming solution and dissolved in suitable BLM material (e.g., n-dodecane and n-butanol solvent 2:1 or 1:1, V/V).

The dry product obtained in the above procedure consists of pigments (chlorophyll a and b as well as a small amount of carotenoids), lipids (glycolipids, including mono- and di-galactosyl dilinolenins), and fatty acids (probably mainly phosphatidylglycerol, etc.) (Goodwin, 1965).

This pigment did not show any physical or chemical change after a storage of several weeks in the refrigerator. Since the extract contained light-sensitive pigments, it was stored in the dark to protect it from deterioration.

Other Chemicals

All compounds used for bathing solutions and photomodifiers were purchased from various chemical companies and were used without further purification in the form of aqueous solutions.

As buffers, acetate solutions were used, and pH was adjusted to the suitable value by adding appropropriate quantities of either HCl or KOH. The pH values of the solutions were measured with a Beckman pH meter against Beckman standard pH buffers at room temperature.

Formation of BLM

The dried pigment-lipid extract was dissolved (as a membrane-forming material) in a mixture of n-dodecane and n-butanol. The membranes were formed on the orifice of a 10 ml Teflon chamber introduced by Tien et al (1967). The whole cell assembly consisted of an outer glass cup of 20 ml and an inner teflon cup of 10 ml. The teflon chamber had a 1.13 mm diameter opening upon which the BLM formed. To eliminate the reflected and scattered light, the inside wall of the white teflon cup behind the orifice was covered with a piece of black plastic film.

To form the BLM, 0.002 ml of membrane-forming solution was injected into the hole with the aid of a Hamilton microsyringe (Model no. PB-600-1, 100 µl). This process was carried out in green light of low intensity and membrane formation was observed visually through a low-powered microscope.

The actual diameter of the bilayer structure was approximately 1.0 mm and its thickness 60-90 Å. The lifetime of the investigated BLM was relatively long (one to two days). However, it should be noted that the physical behavior of BLM containing pigments shows a definite change with time. These problems will be discussed later.

Instrumentation and Principles of the Measurements

Measurement of Membrane Resistance

The D. C. resistance measurements were carried out on the basis of a method given by Tien et al (1967). The circuit diagram for these measurements is shown in Figure 2. It is easy to see that if $R^* >> R_m$ and $R_m \sim R_i$ then the following relation holds:

$$R_m = \frac{E_i}{E^* - E_i} \cdot R_i \qquad (2)$$

where E^* and E_i are the measured potentials without and with external resistance, respectively. (E^* is a function both of E_o and of E_a.) In the case of the present measurements, R^* had a value of 10^{15} ohms, R_i was of the order of 10^8 ohms, and E^* ran about 30-40 mVs. A switch was used to connect the external resistance R_i. Throughout this work the outer solution was grounded, i.e., the active electrode was in the inner cup.

Measurement of Membrane Potential

For measuring the dark membrane potential and the photoelectromotive force, the arrangement shown in Figure 2 was used. The external resistance R_i during these measurements was connected (switch position #3) or disconnected (switch position #2) depending upon whether an external voltage source was employed. In general, the external resistance R_i was always higher by some order of magnitude than that of the membrane. The effective transmembrane potential was measured by the electrometer (Elm Type Cary 31) which had a preamplifier.

Measurement of the Redox Action Spectrum

For measuring the photoelectronic (or redox) action spectrum, the arrangement given in Figure 3 was used. A D.C. Xenon arc lamp (Hanovia, Type 976C, 1000 W) served as the light source. This light first passed through a heat filter and later through a visible grating monochrometer (Bausch and Lomb, Model 5). It was possible to change the wavelength of the exciting light automatically, continuously, and linearly, with time between 350 nm and 800 nm. (The duration time for a complete scanning was three minutes.) The membrane was placed in the path of the monochromatic light beam emitted from the monochromators. Before each scanning the dark baseline was recorded and served as a reference for the photoresponse. For wavelength identification and for evidence that the monochromator motor was running constantly and uniformly, marks were placed on the chart paper at different wavelengths.

To study the influence of electrical field on the spectral photoresponse, the circuit described in paragraph 1 was used under the circumstances given in paragraph 2.

Figure 2--Circuit diagram for the measurements of membrane resistance where:

E_a = external battery

R^* = resistance of the electrometer (Elm)

R_m = the membrane resistance to be measured

C_m = membrane capacitance

E_o = membrane self-electromotive force

R_i = external resistance

R_o = resistance of the external potential source (E)

S_t = switch

Figure 3--the apparatus for BLM formation and measurement of photoelectric action spectrum where:

Xe = Xenon lamp

Mo = monochromator

L_1, L_2 = lenses

GF = grey filter

I = illuminator

GC = glass cup

TC = teflon cup

O = opening

E_1, E_2 = electrodes

Elm = elecrodemeter

R_1, R_2 = recorders

P = power supply box

Sh = shielding

MPh = microphotometer

Ph = phototube

M = microscope

H = heat filter

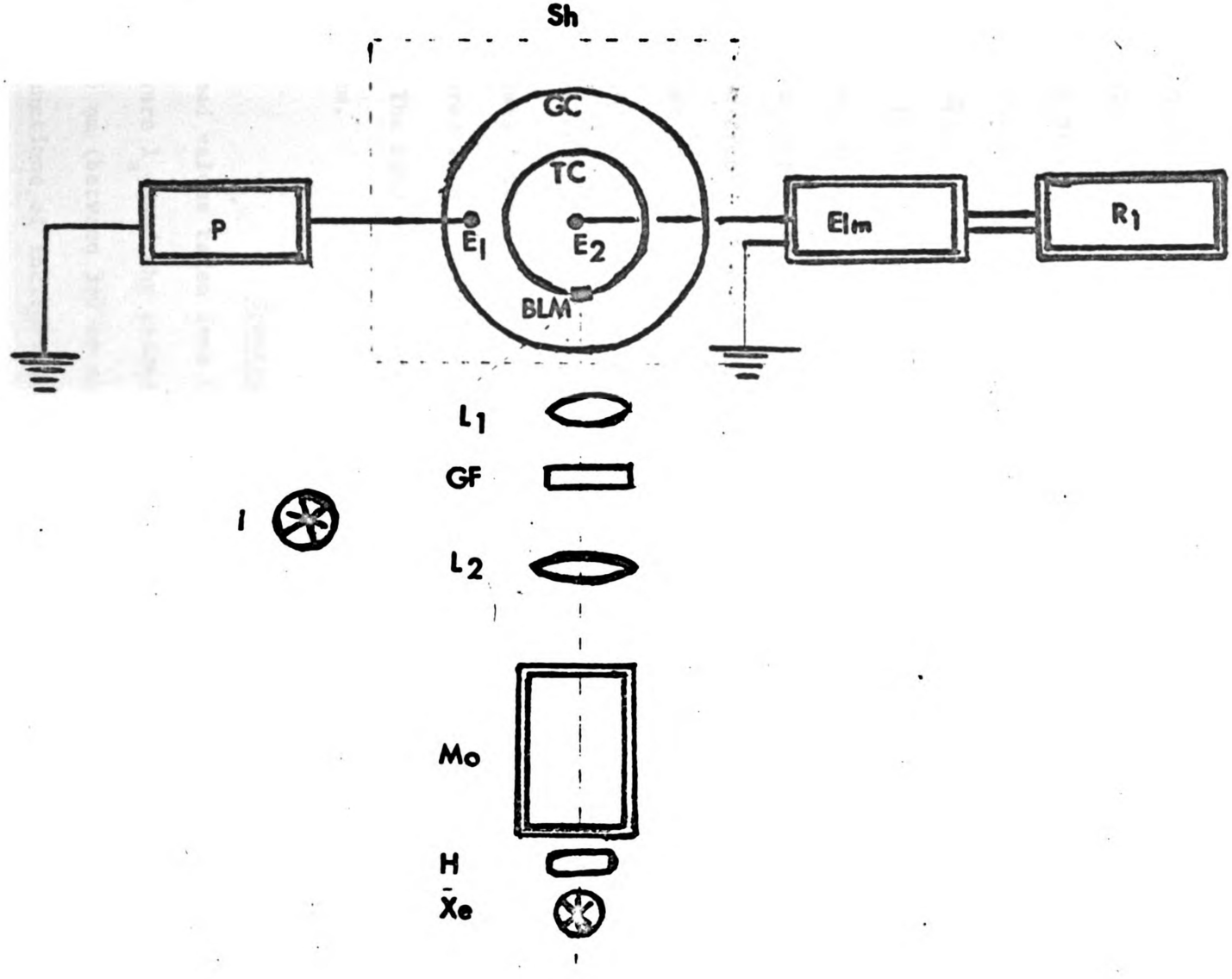
Sh
GC
TC
P
E1
E2
Elm
R1
BLM
L1
GF
I
L2
Mo
H
Xe

The relationship between photoresponse and incident light intensity was also investigated at several discrete wavelengths. In order to gradually decrease the exciting light intensity, grey filters of known optical density were used. The diagram of the apparatus used in these measurements is shown in Figure 3.

Measurement of the Absorption Spectra and Intensity

Absorption spectra of both the membrane-forming solution and the BLM were taken. To measure the absorption spectra of the lipid solutions, a dilution (1:40) of the stock solutions was made and quartz cuvettes of 1 cm pathlength were used. For measuring the absorption spectra of the BLM, a five layer wire screen was used on those membranes formed by using a few drops of the BLM-forming solution. After forming the BLM on each mesh of the screen, the wire frame was carefully transferred into the quartz cuvette which was then filled with acetate buffer at pH 5 and utilized to measure the absorption spectra. The absorption spectra in both cases (diluted BLM-forming solution and the five-layers membrane) were measured with a photoelectric recording grating spectrophotometer Cary 15. The band width in the spectral range investigated did not exceed 0.5 nm.

Spectral Correction

Assumed values taken from the action spectrum and those directly recorded were λ_a, and the relative heights of lamp energy distribution at every 5 nm (between 350 nm and 800 nm, see Figure 4) are λ_b. λ_a and λ_b were functions of incident wavelength. λ, in the present correction, was a series of discrete wavelengths increasing at each 5 nm between 350 nm and 800 nm.

Figure 4--Spectral energy distribution of the incident light (measured by a spectrally flat thermopile), arbitrary unit. (Taken from Dr. N. T. Van)

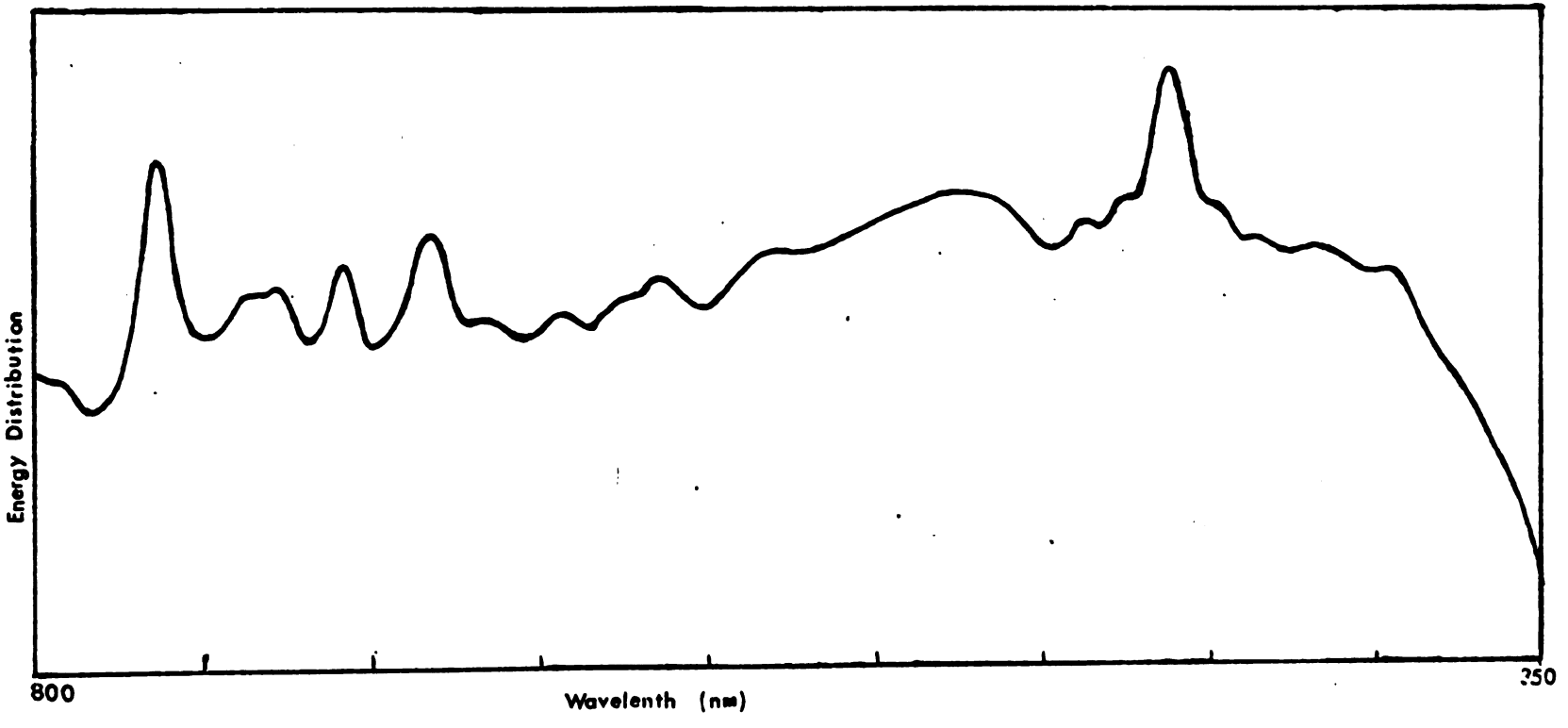
Energy Distribution
800
Wavelenth (nm)
350

Action spectrum corrected for constant incident energy was obtained from the following two steps:

(1) λ_a was divided by λ_b at each fixed wavelength, and a series number was obtained, namely λ_c. (There are 91 numbers in the present work.)

(2) Then the λ_c's were divided with the maxima of themselves, and another series number was obtained (91 numbers), namely λ_d. Plotting each λ_d value versus wavelength, a normalized action spectrum corrected for constant incident energy was received.

Since the corrected spectrum was already normalized, it illustrated the energy efficiencies for different wavelengths.

CHAPTER IV

GENERAL PROPERTIES OF CHL-BLM

The results obtained in the present work are presented in three chapters, namely: (1) general properties of chl-BLM, (2) mechanism of the photogenerated voltage, and (3) action spectra of chl-BLM. In this chapter only the results of Section (1) are given and discussed. The mechanism of photogenerated voltage and photovoltaic spectra will be given and discussed in the next two chapters.

Membrane Resistance and Capacitance

Figure 5 shows the time dependence of membrane resistance and capacitance (R_m and C_m respectively) during the membrane thinning process. It was observed that R_m decreased while C_m increased. However, once black lipid membrane was formed, both of them would remain constant--as long as the system was not disturbed. This result was not unexpected. The value of R_m equals the sum of R_o and R_d where R_o is the resistance due to orderly arranged molecules contained in the thin membrane and R_d is due to randomly arranged molecules sitting in the interior of the thin film, and the C_m is inversely proportional to the thickness. Immediately after the injection of membrane-forming solution to the orifice, it was known that the membrane was not "black" or bimolecular in thickness. It thinned down gradually under the molecular interactions between the membrane-forming solution and the aqueous solution. It took about 30 minutes to decrease the thickness of a newly formed membrane by a hundred times or more and to reach the steady state.

Figure 5a--The time course of the dark membrane resistance as a function of ionic strength.

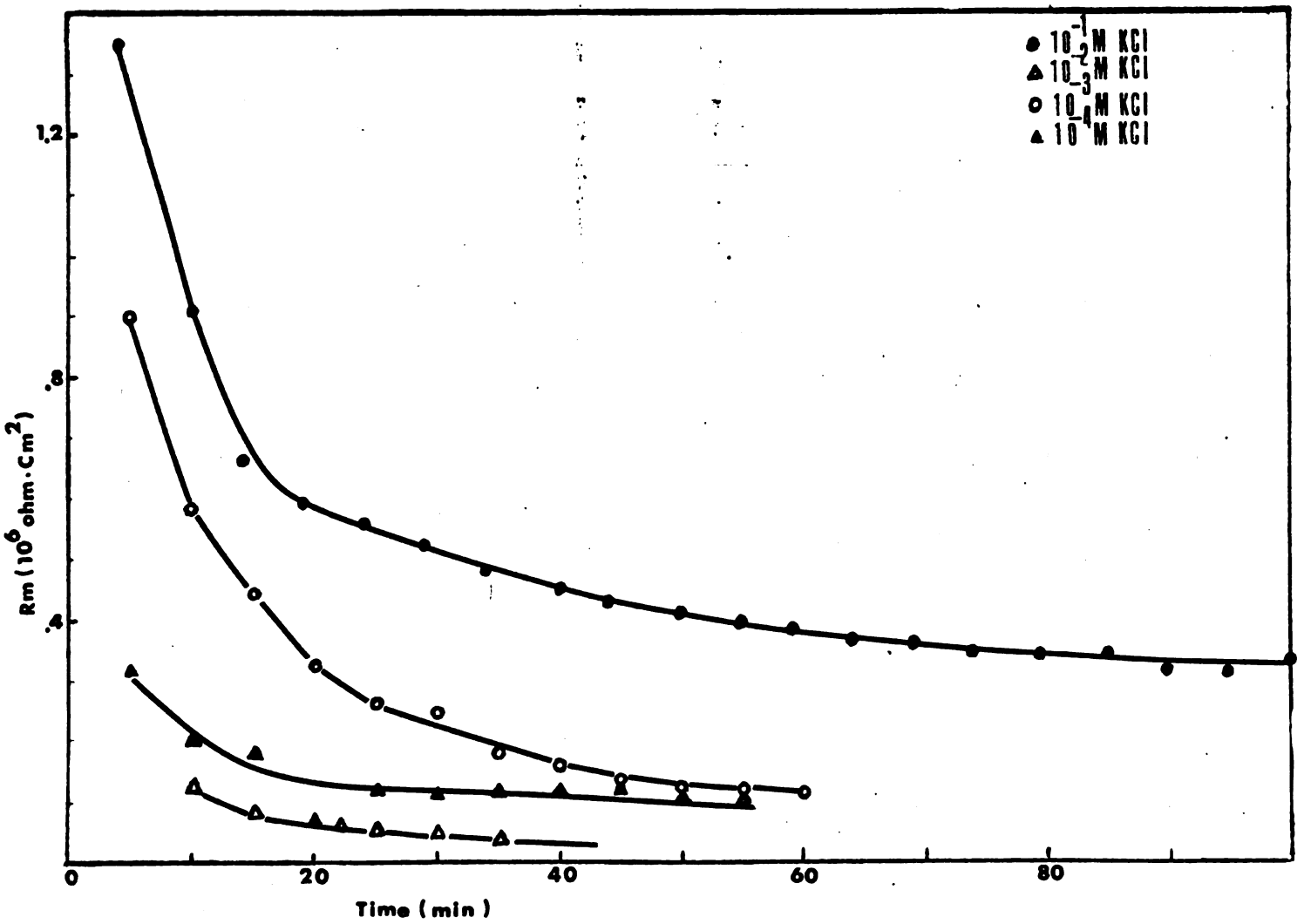
● 10^{-1} M KCl
▲ 10^{-2} M KCl
○ 10^{-3} M KCl
▲ 10^{-4} M KCl
Rm (10^6 ohm.Cm^2)
1.2
.8
.4
0
20
40
60
80
Time (min)

Figure 5b--The time course of the capacitance as the function of ionic strength.

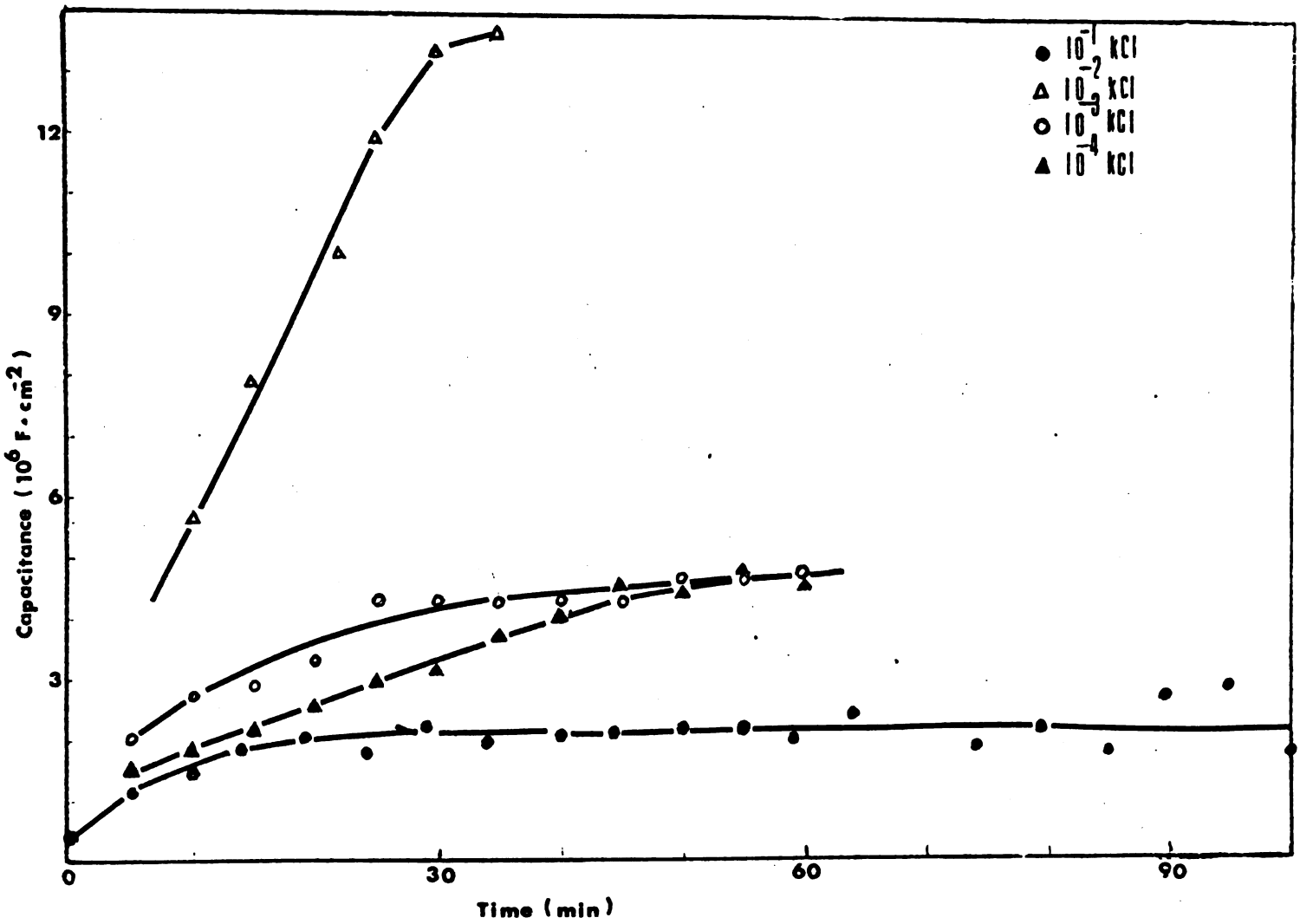
10^{-1} KCl
10^{-2} KCl
10^{-3} KCl
10^{-4} KCl
Capacitance (10^{6} F·cm^{-2})
12
9
6
3
0
30
60
90
Time (min)

Dark Current-Voltage Relationship

The relationship between the dark transmembrane current versus the dark transmembrane potential as a function of the pH of the bathing solution is shown in Figure 6a. The result shows that the I-V curve is not linear at pH above 4. It can be seen that current at fixed transmembrane voltages increases as H^+ ion concentration increases. It probably signifies that H^+ ions contribute to the transmembrane current. Because of its acidic property, assymetrical application of $FeCl_3$ may generate a pH gradient (less than 0.1 pH unit in 0.1 M acetic buffer at pH 5) across the chl-BLM. Figure 6b shows an I-V curve under the effect of 0.1 pH gradient across chl-BLM generated by acid treatment. It can be seen from Figure 6a and 6b that the membrane resistance decreased at high transmembrane voltage, especially when the pH of the bathing solution was higher than 4. This may be the reason that in the study of the transmembrane voltage dependence of photoemf, which is presented in the next chapter, the applied transmembrane voltage was never beyond this limit, namely ± 22 mV. The nonlinearity of the I-V curve has also been observed in many other BLM systems. A variety of theoretical considerations are available in literature (for example, Schlögl, 1969).

Photoinduced Voltage of chl-BLM

The shape of the open-circuit photoemf is shown in Figure 7, containing fast and slow components. The qualitative discussion including the identification of the nature of charge carriers is postponed until the next chapter.

Figure 6a--Dark current-voltage curves as functions of pH. Membranes were formed in 0.1 N KCl solution.

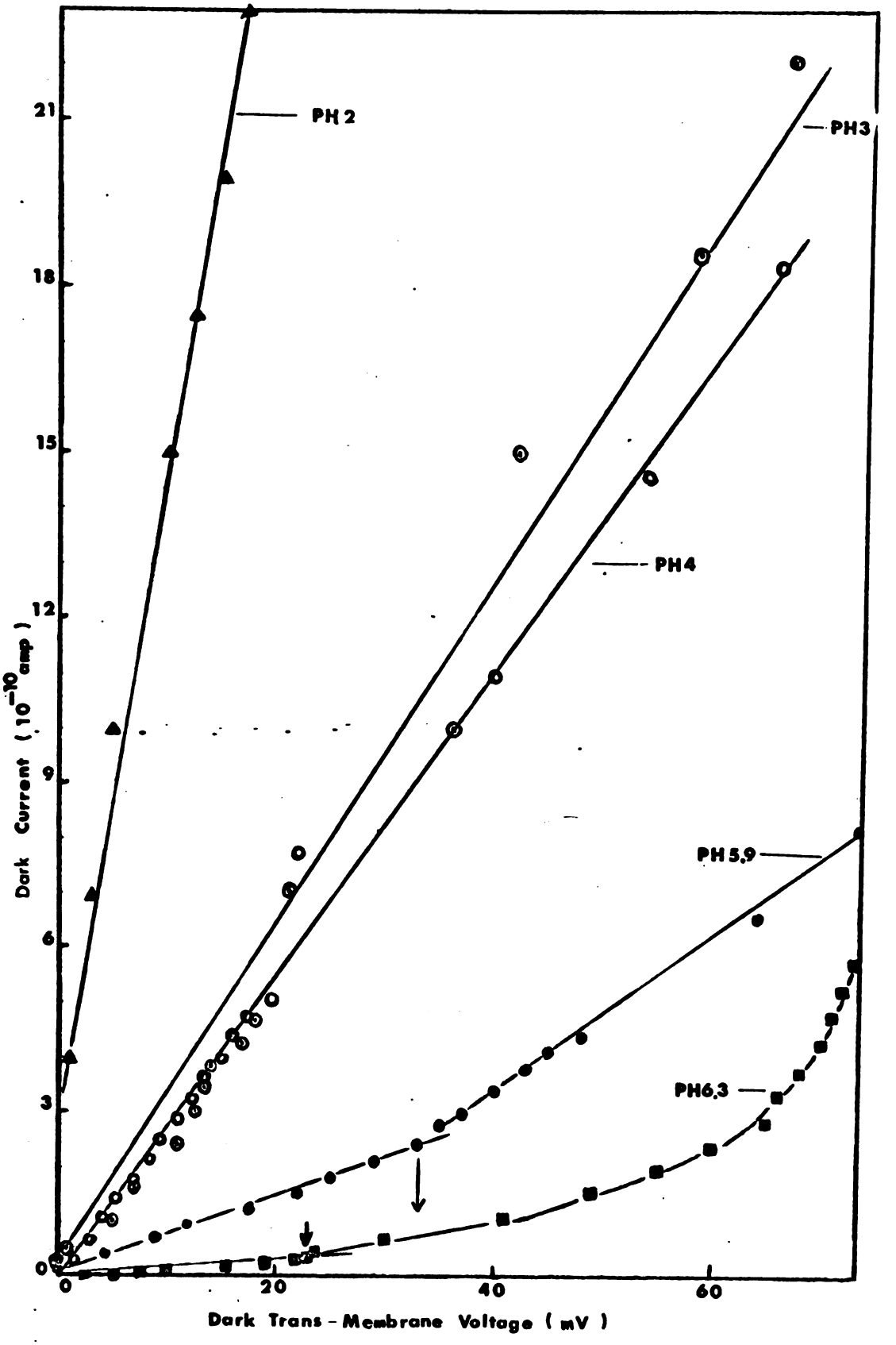
PH 2
PH3
PH4
PH 5.9
PH6.3
21
18
15
12
9
6
3
0
0
20
40
60
Dark Current (10^{-10} amp)
Dark Trans - Membrane Voltage (mV)

Figure 6b--Dark current-voltage curve of a chl-BLM in 0.1 N KCl solution with a pH gradient of 0.1 across the membrane (inside pH 5.1, outside pH 5.0).

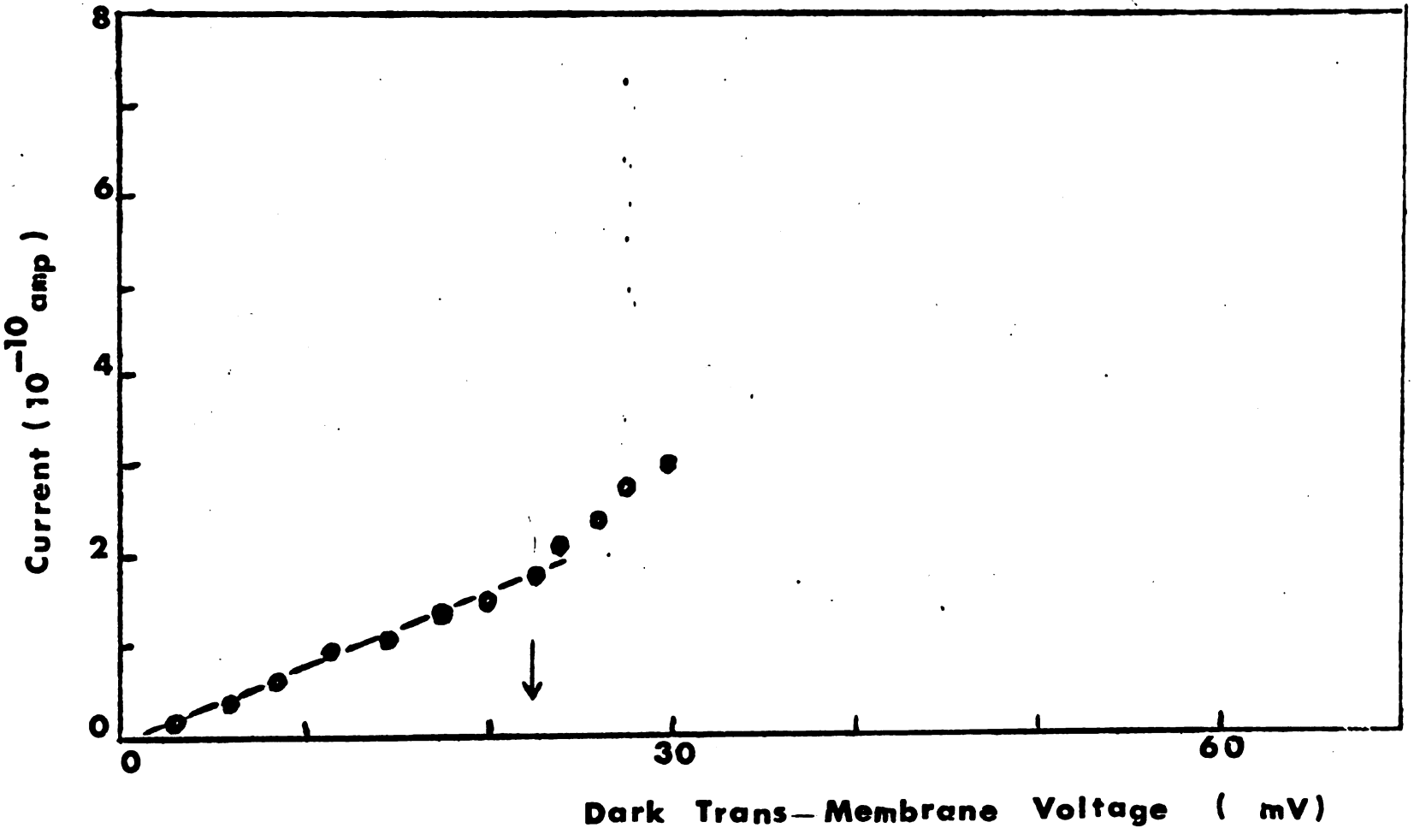
8
6
4
2
0
Current (10^{-10} amp)
0
30
60
Dark Trans—Membrane Voltage (mV)

In order to examine the reproducibility of the result a membrane was repeatedly illuminated and the photoemf was recorded. It was found that the repetitive illumination changed neither the magnitude nor the wave form of the photoresponse appreciably (Figure 8).

Shown in Figure 9 is the effect of duration of illumination. It shows that in order to generate a maximum photoresponse, four seconds is enough. Prolonged illumination does not help at all, but rather depresses it. This is probably due to the competition of two kinds of charge carriers upon illumination. This will be discussed in the next chapter. In regards to the intensity studies, it can be seen in Figure 10 that the increment of the photoemf decreases with increasing light intensity. This is probably because the number of excitable pigments in a BLM is finite. In order to understand the process of generation of photoresponse, redox action spectra were taken by using two different methods. Redox action spectrum is defined as the photo-generated voltage as a function of wavelength of the incident light. In the first method, the action spectra were constructed from responses taken at a number of monochromator settings between 350 nm and 800 nm and are shown in Figure 11. They were also continuously recorded by scanning the wavelength of the incident light from 350 nm to 800 nm and vice versa. The result is shown in Figure 24. The striking resemblance between the absorption spectra of the membrane-forming solution (Figure 27a) and the photoemf action spectra of the membrane indicate that chloroplast pigments contained in chl-BLM are the primary photon absorbers and that all the pigments are functioning at approximately the same efficiencies. Because of the similarity between the two action

Figure 7--The wave pattern of the photoemf of chl-BLM excited with monochromatic light of different wavelengths. Bathing solution is 0.1 N acetic buffer (pH 5) with 10^{-3} M $FeCl_3$ in the inner chamber. Dark transmembrane potential is 0.6 mV.

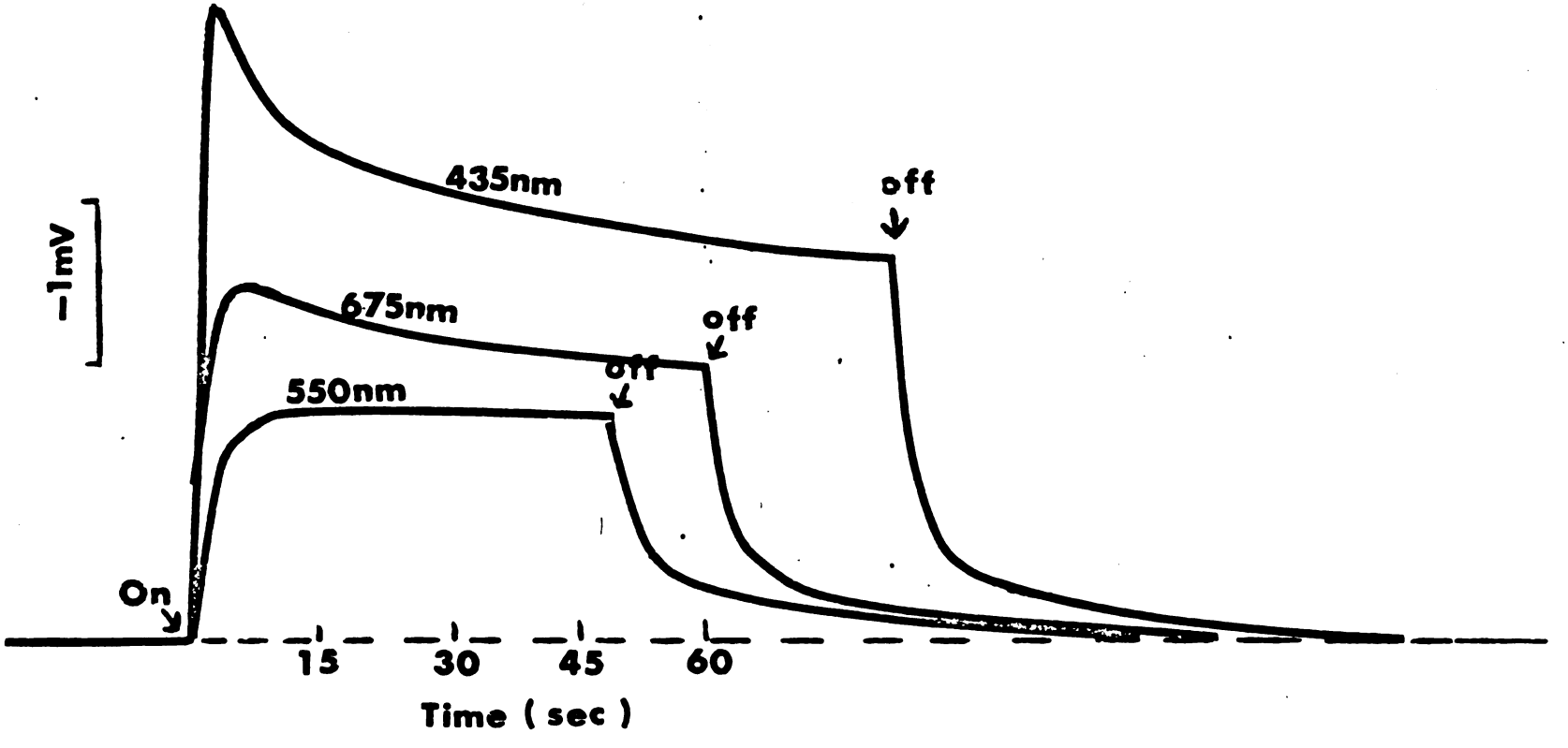
435nm
off
675nm
off
550nm
off
On
-1mV
15
30
45
60
Time (sec)

Figure 8--The effect of repetitive illumination on the photoresponses. Wavelengths of the incident light were set at 425 nm or 650 nm. The membrane was formed in 0.1 N acetic buffer (pH 5) solution, and 10^{-3} M $FeCl_3$ was added to the inner chamber.

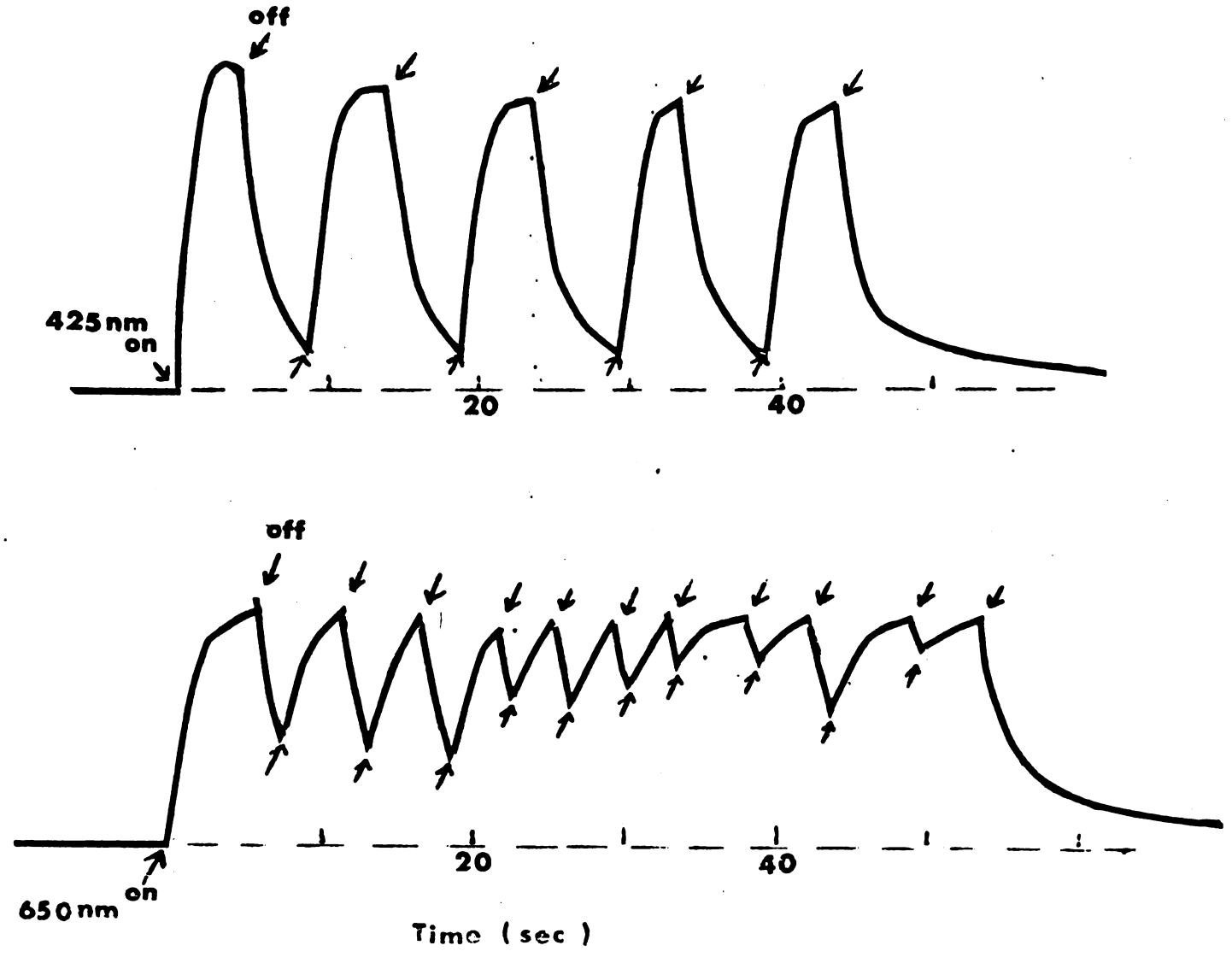
off
425nm
on
1/20
1/40
off
650nm
on
1/20
1/40
Time (sec)

Figure 9--The effect of the duration of illumination on the photoresponse. The wavelength of incident light was set at 440 nm. Rest in dark occurred for 1.5 minutes between two illuminations. The data was recorded from a single membrane formed in 0.1 N acetic buffer solution (pH 5) with 10^{-3} M $FeCl_3$ in the inner chamber.

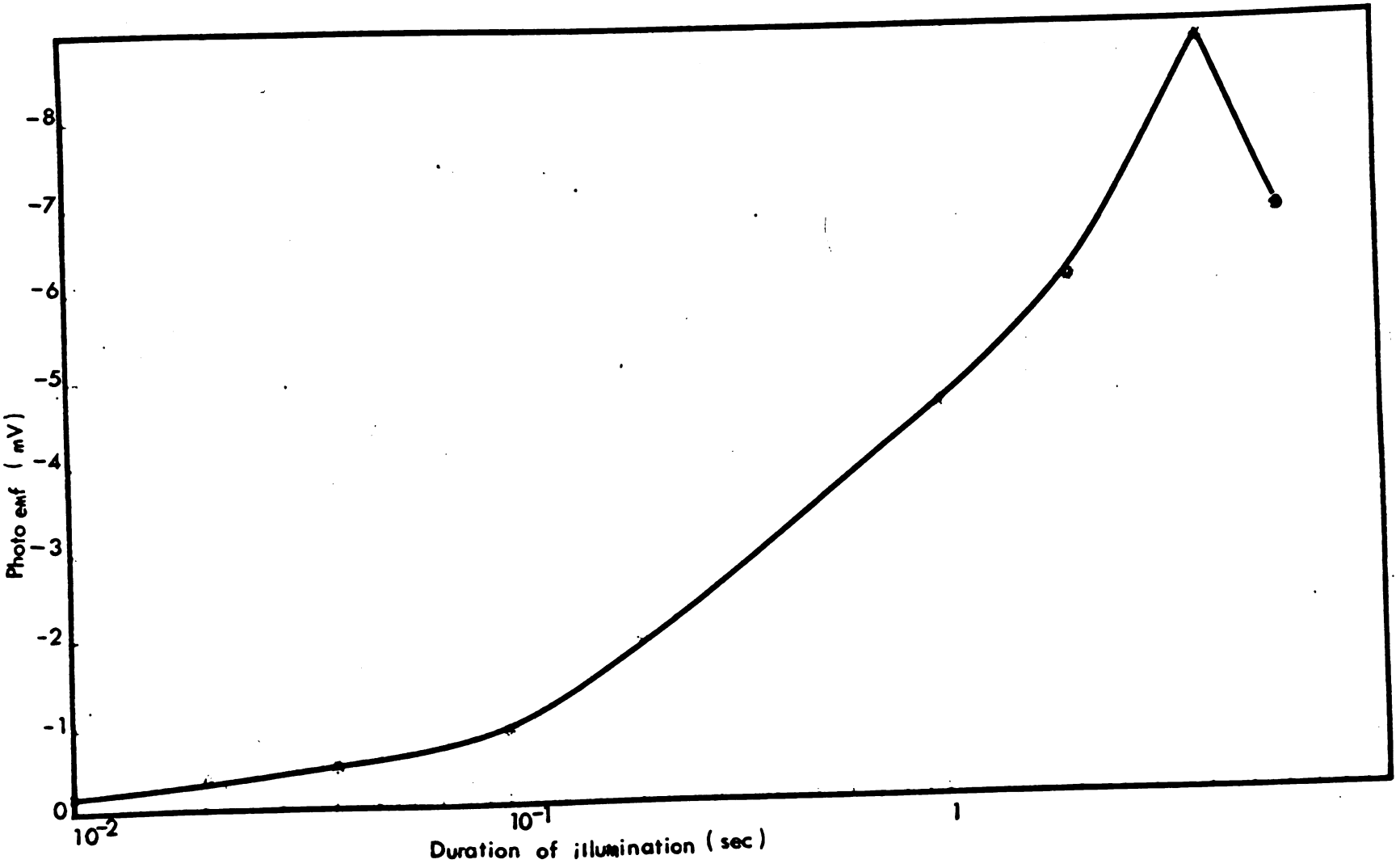
-8
-7
-6
-5
-4
-3
-2
-1
0
Photo emf (mV)
10^{-2}
10^{-1}
1
Duration of illumination (sec)

Figure 10--The effects of relative intensity of incident light on photoemfs of BLM-I (triangles) and BLM-III (circles). The exposure period was seconds in order to detect such a photoemf which contains both the fast and slow components.

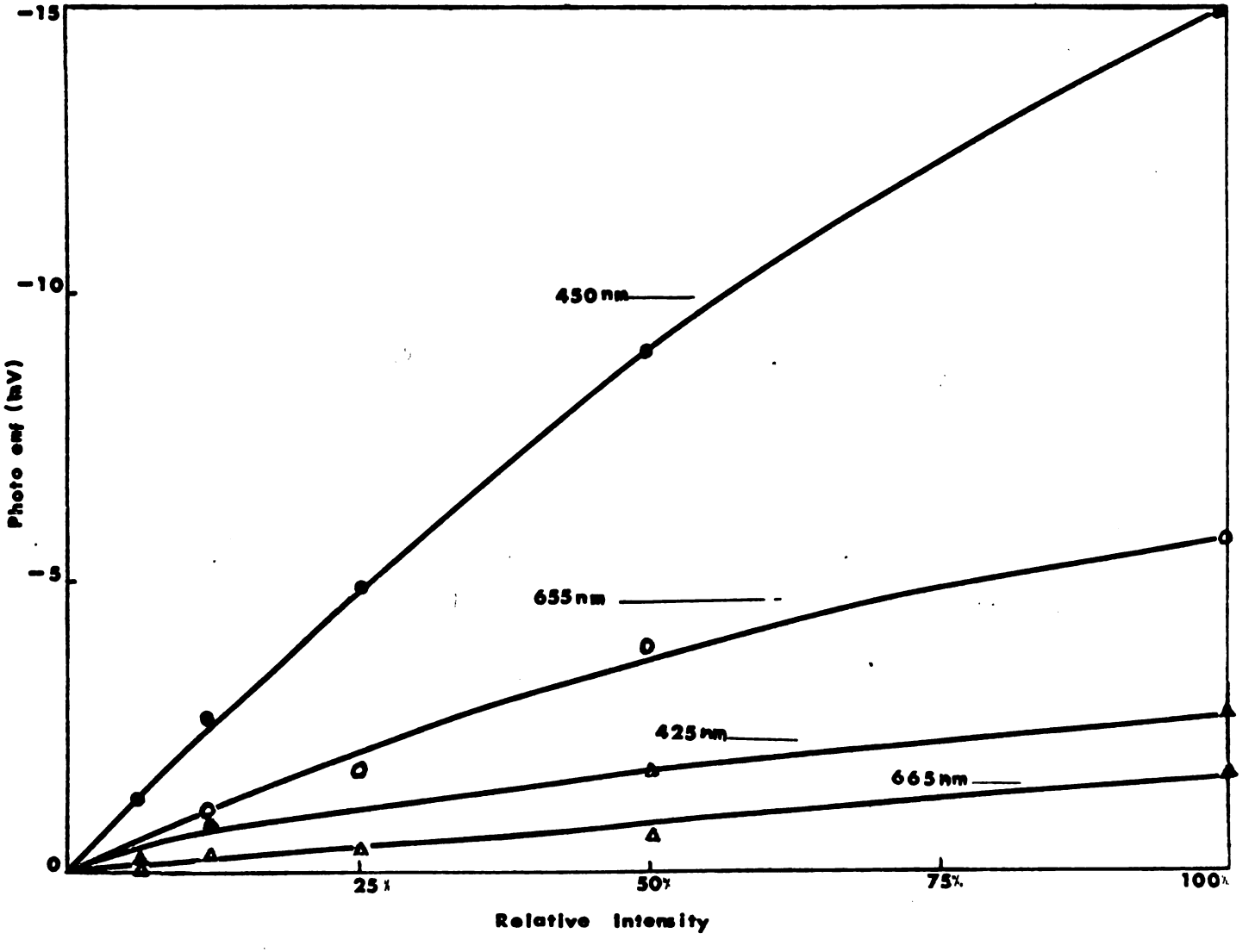
-15
-10
-5
0
Photo emf (mV)
450nm
655nm
425nm
665nm
25%
50%
75%
100%
Relative Intensity

Figure 11--Action spectra of a chl-BLM with a series of discrete monochromatic incident light from 800 nm to 350 nm, and the reverse series. Arrows indicate the direction of wavelength scanning.

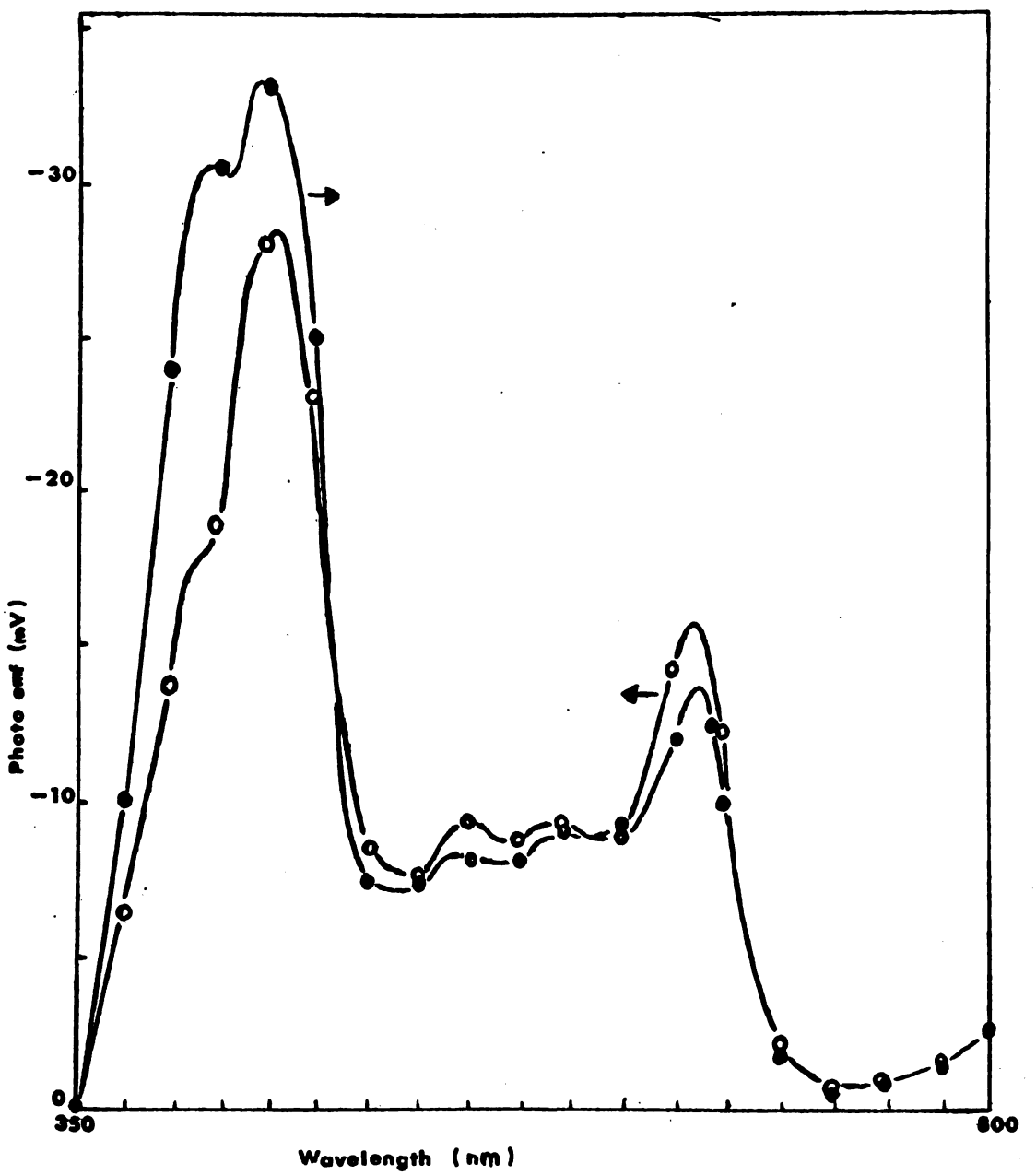
-30
-20
-10
0
Photo emf (mV)
350
800
Wavelength (nm)

spectra taken from the systems with and without $FeCl_3$, it is certain that $FeCl_3$ is not responsible for the photoemf generated by the yellow light. Therefore, the chloroplast pigments contained in chl-BLM undoubtedly absorb quanta, and light energy is converted into electric energy with the aid of highly organized BLM structure. This further confirms that the system used in the present work serves as a very realistic model system in the studies of the primary processes of photosynthesis.

Effect of Modifiers on the Photoemf

It was found that the magnitude of photoemf was enhanced by introducing electron acceptors or donors in one side of the BLM formation chamber. On the other hand, it may also be suppressed by applying the electron uncouplers or proton carriers. The effect of proton carriers on photoemf will be discussed in the next chapter since it is related to the mechanism of photoemf generation. The effects of the rest of the modifiers, however, will be presented here.

(a) Effect of $FeCl_3$

Various electron acceptors and donors have been reported serving as photomodifiers. Among these, $FeCl_3$ was extensively studied in the present work. It was found that the magnitude and wave form of the photoemf did not change by shifting the position of $FeCl_3$ from one side of the chamber to another, whereas the polarity of the photoemf was reversed. The open-circuit photoemf was tremendously enhanced with the presence of $FeCl_3$ in the system, and the side containing $FeCl_3$ was always electrically negative. This might be due to the fact that $FeCl_3$ has a relatively high redox potential (0.77 V), and will withdraw (or trap) electrons from the photoexcited chl-BLM. In clean

systems (without any modifiers), a relatively slow and much smaller photoresponse was observed. The sign of this photoemf was generally in agreement with the small dark membrane potential. This agreement indicated that transmembrane potential plays an important role in the observed photoresponse--probably charge separation.

It has been mentioned in the previous section that the open-circuit photogenerated voltage of chl-BLM formed in 0.1 M acetic buffer (pH 5) is greatly enhanced with the presence of $FeCl_3$ on one side but not both sides of BLM. A typical curve is shown in Figure 12. It is interesting to note that Figure 12 follows approximately the action spectrum of chl-BLM instead of a horizontal line. This means that $FeCl_3$ is more efficient for pigments which have two absorptions at 640 nm and 460 nm (probably chl b) than for other pigments in BLM (e.g., chl a, and carotenoids). Chlorophyll b molecules could transfer an electron from its excited state to the electron acceptors more easily than other pigments could. In order to find out the optimal $FeCl_3$ concentration which would give the maximum photoemf, and how $FeCl_3$ interacts with the chl-BLM, a concentration study was carried out. Experimentally, this was achieved by fixing the bathing solution (0.1 M acetic buffer) at pH 5 and increasing the $FeCl_3$ concentration at the inner chamber. Shown in Figure 13 is the dependence of photoemf on $FeCl_3$ concentration. It can be seen that the presence of 4×10^{-3} M $FeCl_3$ in the inner cup gave a maximum enhancement of the photoresponse. This fact indicates that ferric ions, or their hydrated complex, are bonded reversibly to the BLM surface and the number of binding sites on the chl-BLM is finite. The other evidence that

Figure 12--Enhancement of photoemf by $FeCl_3$. Data was taken from a single membrane in 0.1 N acetic buffer (pH 5). 10^{-3} M $FeCl_3$ had been added to the inner chamber.

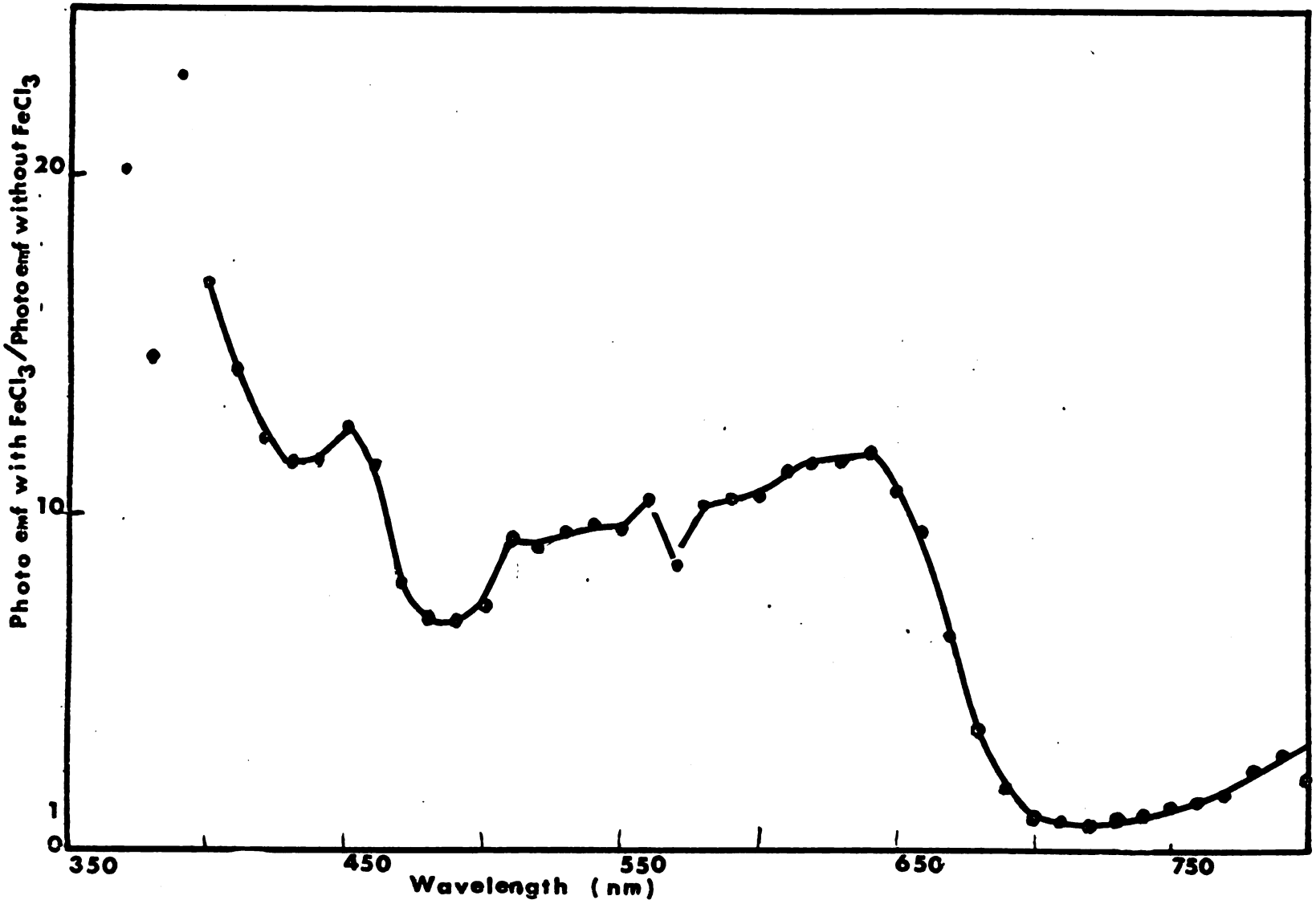
Photo emf with $FeCl_3$/Photo emf without $FeCl_3$
20
10
1
0
350
450
550
650
750
Wavelength (nm)

Figure 13--Dependence of photoemf on $FeCl_3$ concentration in the inner chamber. Curves correspond to two maximum peaks in the action spectrum. Membrane was formed in 0.1 N acetic buffer (pH 5).

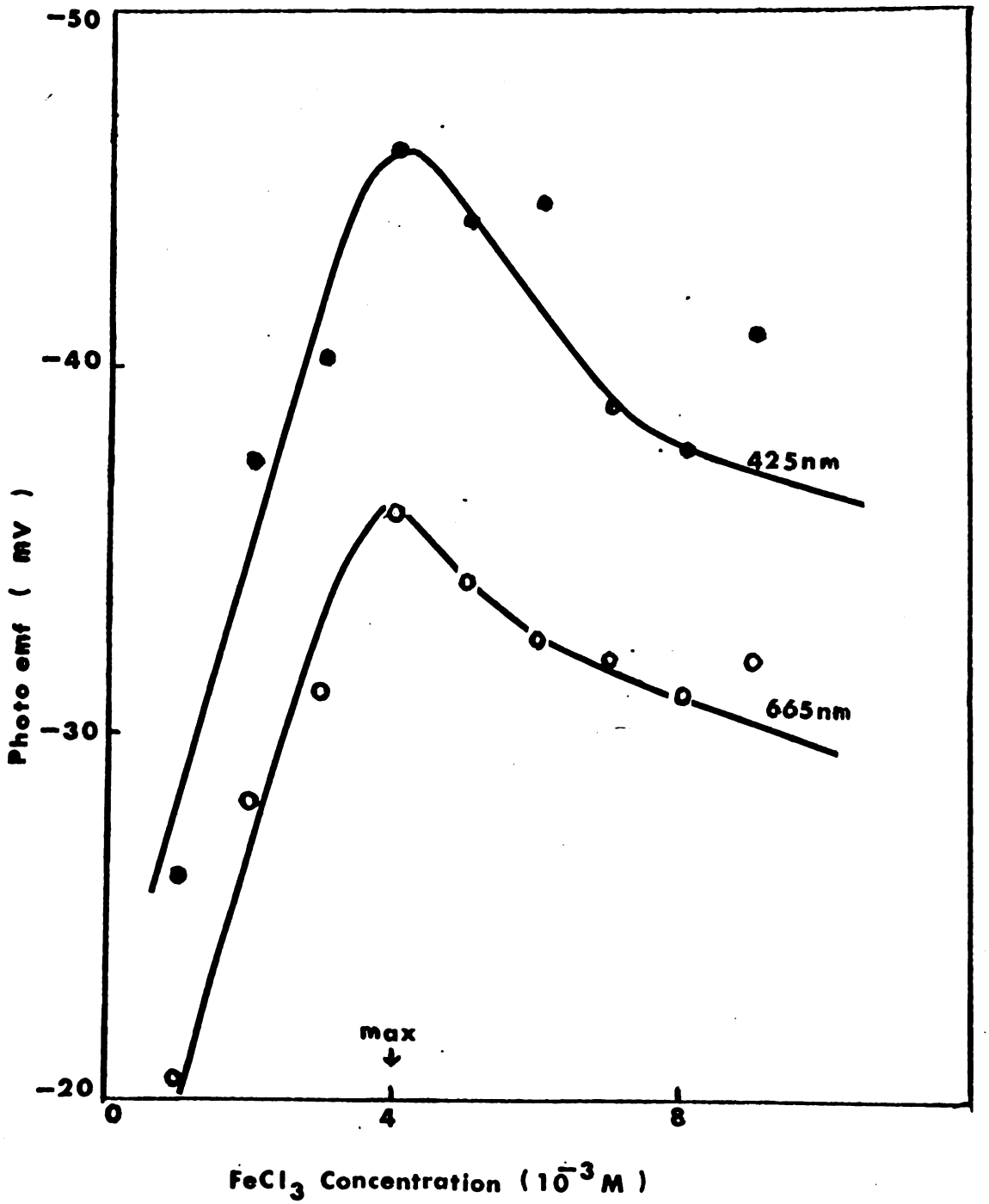
-50
-40
-30
-20
Photo emf (mV)
425nm
665nm
max
0
4
8
FeCl3 Concentration (10-3 M)

supports the above assumption is that in the system containing $FeCl_3$ in the outer chamber, a cloudy layer was observed covering the surface of the BLM. If one sweeps gently with the tip of the microsyringe, this cloudy layer can be removed for a short time.

Figure 14 shows a plot of the dark membrane resistance as a function of $FeCl_3$ concentration in the inner cup. Maximal R_m was observed at a concentration of 2×10^{-3} M $FeCl_3$ in the inner cup. It seems that the magnitude of the photoemf was closely related to the membrane resistance. Very small or no photoemfs could be detected on chl-BLM with a resistance lower than 10^4 ohm-cm^2. It is worth noting that the form of the action spectrum was not changed by changing the $FeCl_3$ concentration in the inner chamber.

(b) Effect of Electron Uncouplers

Two strong electron uncouplers of PS-II, namely DCMU and CMU, were tested in this study. Figure 15 shows the concentration dependence of both photoemf and transmembrane dark voltage. In both cases of inhibiting, the photoemfs decreased with increasing concentration, while the dark transmembrane voltages increased linearly with concentration. Furthermore, the membrane resistance decreased by one order of magnitude in the presence of 4×10^{-3} M DCMU or 5×10^{-3} CMU in the outer chamber. CMU acts to prevent electron flow from water to PS-II (Mueller, Rumberg and Witt, 1963) and DCMU may inhibit electron flow between the primary oxidant, Q^-, and plastoquinone (Kok and Cheniae, 1966) and uncouple the electron flow from H_2O to X (Izawa and Good, 1965). Both DCMU and CMU are electron uncouplers, and in the nonenzymatic BLM system they may act in a similar manner in the electron (hole) flow process of the membrane.

Figure 14--Dark membrane resistance as a function of $FeCl_3$ concentration in the inner chamber. Bathing solution: 0.1 N acetic buffer (pH 5).

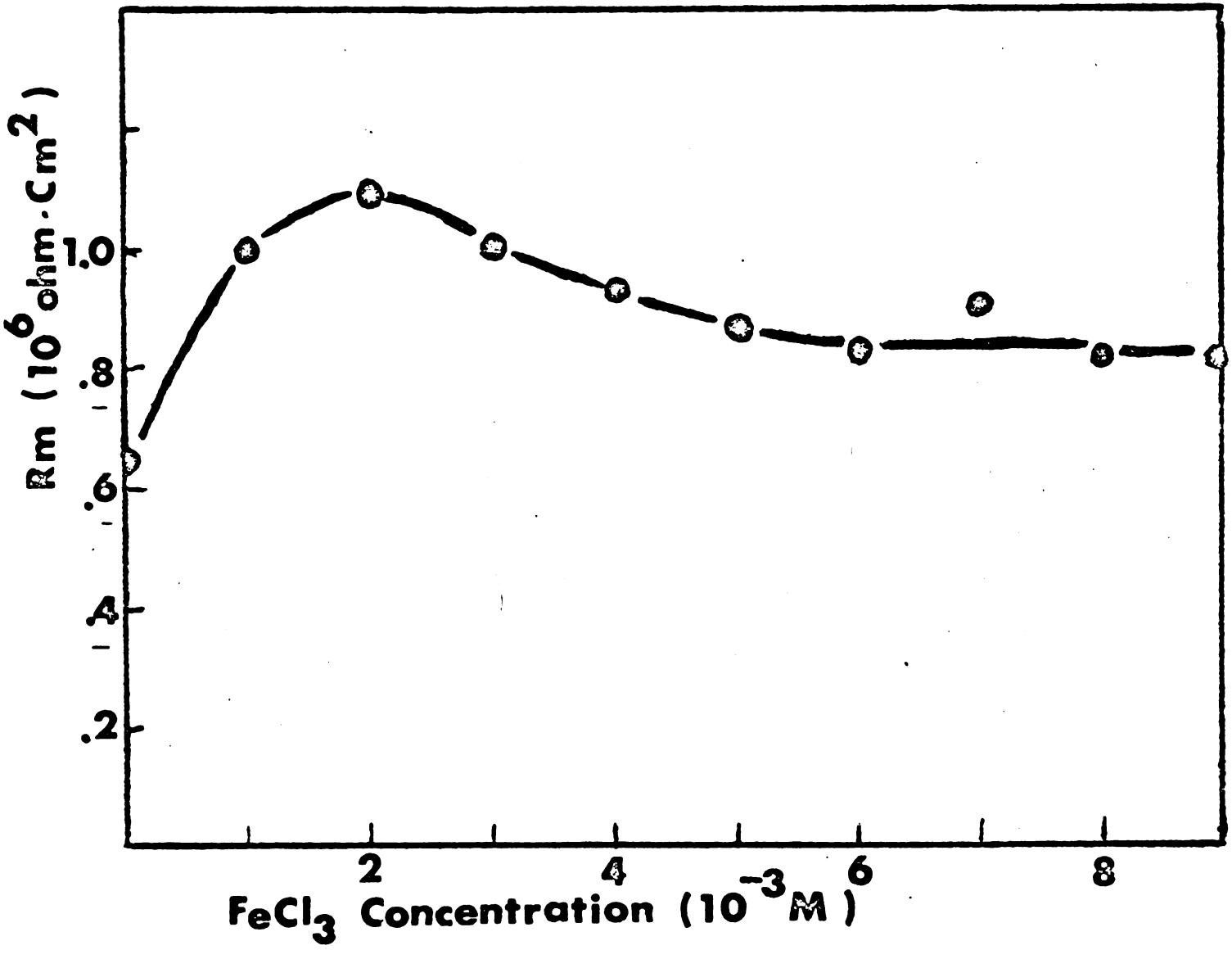
Rm (10^6 ohm·Cm^2)
1.0
.8
.6
.4
.2
2
4
6
8
$FeCl_3$ Concentration (10^{-3} M)

Figure 15--Dependences of photoemf and dark membrane voltage on DCMU and CMU concentrations. Membrane was formed in 0.1 N acetic buffer (pH 5) with DCMU or CMU in the inner chamber and 2.5×10^{-4} M $FeCl_3$ in the outer chamber. Arrows indicate the amount which drops the membrane resistance one order of magnitude (from 10^{6-7} ohm-cm^2 to 10^{5-6} ohm-cm^2).

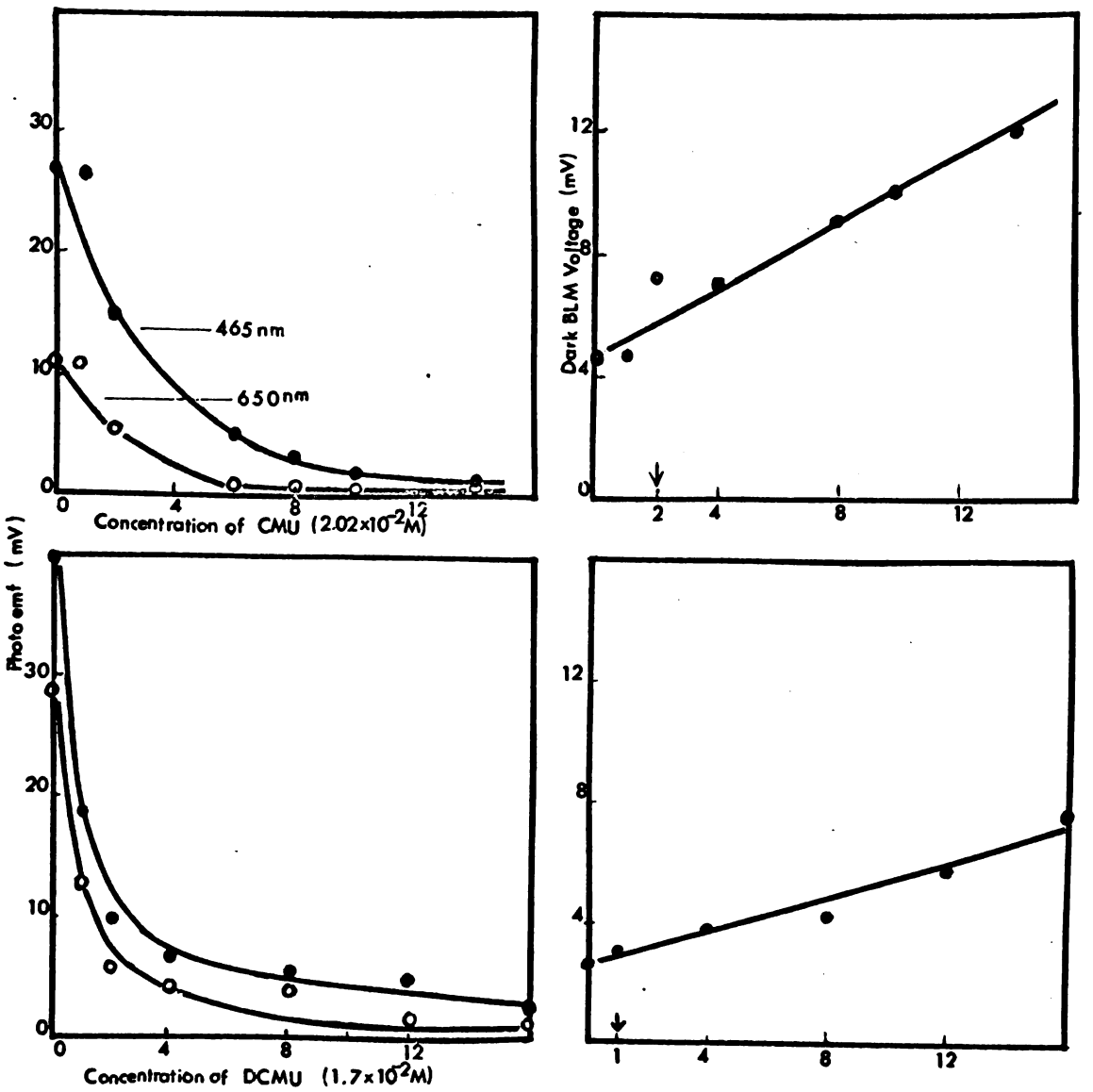
30
20
10
0
465nm
650nm
0
4
8
12
Concentration of CMU (2.02×10⁻²M)
Photo emf (mV)
30
20
10
0
0
4
8
12
Concentration of DCMU (1.7×10⁻²M)
Dark BLM Voltage (mV)
12
8
4
0
2
4
8
12
12
8
4
1
4
8
12

(c) Effect of Bathing Solution pH

As far as the bathing solution was concerned, it was found that photoemfs with fixed amounts of $FeCl_3$ (in the inner chamber) were also pH dependent. By changing pH of the bathing solution from 4 to 5, photoemf increases about 7 times. A systematic investigation on this aspect was also done. Figure 16 shows the pH dependence of membrane resistance. Comparing Figure 5a and Figure 15, it is seen that $FeCl_3$ in one side of the membrane has a certain kind of proper effect on BLM resistance. A maximum membrane resistance was reached at 5. This might be due to the effect of the H^+ ion concentration on the titriable groups contained in chl-BLM. Varying the pH of the bathing solution changed the magnitude of the photoemf; however, the wave form of the action spectrum remained unchanged. Figure 17 shows the relationship between photoemf and pH of the bathing solution. It shows a maximum photoemf at pH slightly above 5. The coincidence that both of the two maxima, resistance and photoemf, fall at pH around 5 again strongly indicates that photoresponse is closely related to BLM resistance.

Selection of a Standard System

Based upon the experiments described in the foregoing paragraphs, it was felt that enough information to select a standard system for further experiments was available, leading to a better understanding of the redox action spectrum and the mechanism of the photoemf generation. The selection of the standard system was based on the following two criteria:

Figure 16--pH dependence of dark BLM resistance. Membranes were formed in 0.1 N acetic buffer with 10^{-3} M $FeCl_3$ in the inner cup.

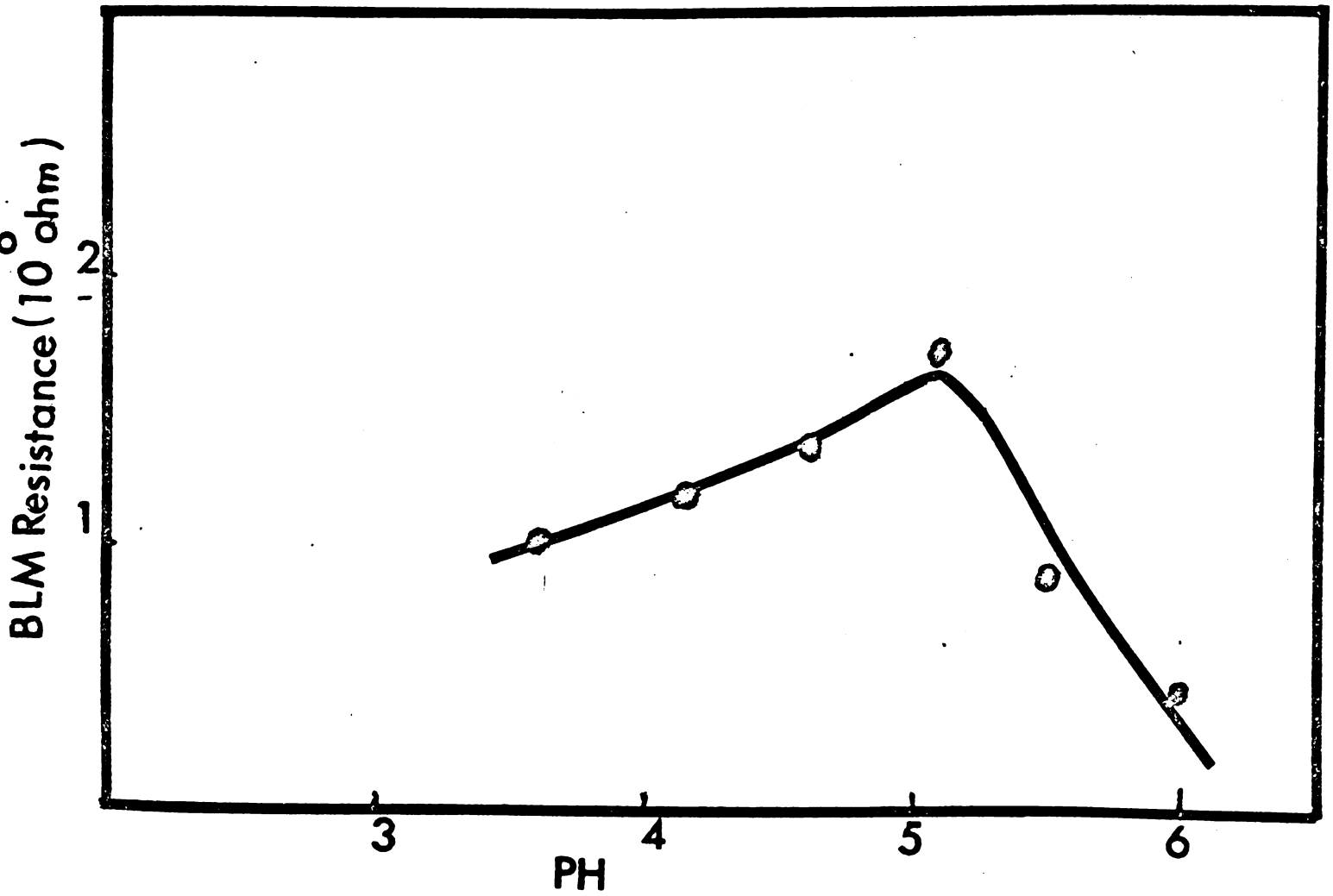
BLM Resistance (10^8 ohm)
2
1
3
4
5
6
PH

Figure 17--The effect of pH on photoemf with incident light of different wavelength. Bathing solutions were 0.1 N acetic buffer with 10^{-3} M $FeCl_3$ in the inner chamber. (Each point is the average of five BLM.) Data are those of action spectra taken at different pH.

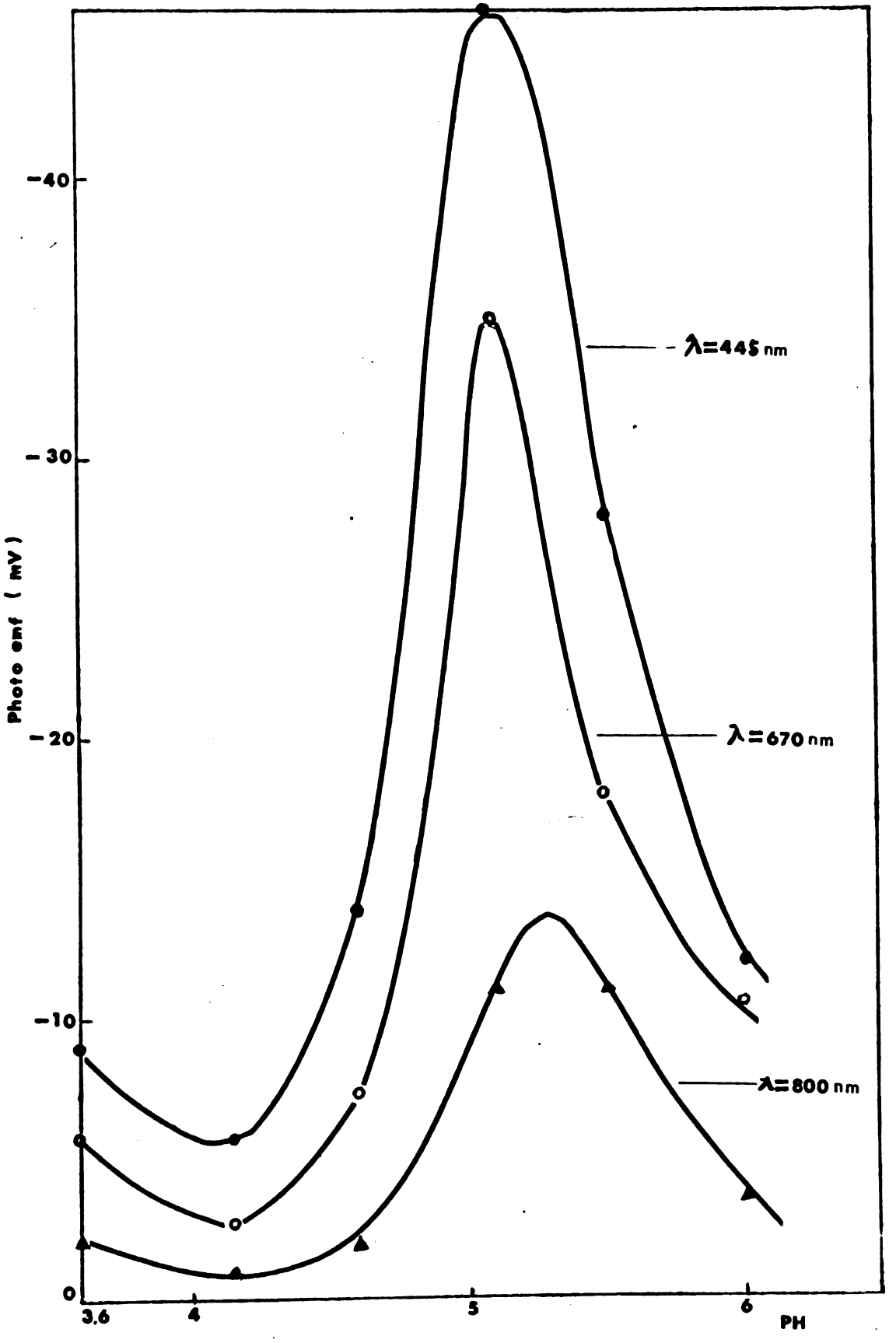
-40
-30
-20
-10
0
Photo emf (mV)
λ=445 nm
λ=670 nm
λ=800 nm
3.6
4
5
6
PH

(1) 0.1 sodium acetic buffer at pH 5 was chosen as bathing solution because at this pH the photoemf was maximum and the membrane was most stable.

(2) Only 10^{-3} M $FeCl_3$ was introduced into the inner chamber after forming a chl-BLM, to enhance the photoemf without generating any detectable pH gradient across the BLM.

The findings using this standard system are considered in the next two chapters.

CHAPTER V

MECHANISM OF THE PHOTOGENERATED VOLTAGE

Introduction

In this chapter the nature of charge carriers and a possible mechanism of the observed "photoelectric" energy conversion are discussed. In the present work this problem is tackled simply by applying an external voltage across the chl-BLM and studying the relationships between the amplitude and polarity changes of the photovoltage and the transmembrane dark voltage. To establish a general overall view of the physical processes, results relevant to this problem will be presented in the first part, and the possible interpretations and a discussion of the mechanism of energy conversion will follow.

Results

Effects of Applied Voltage

The effect of transmembrane dark voltage on the overall photoelectric action spectra is shown in Figure 18. Data shown in Figures 19a and 19b was taken from a single chl-BLM by measuring the transmembrane dark voltage dependence of the photovoltage at maximum light intensity. The chl-BLM was formed in 0.1 N sodium acetic buffer at pH 4.5 with 10^{-3} M $FeCl_3$ in the inner chamber. It should be noted that throughout the present work, the electrode of the inner chamber is assigned to be the cathode and thus the open circuit photoemfs are negative readings. The effect of transmembrane dark voltage on the

Figures 18a and 18b--Photoelectric action spectra under the effect of the external field across the chl-BLM. Curves a, b, c, d, e, and f were taken at the external field equal to -6.0 mV, -4.0 mV, 2.5 mV, 5.0 mV, 8.6 mV, and 14 mV, respectively.

The external resistance was set at 10^9 ohms. Chl-BLM was formed in 0.1 N acetic buffer (pH 5) with 10^{-3} M $FeCl_3$ in the inner chamber. Incident light was scanning from long wavelength to short wavelength.

Figure 18a--Corrected and normalized for constant incident energy.

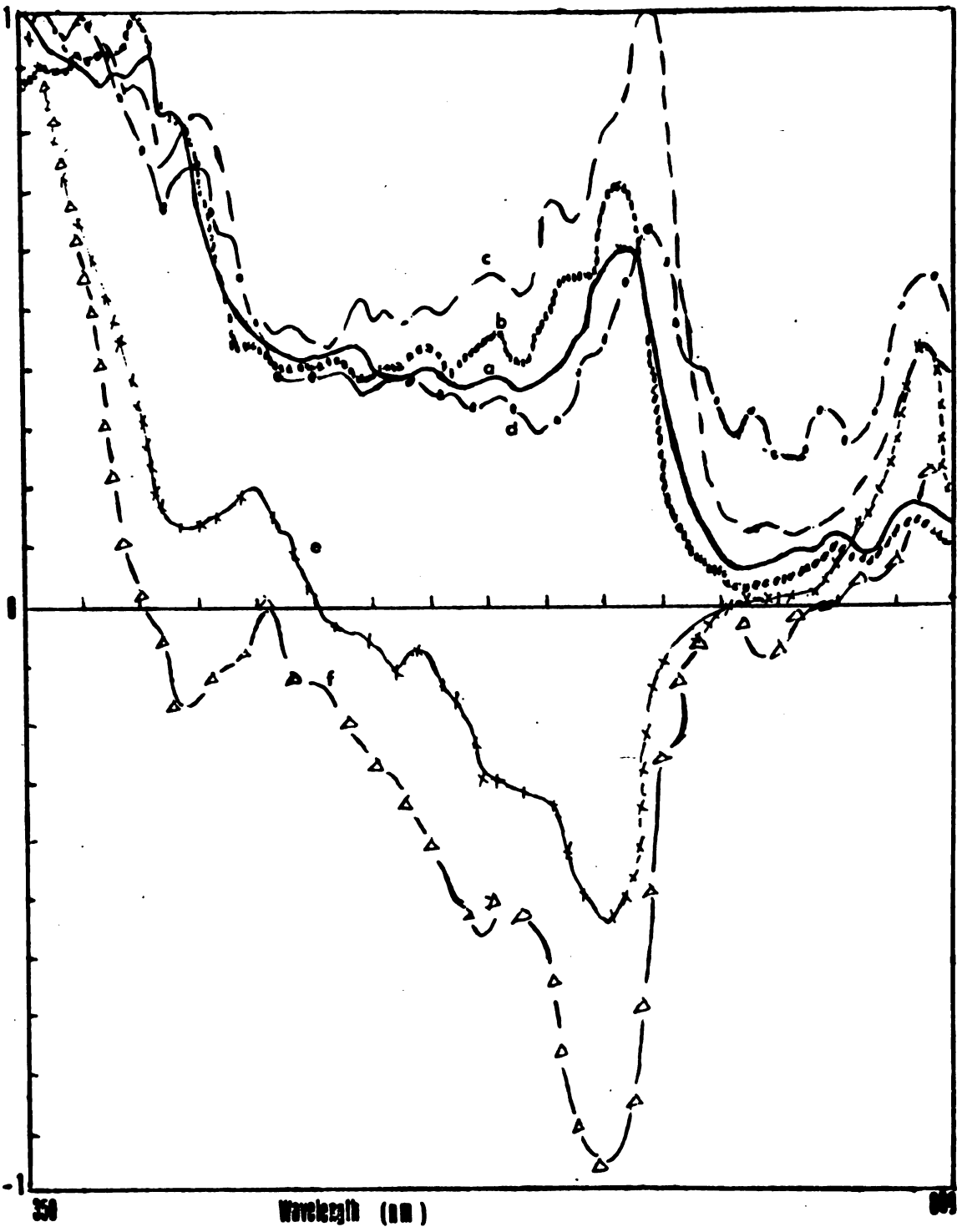
1
0
-1
c
b
a
d
f
350
Wavelength (nm)

Figure 18b--Uncorrected action spectra.

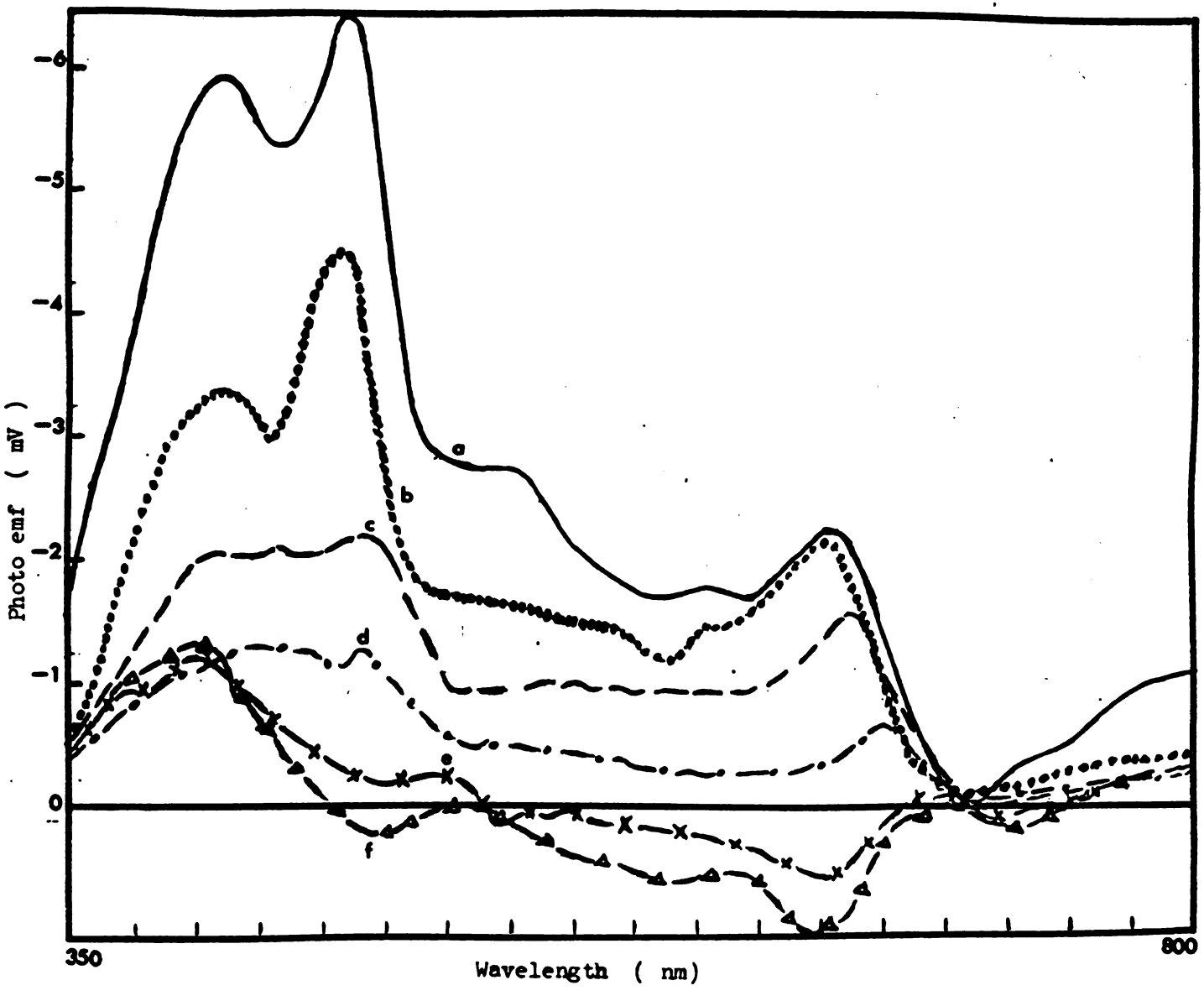
Photo emf (mV)
-6
-5
-4
-3
-2
-1
0
a
b
c
d
f
350
800
Wavelength (nm)

Figures 19a and 19b--Wave forms of photoemfs as functions of transmembrane voltage. Different components are indicated. 10-second exposures were taken with 1.5 minutes between each exposure. Membrane was formed in 0.1 N acetic buffer (pH 5) with 10^{-3} M $FeCl_3$ in the inner chamber.

Figure 19a--Incident wavelength: 460 nm.

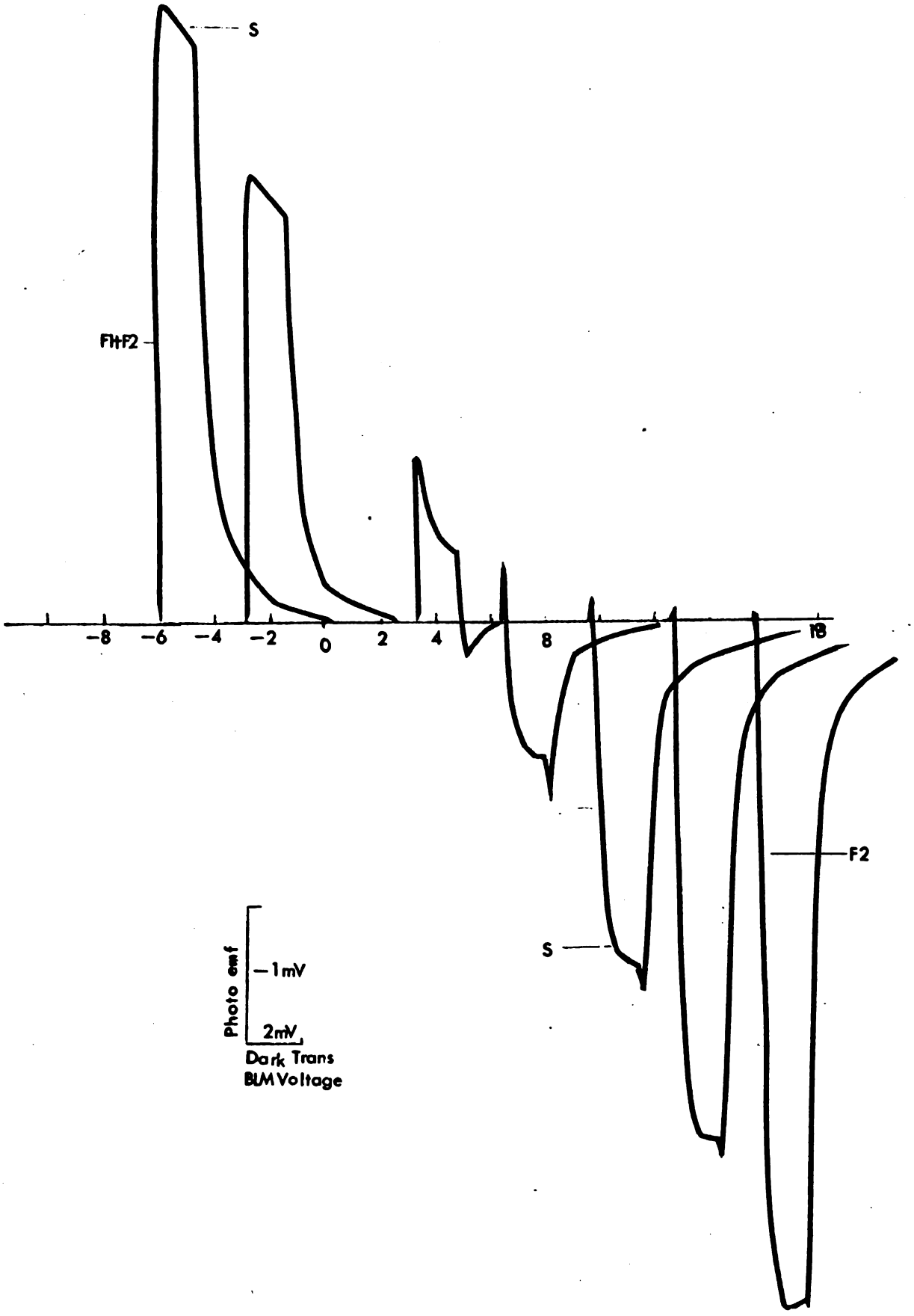
S
F1+F2
-8
-6
-4
-2
0
2
4
8
18
F2
S
Photo emf
1mV
2mV
Dark Trans
BUM Voltage

Figure 19b--Incident wavelength: 665 nm.

photoemf was remarkable, especially at those positive values where the waveforms of the photoemfs are biphasic within a limited range of transmembrane dark voltage (E_t). Beyond this range, biphasic behavior disappears. In contrast, for all negative transmembrane voltages the photovoltages show a monotonic increase. The enlarged pictures of typical biphasic waveforms of the photoemf under the effect of positive and negative dark voltages across chl-BLM is shown in Figures 20a and 20b respectively. From Figure 20a the waveform of the photovoltage can be analyzed into the following four components:

(i) Component F1: The sign of F1 was totally dependent on the side of the chl-BLM on which the electron acceptor was present. However, its absolute value decreased (perhaps exponentially, see Figure 21) with increasing E_t.

(ii) Component F2: This component was strongly dependent on the magnitude and polarity of the transmembrane voltage.

(iii) Component S: This component showed rather special behavior. Its absolute value increased with the increasing algebraic sum of components F1 and F2. The polarity of S was controlled not only by the E_t, but also by the concentration gradient of protons generated across the membrane which will be discussed later.

(iv) Component E: This is nothing but the steady state summation of all previous components.

When the light was off, component F1 disappeared almost instantaneously. The residual F2 component thus overshot to the positive

Figures 20a and 20b--Enlarged wave patterns of the photoemf under the effect of positive external field (20a) and negative external field (20b) across the BLM. Components are indicated. Experimental conditions were the same as those in Figures 19a and 19b.

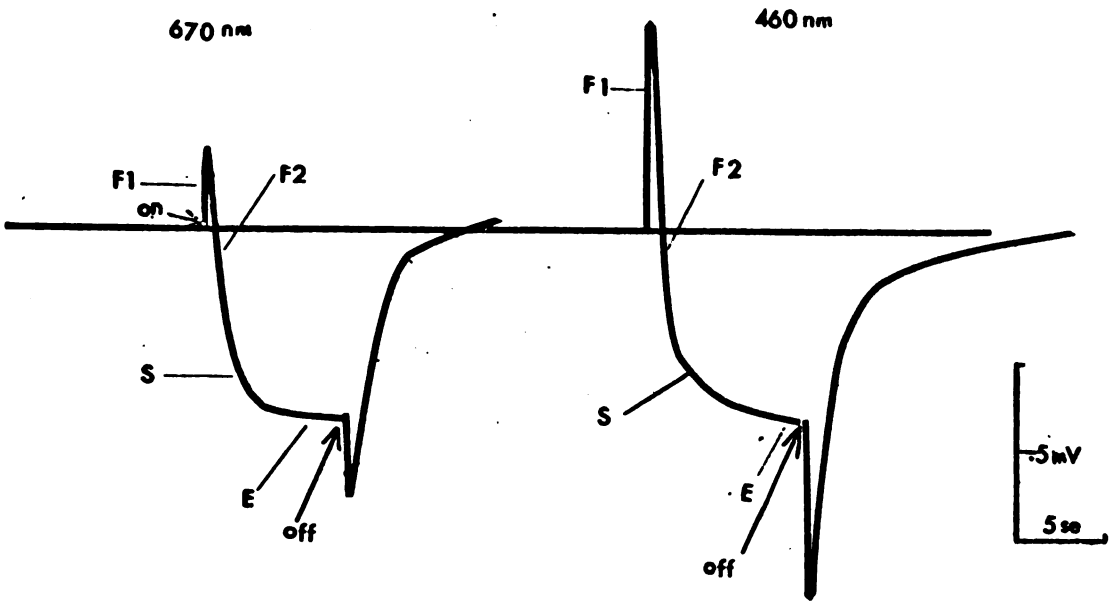
670 nm
460 nm
F1
F2
on
S
E
off
.5mV
5se

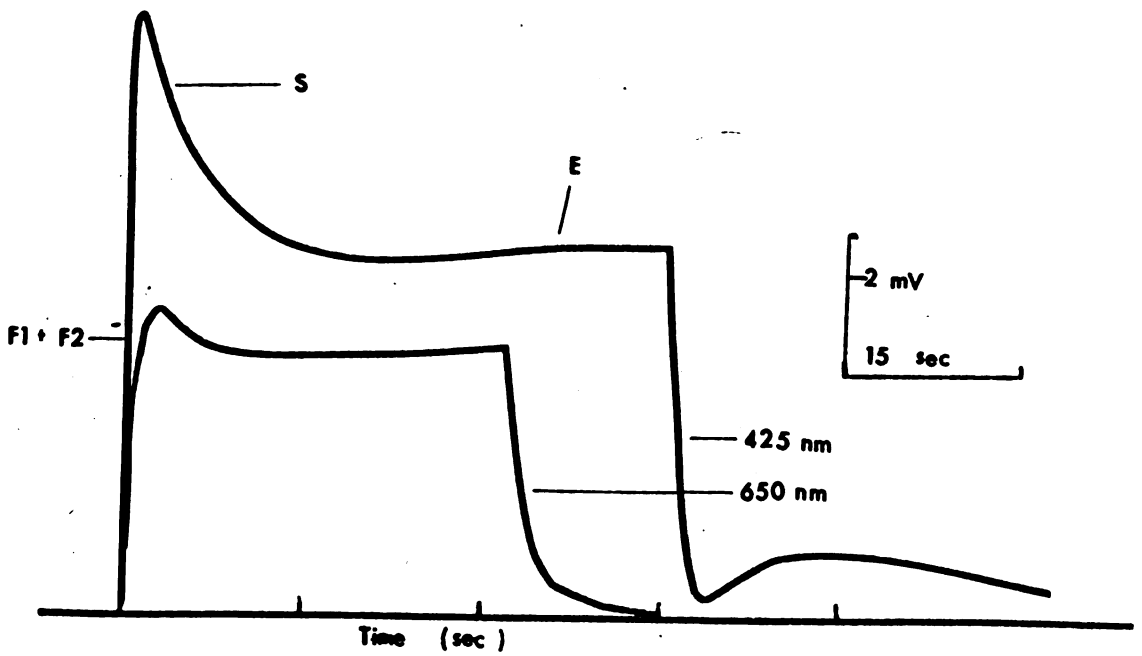
S
E
F1 + F2
2 mV
15 sec
425 nm
650 nm
Time (sec)

direction until the disappearance of components F2 and S caught up and finally decayed to the baseline.

Effect of the Proton Carrier

The effect of DNP (2,4-dinitrophenol), a well-known proton carrier, on the photoemf of the chl-BLM has also been examined. It was observed that by introducing 2.5×10^{-4} M DNP in the outer chamber, membrane resistance decreased to about 60% of the original value. For 5×10^{-4} M DNP, it further decreased to 40%. The photovoltage was completely eliminated after 40 minutes, no matter what the concentration of DNP or on which side of the membrane the DNP was introduced.

Figure 22 shows that under the influence of DNP the slow component, namely S, declined faster as the membrane became older. This result strongly indicates that the charge carrier responsible for the slow component S is the proton.

Figure 21--The dependence of the F1 component of photoemf on the dark transmembrane voltage.

Figure 22--Effect of DNP on wave patterns of photoemf. Membrane was formed in 0.1 N acetic buffer (pH 5) with 2.5×10^{-4} M DNP in the outer chamber and 10^{-3} M $FeCl_3$ in the inner chamber. Wavelength of excitation light was 465 nm.

Curve a--before introducing DNP

Curve b--10 minutes after introducing DNP

Curve c--15 minutes after introducing DNP

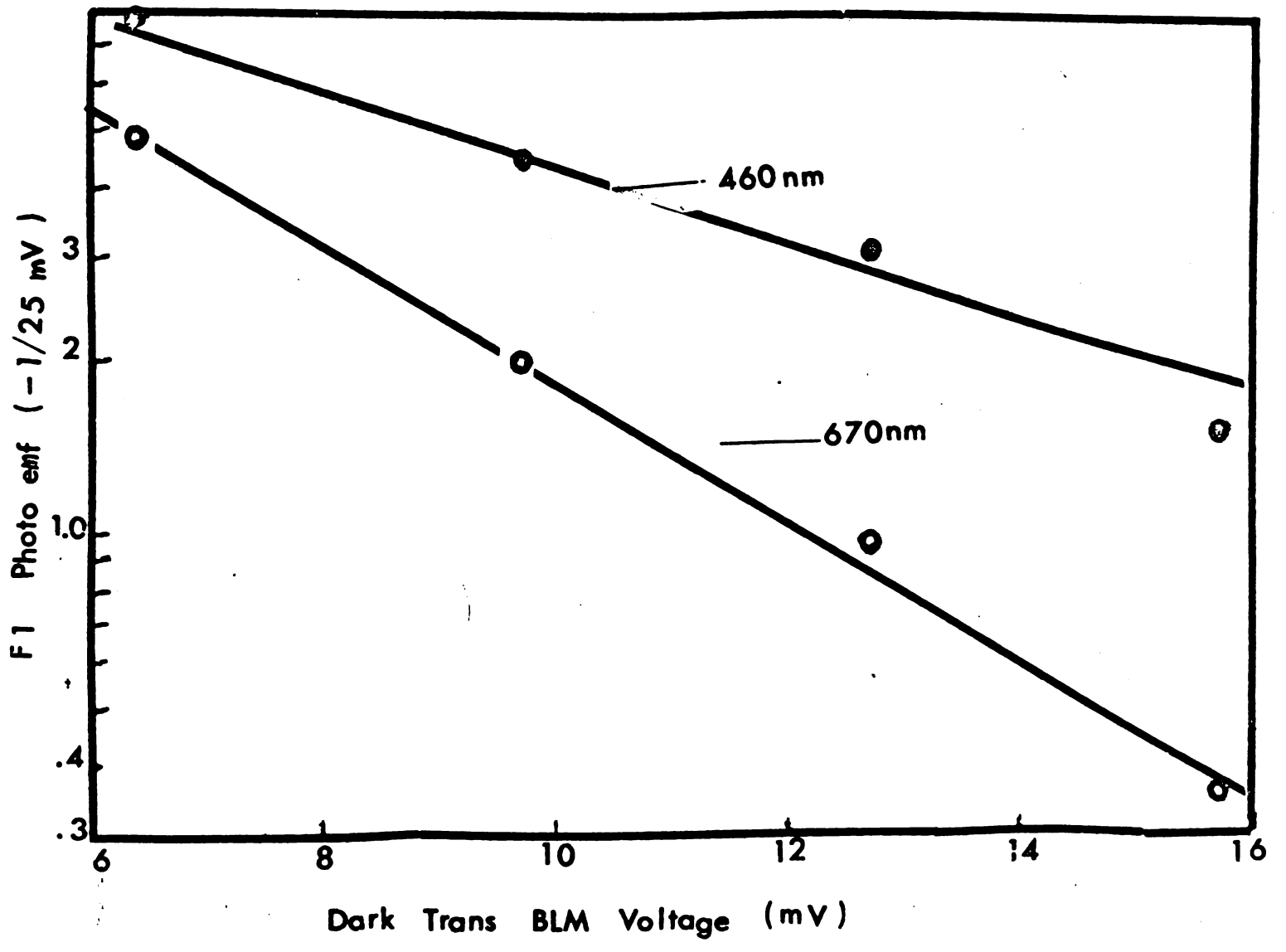
460 nm
670nm
F1 Photo emf (−1/25 mV)
3
2
1.0
.4
.3
6
8
10
12
14
16
Dark Trans BLM Voltage (mV)

A Suggested Mechanism

In order to understand the origin of each component we have to consider all possible factors which may influence the photoresponse. In the present experiment, temperature, pH of the bathing solution, and the intensity of incident light were kept constant; therefore, the total number of pigments excited by a constant incident light per unit time should be a constant.

The following three factors are primary variables responsible for the observed results:

(1) $FeCl_3$ asymmetrically applied in one side of chl-BLM,

(2) transmembrane potential (E_t), and

(3) hole generation leading to water oxidation.

Considering these three factors, the following mechanism is proposed.

The present membrane system is believed to be constructed as a liquid crystal with the polar groups of lipid molecules and chromophores of pigment molecules arranged in more or less regular manner at the surfaces of the membrane, and the hydrocarbon tails of these molecules randomly located in the center of the membrane as a liquid phase (Tien, 1968a).

It is proposed that upon illumination, excitons are first generated by the pigments (primarily chlorophylls) contained in the membrane surfaces. Some excitons will be trapped by the ferric ions immediately and lead to the reduction of ferric ions to ferrous ions. Once formed, these ferrous ions are readily replaced by the ferric ions stored in the inner aqueous phase. Products of this trapping process are the holes left at the inner surface of the membrane. The rest of the

excitons can also be either trapped by some other electron acceptors or donors contaminating the chl-BLM or recombined to give fluorescence or phosphorescence, depending upon whether the exciton is in singlet or triplet state. The diffusion of the holes can be enhanced or retarded by the external electric field, depending upon the direction of the field. Therefore, the accumulation of holes can occur in either surface of the membrane, lead to oxidation of water molecules, and, hence, the generation of protons by these holes. These protons asymmetrically accumulated in one side of the membrane surface can diffuse through the membrane and reduce the established photovoltage. Of course, this last process will be affected by the external electric field, too. The above hypothesis can be summarized as follows:

$$\text{pigment} \xrightarrow{h\nu} \text{pigment}^* \qquad (3)$$

$$\text{pigment}^* \longrightarrow \text{pigment} + \text{exciton} \qquad (4)$$

$$\text{exciton} + Fe^{+3} \longrightarrow \text{hole} + Fe^{+2} \qquad (5)$$

$$\text{electron} + \text{hole} \longrightarrow \text{luminescence} \qquad (6)$$

$$\text{hole} + 1/2\ H_2O \longrightarrow H^+ + 1/4\ O_2 \qquad (7)$$

The overall reaction is:

$$1/2\ H_2O + Fe^{+3} \longrightarrow H^+ + 1/4\ O_2 + Fe^{+2} \qquad (8)$$

Based on this hypothesis, the component F1 is thought to be the accumulation of holes at the outer surface of the membrane as the result of diffusion (see Figure 23). That is why the polarity of F1 is solely dependent on the side of the membrane on which the electron acceptors are present, i.e., on the surface of the membrane from which the holes

Figure 23--Schematic illustration of the basic electronic (hole) and protonic charge transfer processes in photoactive chl-BLM separating two aqueous solutions. $\ominus$ = electron; $\oplus$ = hole; $\ominus\oplus$ = exciton.

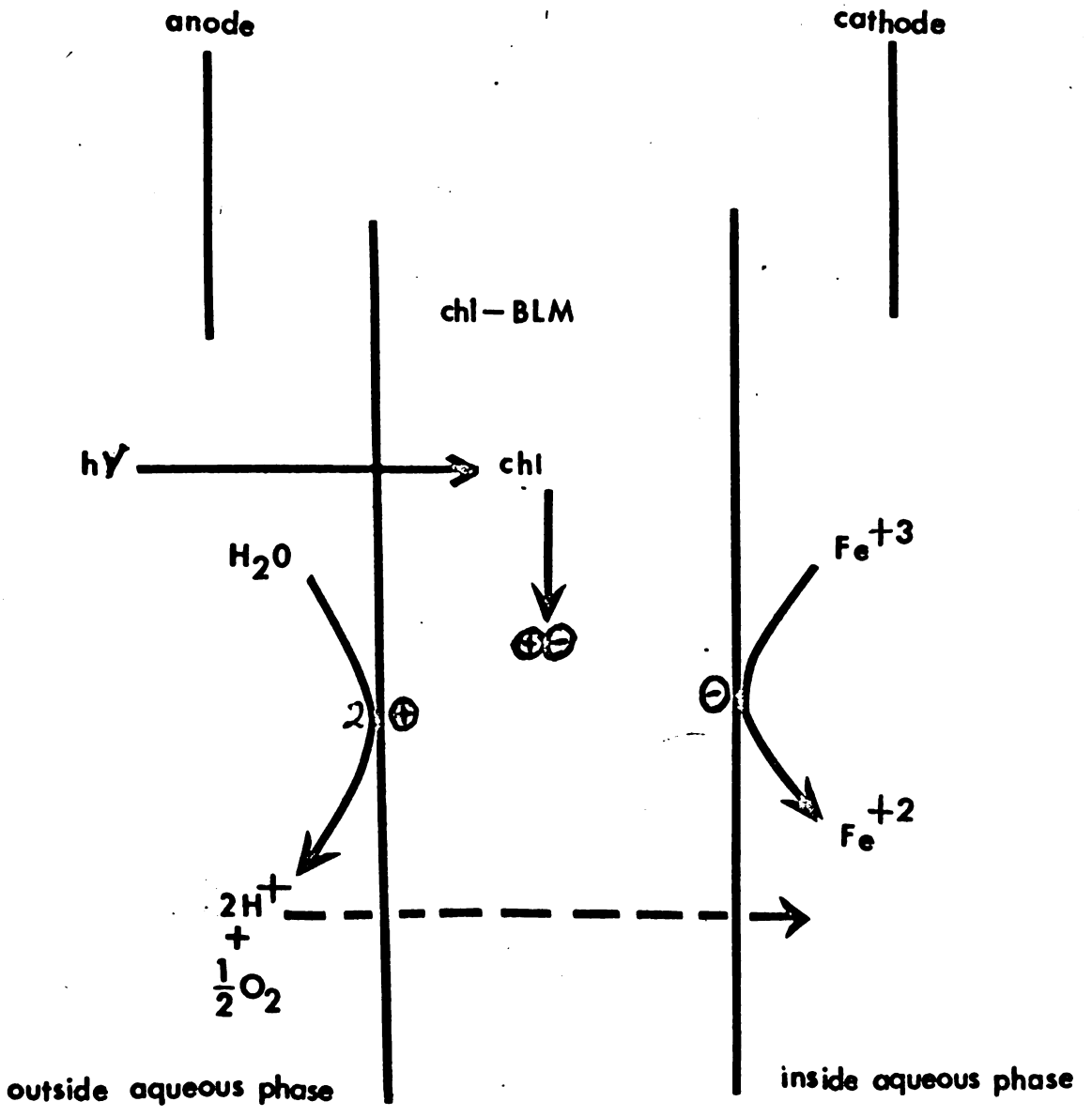
anode
cathode
chl – BLM
hν
chl
H_2O
Fe^{+3}
Fe^{+2}
$2H^+$
+
$\frac{1}{2}O_2$
outside aqueous phase
inside aqueous phase

are diffused. The component F2 is considered to be the separation of excitons into electrons and holes and is thus strongly dependent on the direction and magnitude of the external field. That the F2 component is thought to be relatively slower than F1 is based on the fact that in a clean case (without $FeCl_3$), photovoltage was observed relatively slower. The diffusion of protons through the membrane, as a result of components F1 plus F2 and water oxidation, is identified as the slow component S which tends to decrease the established photovoltage.

If the external field is set such that the positive holes are readily able to drift from the inner to the outer surface of the membrane (negative E_t), the direction of component F2 is the same as F1, and thus the negative photovoltage is greatly enhanced (see Figures 19a and 19b). If the direction of the external field is reversed, component S will tend to decrease or even overwhelm the photovoltage established by F1, provided that the field strength is large enough. The resulting waveform is a small overshoot in the negative direction followed by a large positive component.

As far as the magnitude of the F1 component is concerned, there are two possible explanations:

(1) A positive E_t tends to draw ferric ions away from chl-BLM thus decreasing the total number of ferric ions on the surface of chl-BLM.

(2) A positive (or negative) E_t decreases (or increases) the binding strength of ferric ions and chl-BLM, thus decreasing (or increasing) the efficiency of trapping electrons in the excited state.

The exponential relationship of F1 and E_t favors the second explanation, if we assume the binding strength is directly proportional to the dark transmembrane voltage (E_t) and follows the following equation:

$$E_t = c(E_g - b)/2KT \tag{9}$$

where E_g is the binding strength between Fe^{+3} and chl-BLM, and b and c are positive constants. The exponential relationship of F1 and E_t can be written as (from Figure 21):

$$F1 = \exp(a/m)\ \exp(-E_t/m) \tag{10}$$

where a = 14, b = -0.5 for incident light at 665 nm (Figure 19b); and a = 17.2, m = -0.354 for incident light at 460 nm (Figure 19a).

Then the effect of field strength on the magnitude of the F1 component can be easily explained by the following equation, in terms of binding strength, E_g:

$$F1 = \exp(a/m)\ \exp(cb/2KT)\ \exp(-cE_g/2KT) \tag{11}$$

This equation was obtained by combining Equations 9 and 10.

Because of the involvement of proton diffusion (or drifting) in the suggested mechanism, the observed fact that the photoresponse does not return to the dark baseline at the offset of incident light if the bathing solution is KCl instead of buffer solution can be understood. The effect of DNP on the S component can also be interpreted on the basis of this hypothesis. Since DNP was applied in the outer chamber, protons generated by water oxidation would soon be removed

by this proton carrier and would lead to the faster declination of photovoltage in the S component (see Figure 22).

This suggested mechanism can be used to predict several observations which need further investigation:

(1) Since the photogenerated excitons are either trapped by electron acceptors or recombined to give luminescence, large photovoltage will result in small luminescence, and vice versa.

(2) Oxygen evolution should be observed upon illumination.

(3) Since the generation and diffusion of protons are involved in this proposed mechanism, a reasonably large pH gradient across the membrane will modify the wave pattern of photovoltage to an appreciable extent.

According to this analysis, the F2 component will be missing if the external field is absent. Unfortunately, the data for this specific case is lacking due to experimental difficulty.

Conclusion

The following conclusions can be drawn:

(1) Charge carriers involved in the photoelectric effect of the present system are both electronic (hole) and protonic.

(2) Chl-BLM is not only an energy transducer but also a chemical reaction frame.

(3) This photo-induced H^+ accumulation at one side of the chl-BLM using the highly insulated membrane structure and the movement of H^+ ions occurs only at high pH gradient and/or transmembrane voltage and strongly indicates that the native charged BLM is rather impermeable to the H^+ ion. This water oxidation resulting in H^+ generation and accumulation has been widely observed in photosynthesis study, both in vivo and in vitro. Izawa and Hind (1967) can even directly measure the pH rises asymmetrically in illuminated chloroplast suspension.

This coincidence reminds us of the so-called chemo-osmotic hypothesis suggested by Mitchell (1966). It is thus postulated that the phenomenon of H^+ flux across chl-BLM at high concentration gradient probably supplies the energy required for ATP formation.

CHAPTER VI

ACTION SPECTRUM OF CHL-BLM

Introduction

In this chapter three typical photoelectric action spectra of chl-BLM are discussed. Attention is focused on the peak analysis and the time dependent peak ratio (E) change. Current viewpoints about the action spectrum principle mentioned in the literature review will not be repeated here.

It is generally accepted that the action spectrum for photosynthesis is parallel to the absorption spectrum of the same sample. This kind of spectrum is characterized by a major band around 430 nm and a minor band around 670 nm, caused by the constitutional pigments chl a and the red-peak/blue-peak ratio Y, which is usually less than 1. Nevertheless, recent investigations have reported higher red peaks in leaves of higher plants such as bean and radish (Table 1).

The action spectra of chl-BLM formed with fresh lipid solution exhibited three distinctive spectral characteristics with time after the membranes were formed. Among these three types of action spectra, only the one taken at the final stage, designated as BLM-III, was in agreement with the above statement; i.e., it followed the absorption spectrum of the same BLM-forming solution. Since it has been reported that aging, heat, and radiation treatments of chloroplast preparations result in loss of photosynthetic activity (Kok, 1965), the time dependent spectral change of the chl-BLM becomes very intriguing.

Results

The majority of the photoelectric action spectra reported in this study have been calibrated for constant incident energy, and only these spectra are used for critical discussion.

Shown in Figures 24a and 24b are the three distinctive types of photoelectric action spectra calibrated for constant incident energy and taken from a single BLM at 0.5 hours, 2 hours, and 3.5 hours after the addition of 10^{-3} M $FeCl_3$ in the inner chamber. Their uncalibrated spectra are shown in Figures 24c and 24d. All the experimental conditions in Figures 24a, 24b, 24c, and 24d were the same, except the direction of wavelength scanning. The spectral patterns recorded by scanning from 350 nm to 800 nm (Figures 24b and 24d) were similar, while those scanned from 800 nm to 350 nm (Figures 24a and 24c) show the following three obvious differences:

(1) photovoltage increased with time,

(2) E was time dependent, and

(3) a blue shift of red peak was observed.

These three types designated as BLM-I, BLM-II, and BLM-III, are classified with a parameter, E, which is equal to the ratio of red peak height to the blue peak height of the uncalibrated action spectrum. The peak ratio calculated from the uncalibrated spectra is defined as Y. The ratio Q shown in Table 2 is the peak ratio (red/blue) taken from the spectra calibrated for a constant incident quanta. BLM-I is defined as the action spectrum observed with chl-BLM formed with fresh lipid solution (less than 1 hour old). This kind of spectrum has an E value larger than 1. BLM-II is thought to be a transition state between BLM-I and BLM-III. It was observed that chl-BLM formed

Figures 24a, 24b, 24c, and 24d--Three different types of action spectra of a single chl-BLM. BLM-I, BLM-II, and BLM-III are spectra taken at 0.5 hours, 2 hours, and 3.5 hours, respectively, after the addition of 10^{-3} M $FeCl_3$.

Figure 24a--Scanned from 800 nm to 350 nm, calibrated for constant incident energy.

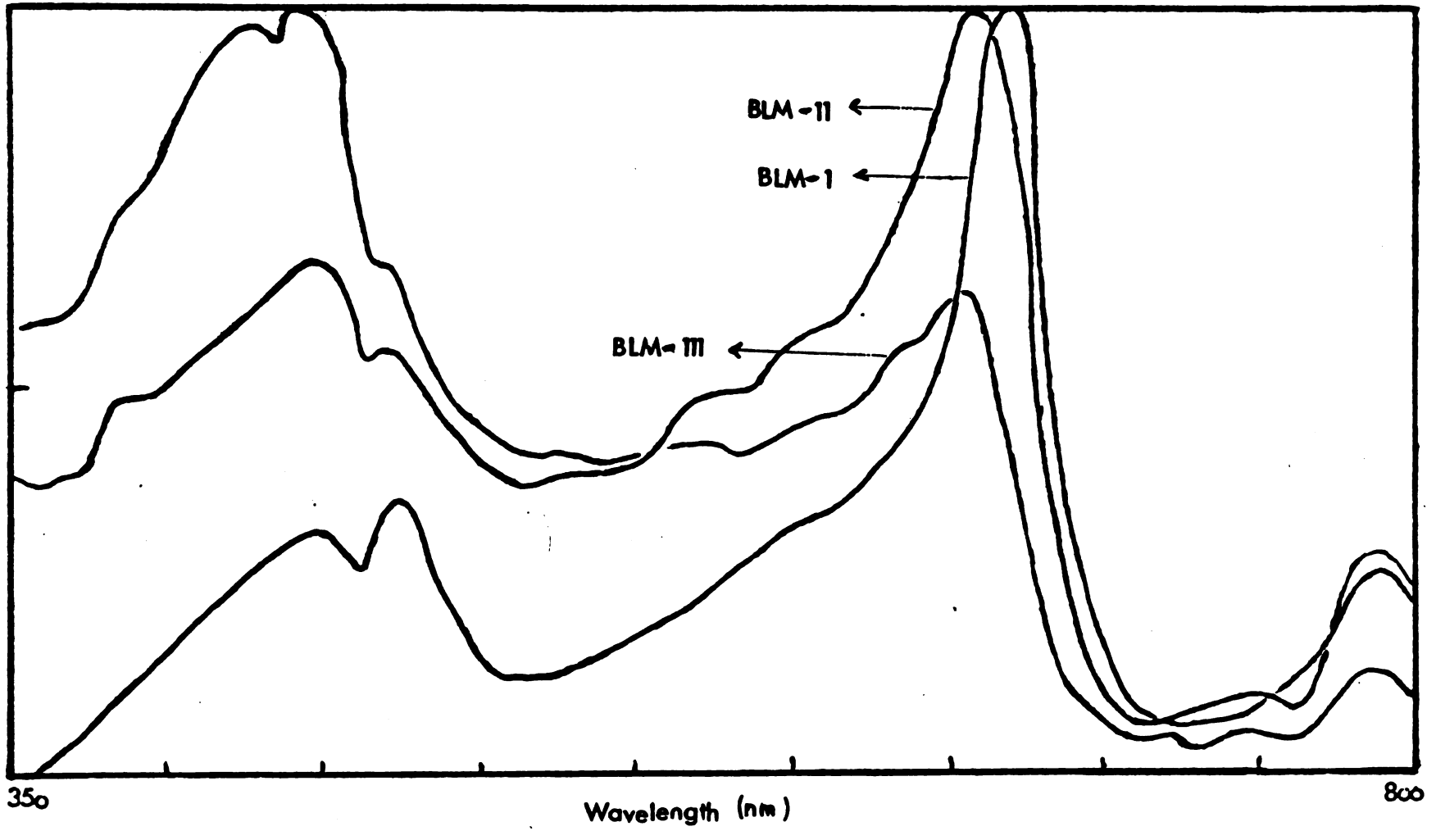
1
BLM-II
BLM-I
BLM-III
350
Wavelength (nm)
800

Figure 24b--Scanned from 350 nm to 800 nm, calibrated for constant incident energy.

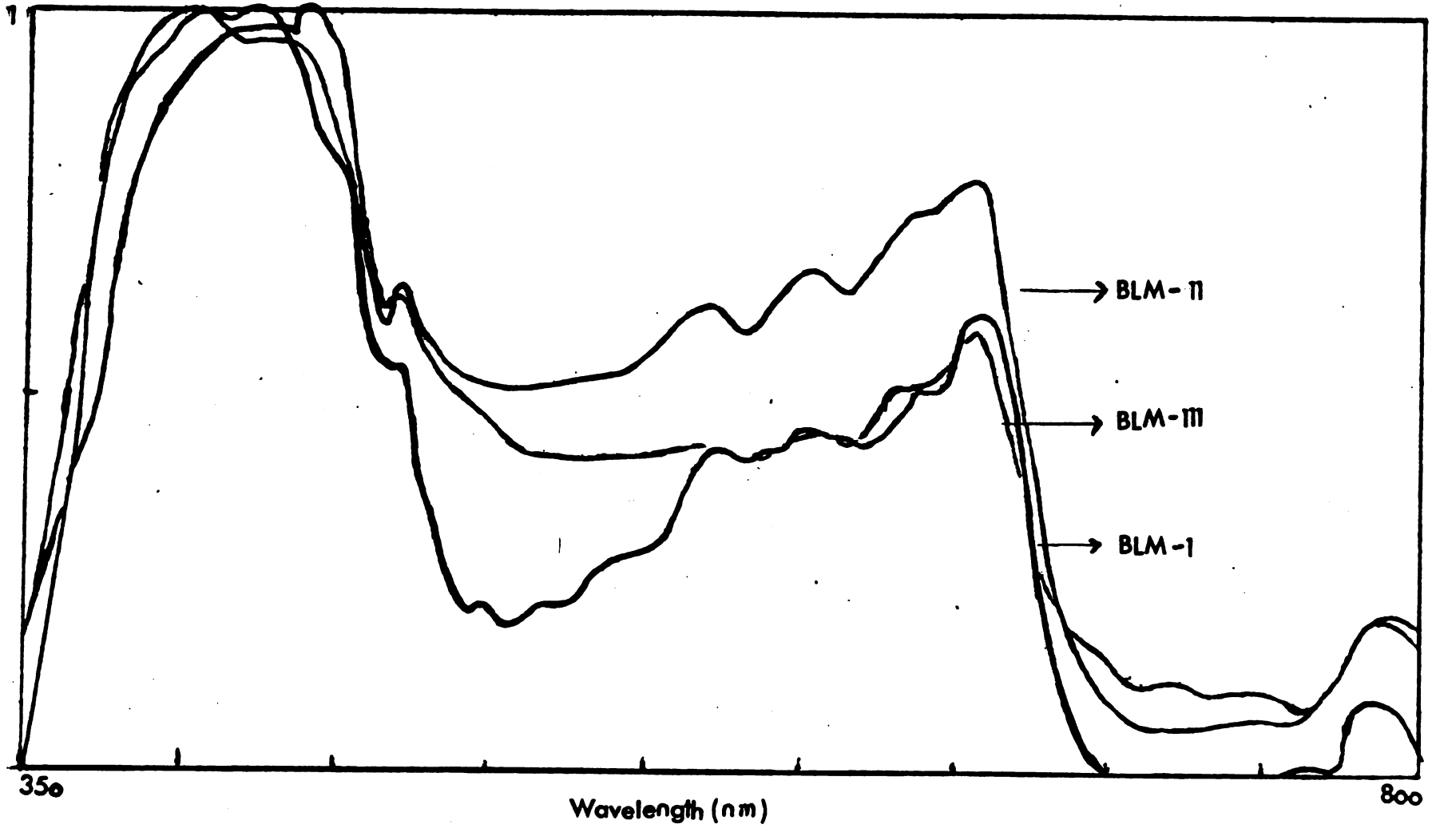
1
BLM-II
BLM-III
BLM-I
350
800
Wavelength (nm)

Figure 24c--Scanned from 800 nm to 350 nm, recorded directly.

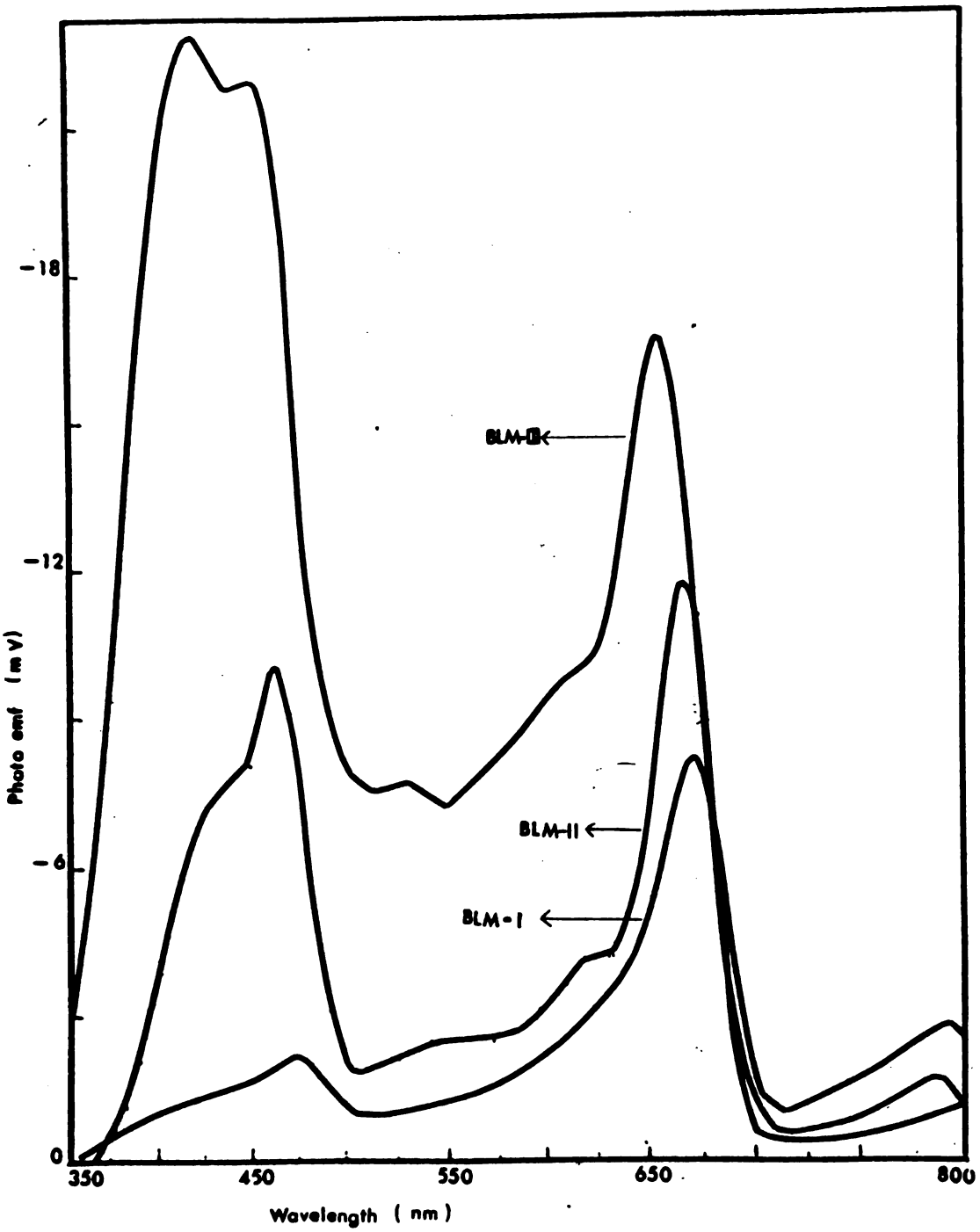
-18
-12
-6
0
Photo emf (mV)
BLM-III
BLM-II
BLM-I
350
450
550
650
800
Wavelength (nm)

Figure 24d--Scanned from 350 nm to 800 nm, recorded directly.

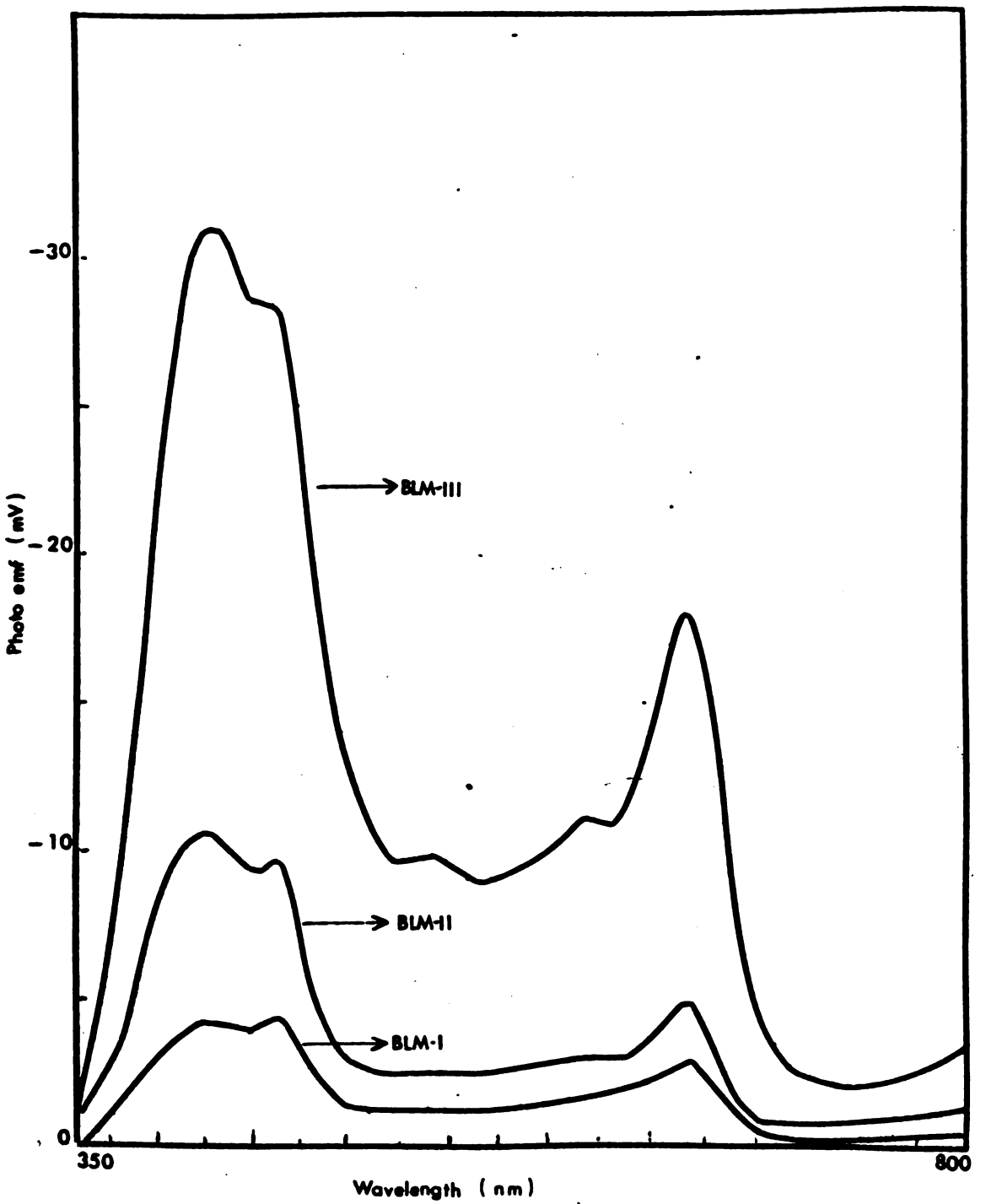
-30
-20
-10
0
Photo emf (mV)
BLM-III
BLM-II
BLM-I
350
800
Wavelength (nm)

with fresh solution or chl-BLM formed with aged lipid solution and has an E value around 1. BLM-III was observed from chl-BLM formed with either fresh or aged lipid solution. This type of spectrum had an E value smaller than 1. The detailed characteristics of the three types of calibrated action spectra are shown in Table 2. It is interesting to note that the red peak position shifted from 670 nm through 660 nm to 655 nm. The peak ratio, Y, decayed with time after the formation of the membrane. It leveled off after 70 minutes and increased slightly after 2 hours (Figure 25). This time dependence of spectrum change was also detected from chl-BLM formed with aged lipid solution (e.g., 61 days in the refrigerator at 4 °C in the dark). It is worth noting that in this case only BLM-III could be observed. The increase of chl-BLM resistance from BLM-I (1×10^5 ohm-cm^2) through BLM-II (5×10^5 ohm-cm^2) to BLM-III (7.5×10^5 ohm-cm^2) was also noticed. The efficiency for energy conversion in BLM-III was higher than that in BLM-I and BLM-II (shown in Figures 24c and 24d). Action spectra were also recorded on chl-BLM before and after illumination for long time periods. In comparison, spectra 1 and 2 in Figure 26 show apparent spectral changes. There were two obvious differences after prolonged illumination:

(1) Photovoltage decreased throughout the whole range of spectrum, and

(2) Peak ratio E decreased from a value larger than 1 to a value smaller than 1.

A certain kind of recovery seemed to exist by letting the membrane rest in the dark after prolonged illumination. Spectra in Figure 26 were all

Table 2--Peak positions and peak ratios of chl-BLM photoelectric action spectra which have been calibrated for constant incident energy.

	RED SIDE (nm)			BLUE SIDE (nm)			dip(s)	peak beyond 700 nm	$E^{(i)}$	$Q^{(ii)}$
	major	minor	shoulder	major	minor	shoulder				
Figure 22a (BLM-I)	670	630, 600		437-445	470		500	725-800	2.86	2.0
Figure 22b (BLM-I)	660	630, 600		437-445	470		500	725-800	0.6	0.37
Figure 22a (BLM-II)	665	600	670	440	470		no	725-800	1.54	0.92
Figure 22b (BLM-II)	655	605	670	430	470		no	725-800	0.77	0.60
Figure 22a (BLM-III)	655	630-635 600-615	670	437-445 425-430	470		430-435	725-800	0.60	0.40
Figure 22a (BLM-III)	655	630-635 600-615	670	437-445 425-430	470		430-435	725-800	0.60	0.40

(i) E = red peak maximum/blue peak maximum. Data were from those action spectra calibrated for constant incident energy.

(ii) Q = maximum of red peak/blue peak. Action spectra used were those calibrated for constant incident quanta.

Figure 25--Relative ratio of red peak and blue peak in chl-BLM action spectra as a function of resting time in dark. Standard experimental conditions.

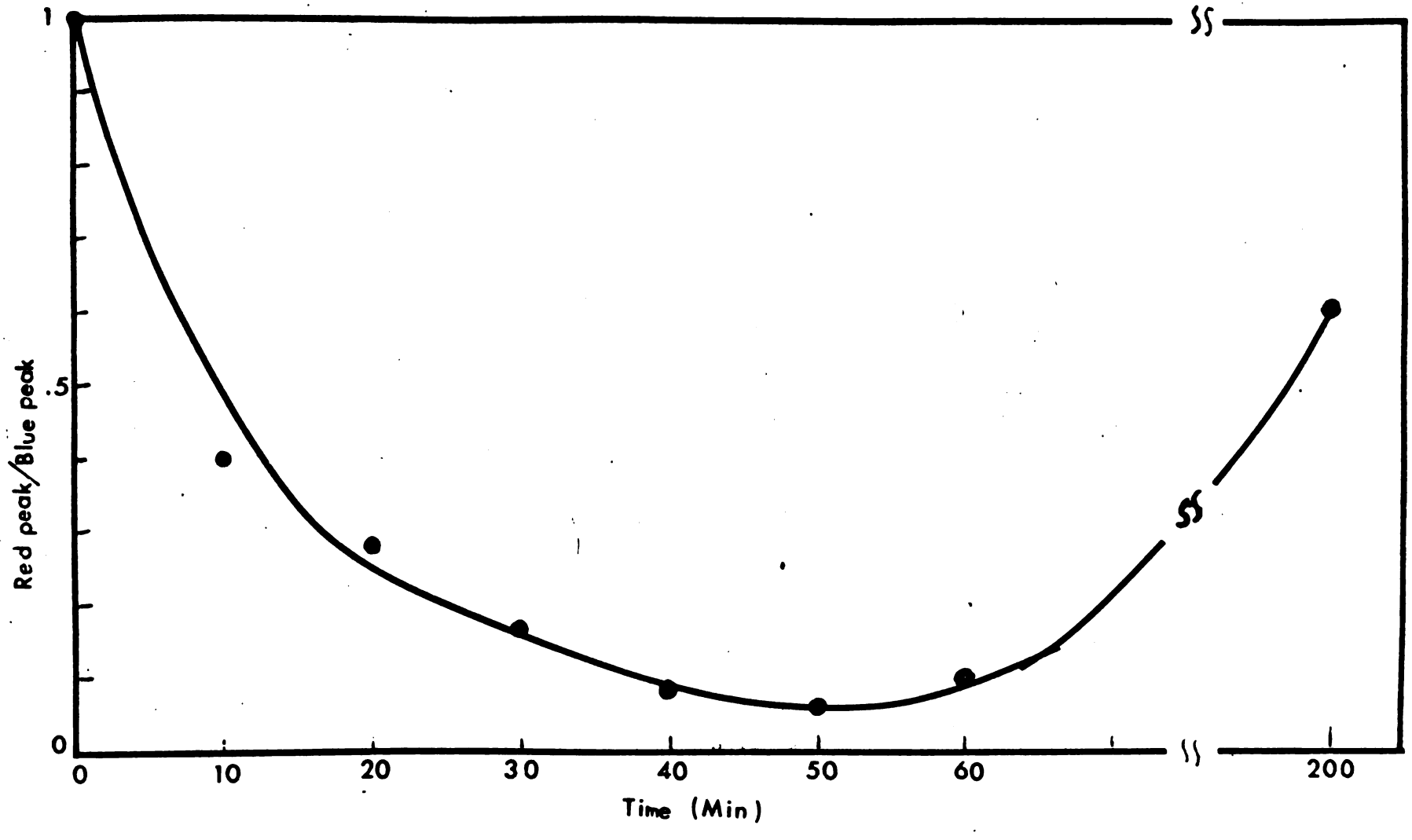
1
.5
0
Red peak/Blue peak
0
10
20
30
40
50
60
200
Time (Min)

Figure 26a--Peak height recovery of chl-BLM by resting in the dark. Calibrated for constant incident energy and normalized.

Curve 1--Action spectrum taken from newly-formed chl-BLM.

Curve 2--Action spectrum taken after 1 hour with alternative illumination at 670 nm and 440 nm.

Curve 3--Action spectrum taken after resting in the dark for 2 hours.

BLM were formed under the standard experimental conditions.

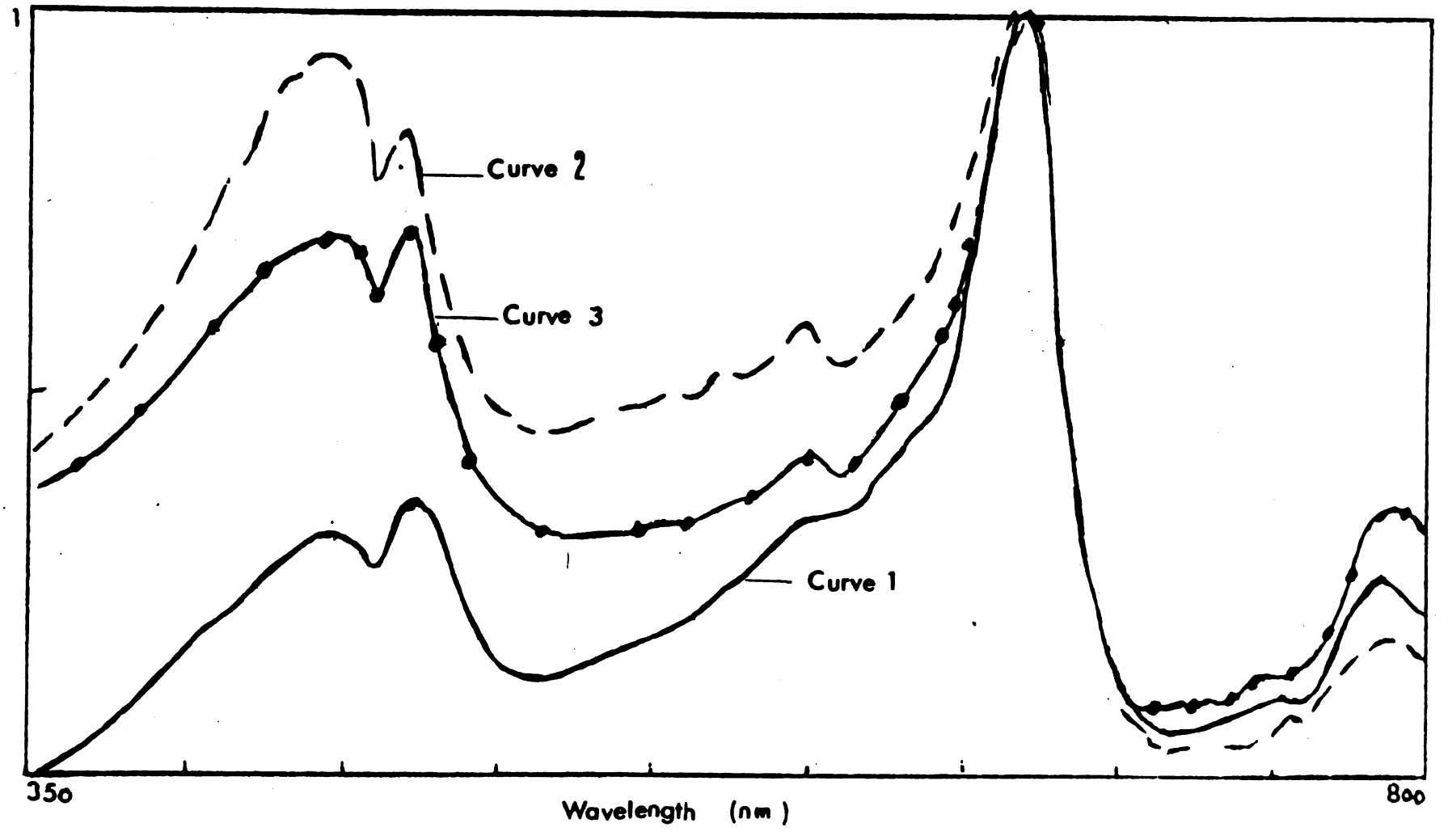
1
Curve 2
Curve 3
Curve 1
350
800
Wavelength (nm)

Figure 26b--Peak height recovery of chl-BLM by resting in the dark. Spectra were taken directly from the recorded. BLM were formed under standard experimental conditions:

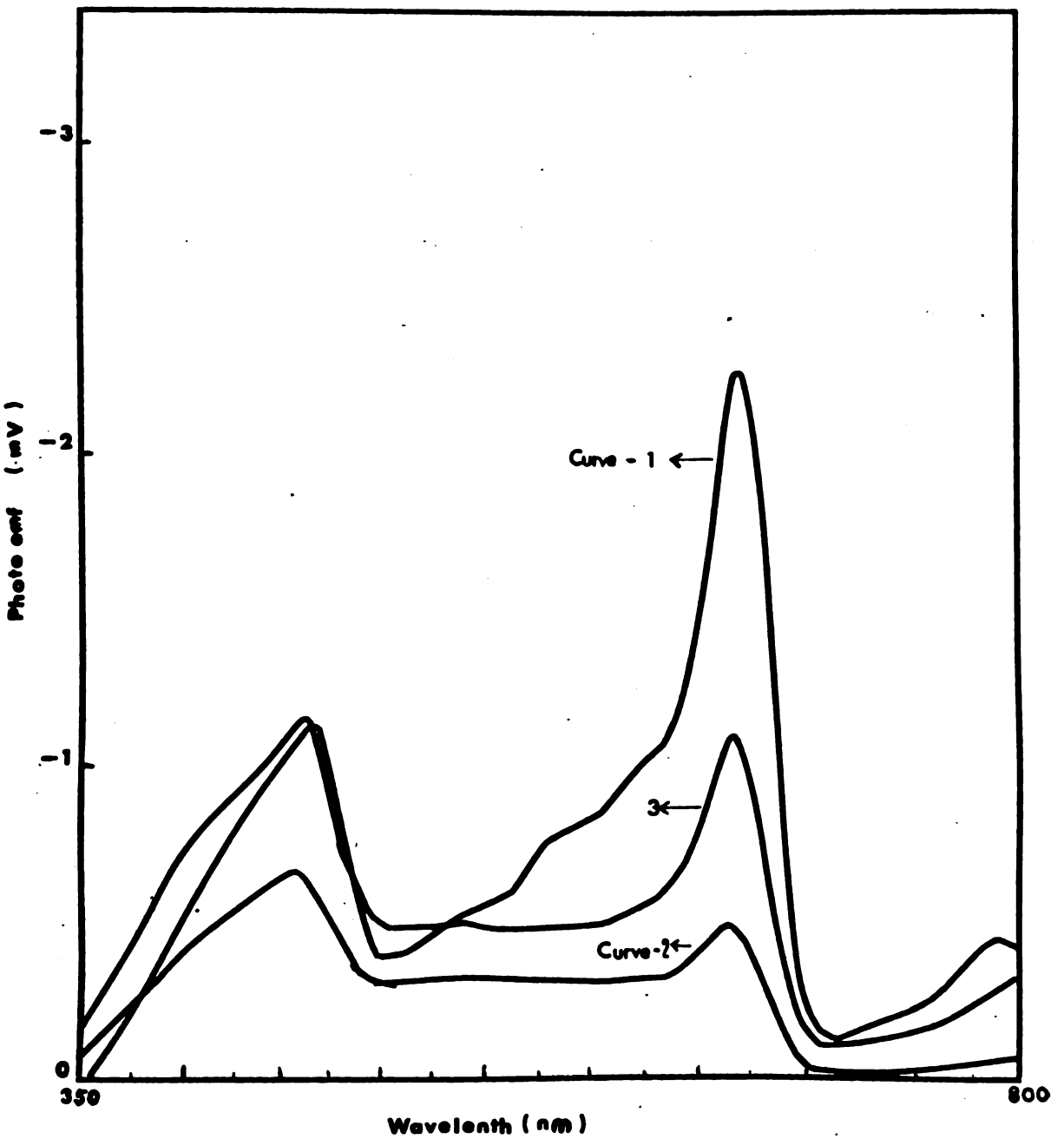
-3
-2
-1
0
Photo emf (mV)
Curve - 1
3
Curve-2
350
800
Wavelenth (nm)

recorded from a single membrane. Spectrum 2 in Figure 26 was taken after one hour of alternative illumination at 670 nm and 440 nm. Appreciable decreases in both absoluted peak heights and the E values were observed as compared with spectrum 1 which was taken from freshly formed membrane. After a spectrum was recorded, the membrane was allowed to rest in the dark for 1.5 hours and then spectrum 3 was taken. The blue peak showed 100% recovery while the red peak showed only about 50%. It should be noted that the Y value of the spectrum scanned from shorter wavelength is always smaller than the one scanned from longer wavelength.

In order to understand the causes of the above observations, absorption spectra of fresh as well as aged membrane-forming solutions and chl-BLMs formed with these solutions were taken (shown in Figures 27a and 27b). Notice that the change in blue peak was observed in absorption spectra taken from aged and fresh BLM-forming solution. It was also surprising that the absorption spectrum of chl-BLM formed with fresh lipid solution showed an unusual difference from others, namely, that the red peak absorbance was higher than the blue one. Another interesting finding was that the red peak maximum in the absorption spectrum of chl-BLM formed with aged solution, shifted from 670 nm to 660 nm as compared with the one formed with fresh solution. This shift seems responsible for the observed blue shift of red peaks in the action spectra mentioned previously. A summary of the absorption spectra is shown in Table 3.

Figure 27a—Absorption spectra of chl-BLM forming solution. Open circles: freshly prepared membrane-forming solution; closed circles: prepared at least six months before taking spectra.

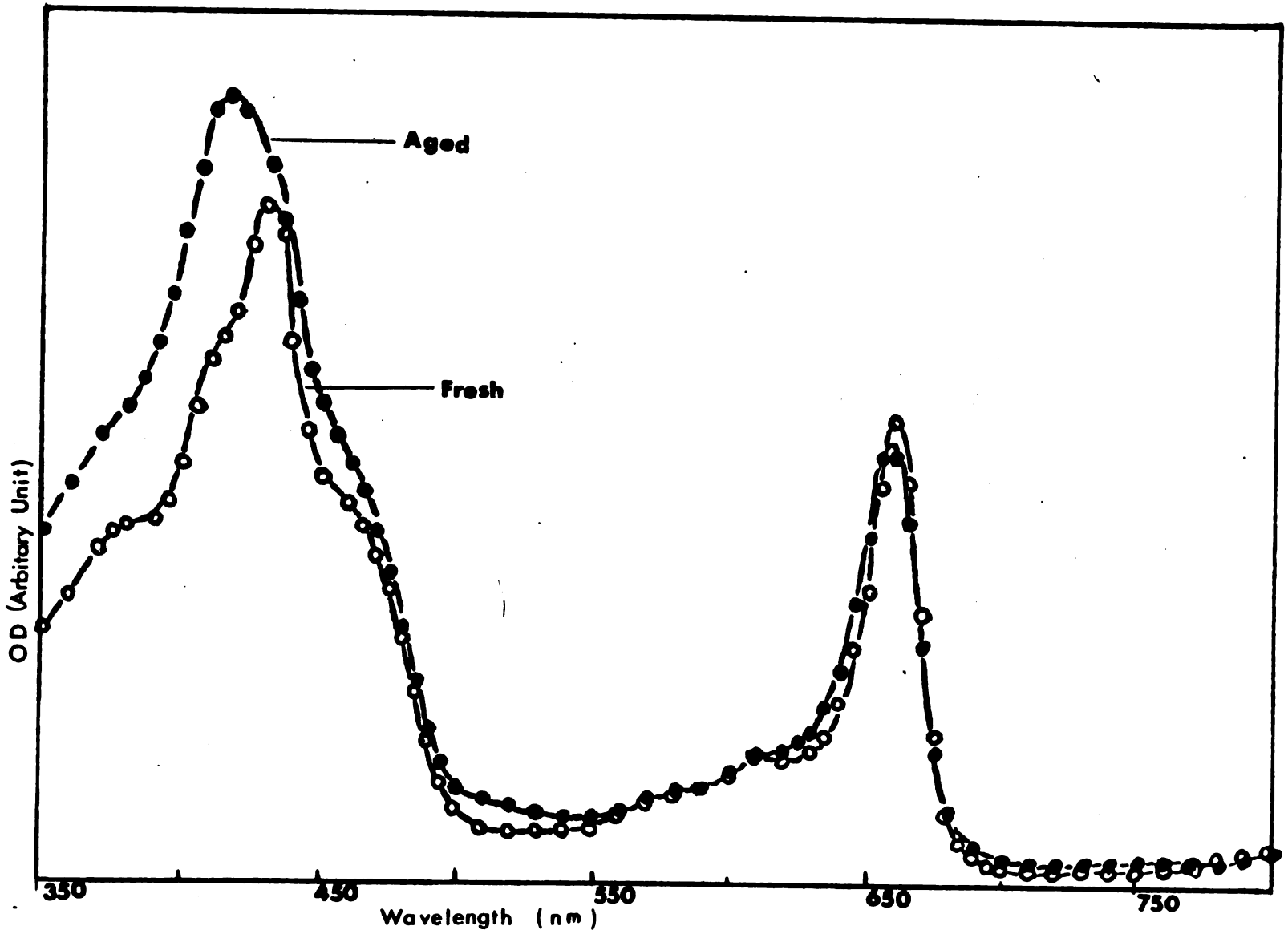
Aged
Fresh
OD (Arbitary Unit)
350
450
550
650
750
Wavelength (nm)

Figure 27b--Absorption spectra of chl-BLM. Open circles: chl-BLM formed with fresh lipid solution; closed circles: chl-BLM formed with aged lipid solution. The aged lipid solution was stored in the refrigerator, at 4°C in the dark.

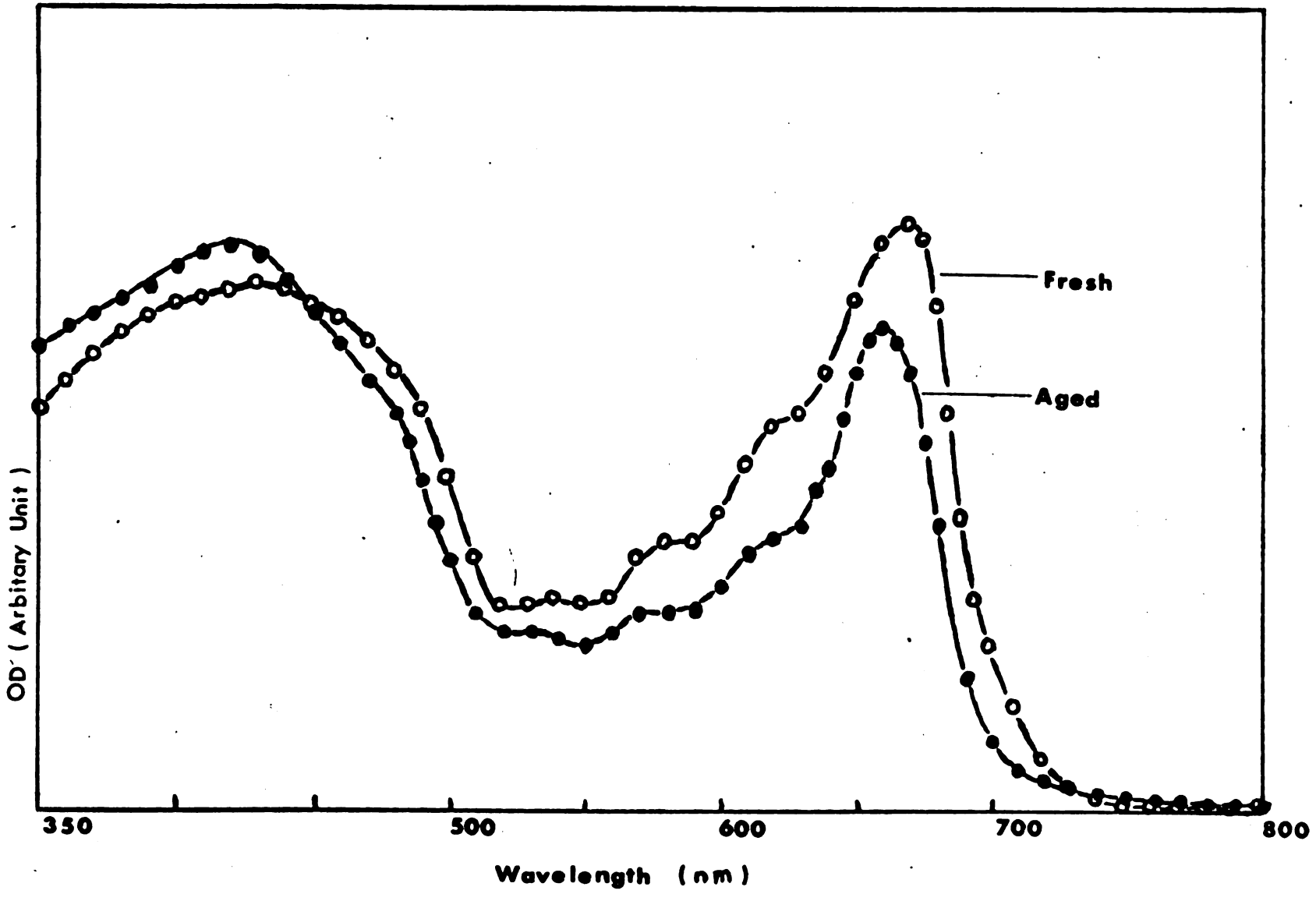
Fresh
Aged
OD' (Arbitary Unit)
350
500
600
700
800
Wavelength (nm)

Table 3--Absorption spectra peak positions and peak ratios

		RED SIDE (nm)			BLUE SIDE (nm)			
		major	shoulder		shoulder	major		Y
1	Figure 27a (fresh)	660	600-612		465-480, 420	435		0.69
2	Figure 27a (aged)	655	600-612		465-480, 435	420		0.55
3	Figure 27b (fresh)	670	612, 570 670					
4	Figure 27b (aged)	660	612, 570					
5	chloroplast pigments in diethyl ether	660				430		
6	chloroplast pigments in living cells	675				440		

Discussion

Since the difference or similarity between the chl-BLM photoelectric action spectrum obtained in the present work and the action spectra for photosynthesis reported in literature is not known, a direct comparison between these two kinds of action spectra seems impractical. However, it is possible to compare the absorption spectra shown in Figure 27a with the absorption spectra of chloroplast pigments in solution. It is also possible to compare the absorption spectra of chl-BLM shown in Figures 27a and 27b to the absorption spectra reported by Rabinowitch and Govindjee (1969).

In the following, information obtained from peak analysis concerning the different features of the action spectrum of chl-BLM and the action spectra for photosynthesis is summarized in Table 3.

It can be seen from Table 3 that the absorption spectra shown in Figure 27a have a blue band around 430 nm and a red band around 660 nm. The absorption spectra of chloroplast pigments in diethyl ether as determined by Rabinowitch and Govindjee (1969) confirmed the two peaks at 430 nm and 660 nm, respectively.

The red absorption band at 670 nm (see Figure 27b--fresh) probably corresponds to the red absorption at 675 nm reported by Rabinowitch and Govindjee (1969) after working on the absorption spectrum of chloroplast pigments in living cells.

It has been reported and widely accepted that the red absorption band of chlorophyll a in solution is much narrower than in living cells (Rabinowitch and Govindjee, 1969). Recently, careful observations suggested that the broad nature of the red band in vivo is due

to the presence of more than one component, namely chl a 670 nm, chl a 680 nm, and chl b 650 nm (Rabinowitch and Govindjee, 1969). Similar observations can be found in the present work. Looking at the red absorption bands of chloroplast pigments in chl-BLM (Figure 27b), one notes its greater width compared to the corresponding bands in solution (Figure 27a). This probably indicates the following:

(i) Membrane structure might be crucial in order to detect more than one form of chl a,

(ii) In a chl-BLM newly formed with fresh lipid solution, two forms of chl a may exist, and

(iii) Since the red absorption maximum is strong at 670 nm in chl-BLM prepared from fresh solution (Figure 27b--fresh), but in aged solution showed only a small shoulder (Figure 27b--aged), it is suggested that chl a, which has an absorption band at the longer wavelength side in the absorption bands of the two chl a forms, might be unstable.

Peak Identification

Among the three types of action spectra, BLM-I, -II, and -III, only the spectral pattern of BLM-III did not show any apparent change in magnitude and peak position when the direction of scanning was reversed. Therefore, in the analysis of action spectrum peak positions, attention will be paid mostly to the BLM-III. Differences between the three types of action spectrum will be compared and discussed after the peak identification.

It can be seen from Figures 24, 27a, and 27b that BLM-IIIs follow approximately the analysis of the spectrum in terms of absorption peaks of the same samples (both in the form of BLM and in solution), except for one or more additional regions with distinct maxima in the far-red region of the action spectra.

Peak Beyond 700 nm

First of all, a remarkable difference was found in the chl-BLM action spectra in the far-red region. One to three minor but distinct maxima were observed in the action spectrum above 700 nm (i.e., 720 nm, 745 nm, and 790 nm), whereas the absorption spectra (Figures 27a and 27b) showed no band in the same region. This result indicates the presence of a small amount of pigment (or pigments) which absorbed the far-red light both in chl-BLM and in its forming solution. The absence of this (or these) peaks(s) in the absorption spectra was probably due to the fact that the light energy absorbed by this pigment (or pigments) was much more efficiently utilized for photoelectric energy conversion than was the energy absorbed by chlorophylls and carotenoids. The presence of these peaks in all three types of action spectra (BLM-I, -II, and -III) indicates that the pigment (or pigments) responsible for these peaks is quite stable.

Actually, similar arguments for the existence of this pigment (or pigments) have appeared in the literature in various systems related to photosynthesis.

As early as 1952, Duysens had postulated the presence of very low concentration of a pigment which had an absorption band in the region of the fluorescence band of chlorophyll a. In 1953-1954, Jacobs et al,

working with the microcrystals or monolayers of chl a, observed an absorption band around 735 nm. Six years later, Rabinowitch (1960) reported the inhibition of photosynthesis by additional far-red illumination (maximum at 745 nm). In 1961, Govindjee, Cederstand, and Rabinowitch identified an absorption around the 740 nm to 760 nm region. Izawa et al (1963), after measuring the light-induced shrinkage of chloroplast suspension identified an absorption peak around the 720 to 740 nm region. A similar conclusion was also made by Lundegardh (1966) after studying a wide range of incident wavelengths on higher plant leaves; and by Ichimura (1960) on the photoconductivity of chloroplasts.

Peak in Red Region (665-660 nm)
and in Blue Region (425-430 nm)

The two peaks which are known to have two absorption peaks at 660 nm and 430 nm (Zscheile and Comar, 1941), are probably due to the absorption of chl a. The ratios of red peak (660 nm)/blue peak (430 nm) for the absorption spectra shown in Figure 27a-aged, and the action spectra, BLM-III (Figures 24a and 24b), were approximately equal, 0.61 and 0.623, respectively. This indicates that light absorbed by these bands (430 nm and 660 nm) had the same efficiency on the photoelectric energy conversion.

Shoulder between 670 nm and 675 nm
and Peak in the Blue Region--
437 nm to 445 nm

The shoulder at the long wavelength side of the red band and the maximum at 437-445 nm was probably due to one of the two forms of chl a

which was reported to have two red bands at 673 nm and 683 nm (Kranovsky and Kosobutskaya, cited by Rabinowitch, 1951, and Butler, 1965). A blue band at the 437 nm to 438 nm region was also reported (French, 1959). These peak positions in BLM action spectra agree with those of Soret and the red bands of chl a in the action spectra for CO_2 fixation of bean plants as determined by Balegh and Biddulph (1970; 437 nm and 670 nm).

The small maximum or shoulder at 605 nm, 570 nm, and 405 nm might have been due to the absorption of chl a with a secondary absorption peak reported at 615 nm, 575 nm, and 410 nm, respectively (Zscheile and Comar, 1941).

The shoulder between 630 nm and 640 nm is quite difficult to analyze; it might have been due to the chl a secondary absorption band or a chl a doublet (French, 1968). Another possibility is chl b having an absorbing maximum at 640 nm in solution (Zscheile and Comar, 1941). If indeed chl b should be responsible for the shoulder between 630 nm and 640 nm, the shoulder between 450 nm and 455 nm may correspond to its blue absorption band. Since carotenoids absorb light significantly from 530 nm downward (Emerson and Lewis, 1943), the shoulder between 450 nm and 455 nm could also be due to the absorption of carotenoids.

The minor peak at 470 nm is probably due to the absorption of chl b (Sauer and Calvin, 1962).

Comparison of Three Types of chl-BLM Action Spectra

The three remarkable differences among BLM-I, -II, and -III mentioned in the results will be discussed here.

The time-dependent blue shift of the red maximum from BLM-I (670 nm) through BLM-II (660 nm) to BLM-III (655 nm) and the relatively narrow band width in the red region of BLM-I indicates:

(1) the existence of two forms of chl a in chl-BLM, and

(2) only chl a (670 nm to 675 nm, 437 nm to 455 nm) and probably carotenoids or chl b (470 nm) could be detected in the early period (for newly-formed chl-BLM from fresh lipid solution).

The reason why an E value larger than the one observed in BLM-I (scanning from 800 nm to 350 nm but not in reverse scanning or other cases) might be explained by either one of the following assumptions:

(1) In the early period, the light energy absorbed by chl a in the red region (670 nm) was much more effectively utilized in the generation of photoelectric voltage than in the blue (437 nm), and

(2) This pigment (670 nm and 437 nm) was unstable and could be deactivated or change its form (due to, say, certain chemical reactions) both in light and in dark.

That photovoltage increased with time can be easily explained in terms of dark resistance. It was found that membrane resistance increased 7.5 times as the action spectra changed from BLM-I to BLM-III. The most probable reason why the membrane resistance was increased is that the membrane constitutional substances had changed. Perhaps certain pigments, which undergo certain kinds of chemical reactions, either in the dark and/or in the light, can alter the chl-BLM conformation and increases the resistivity of the membrane. It is also possible that the

chl-BLM may have lost solvent, which can also change the pigment environment. In regard to the blue shift in the red region, similar observations were reported by Litvin and Ho (1967). They found that:

(i) the maximum of high plant leaves (Elodea) action spectrum for O_2 evolution was shifted with time from 680 nm to 670 nm,

(ii) an increase of light intensity resulted in a shift of maxima in action spectrum from 680 nm to 650 nm, and

(iii) in early periods of photosynthesis no chl b (650 nm) was detected in action spectra, whereas an appreciable amount of chl a was found between 685 nm and 690 nm.

In order to interpret the results presented in this chapter, the following hypothesis is advanced.

We can specify the changeable substance which may have caused the increase of chl-BLM resistance as chl a 670 nm. This pigment is thought to have two different forms, designated as "A" and "B". In freshly prepared membrane-forming solution, A form is predominant. It is believed that A form undergoes a transformation (or bleaching) to B form both in the dark or catalized by light.

$$\text{A (670 nm)} \xrightarrow[\text{dark}]{\text{dark or light}} \text{B (probably chl a 660 nm or a deactivated chl a 670 nm)}$$

This may be a reason why the action spectrum of a BLM formed with fresh solution when scanned from long wavelength to short wavelength, will gradually shift the maximum of the red peak from 670 nm to 660 nm (Figure 24a). However, if the spectrum was scanned from short wavelength

to long wavelength, the pigment would quickly be transformed (or bleached) from A form to B form by the short wavelength light before the scan reached the red band. As a result, no apparent blue shift was observed in this case (Figure 24b). Since the transformation (or chemical reaction) could proceed in the bulk phase, too, in the aged membrane-forming solution, A form of the pigment was not detectable. Consequently, no BLM-I type spectrum was observed in the membrane formed with aged solution. The evidence supporting this hypothesis also comes from the absorption spectra of chl-BLM (Figures 27a and 27b). Note that the spectra formed with fresh solution had a maximum absorption band at 670 nm in the red region, while the other formed with aged solution had an absorption maximum at 660 nm. In the dark, this transformation (or bleaching of chemical reaction) could be reversed slowly. Prolonged illumination could deactivate (or bleach) all the pigments contained in the chl-BLM, and, as a consequence, a decrease in efficiency of energy conversion mediated by BLM would take place. The recovery by resting in the dark can be similarly explained (Figure 26). Further, this may explain the fact that the E value of the spectrum scanned from shorter wavelength is always smaller than the one scanned from longer wavelength.

Finally, it has been reported that chlorophyll molecules tend to spontaneously lose their Mg atoms, which only absorb light in the blue region (425 nm). This would appear to give a good interpretation to the observed decay of the E value (Table 2). Alternatively, the last possible reason might be due to the intrinsic properties of chl a and b (the Y value of chl a is always larger than the Y value of chl b,

Table 3). In order for this to be true, the assumption must be made that in early periods only an appreciable amount of chl a can be detected.

Conclusions

The following conclusions can be drawn:

(1) Pigment(s) absorption of far-red light (beyond 700 nm) is believed to exist.

(2) The decrease of photosynthetic activity in chloroplast preparation by aging, heating, digitonin (detergent), or radiation (Kok, 1965), was probably due to the disappearance of a pigment (probably chl a) which had an absorption maximum at the longer wavelength side of the red band. This pigment (chl a 670 nm in the present experiment) was either structurally or environmentally dependent or both, because only in that BLM which was immersed in a polar solution (e.g., 0.1 M acetic buffer, pH 5), was it observed.

CHAPTER VII

SUMMARY

In the present work the photoelectric effect of chl-BLM formed with extract of spinach leaves was studied. The dark current voltage curve shows nonlinear behavior, especially when the pH of the bathing solution is higher than 4. The photoelectric action spectrum of chl-BLM showed a striking resemblance to the absorption spectrum of the same sample and indicated that chloroplast pigments contained in the membrane were the primary light absorbers and were functioning at approximately the same efficiencies. Asymmetrical addition of $FeCl_3$ on the membrane system enormously enhanced the photovoltage, probably via the trapping of electrons by ferric ions. Pigments which had an absorption maximum at 640 nm in the red region and an absorption maximum in the blue region (perhaps chl b) showed greater ability to transfer electrons in the excited state to this electron acceptor than other pigments do (like chl a, carotenoids). Electron uncouplers (or Hill reaction inhibitors) suppressed photoresponse of chl-BLM effectively. The optimal bathing solution pH for the present experiment was 5 which gave maximum photovoltage and stable chl-BLM. The membrane resistance was closely related to the photovoltage. Membranes of large resistance usually gave large photovoltage. Very little or no photovoltage could be detected if the resistance was below 1×10^4 ohm-cm^2.

The membrane was considered to be a liquid crystalline structure which generated excitons upon illumination. Charge separation was influenced by Fe^{+3} via trapping of electrons or by some other unidentified impurities contaminating the chl-BLM. Photolysis of water was postulated to take place on the surface of the chl-BLM. Charge carriers involved in the photoelectric effect of the chl-BLM system were both electronic (hole) and protonic. Therefore, the chl-BLM functions not only as an energy transducer but also serves as a substrate for chemical reactions.

Further analysis of the action and absorption spectra of chl-BLM led to the qualitative identification of pigment molecules responsible for the observed peaks. Three types of action spectra at different ages of the membrane were found to correspond with three different states of the membrane. The extra peaks in the far-red region of the action spectra indicated the existence of a pigment-absorbing far-red light (higher than 700 nm). The maximum red band showed a time dependent blue shift, namely from 670 nm to 660 nm and then to 655 nm.

BIBLIOGRAPHY

Alamuti, N. and Lauger, P. (1970), Biochim. Biophys. Acta 211, 362.

Balegh, S. E. and Biddulph, O. (1970), Plant Physiol. 46, 1.

Bangham, A. D. (1968), Prog. Biophys. Molec. Biol. 18, 29.

Barer, R. (1955), Science 121, 709.

Bassham, J. A. and Calvin, M. (1957), "The Path of Carbon in Photosynthesis".

Black. C. C., Turner, J. F., Gibbs, M., Krogman, D. W., and Gordon, S. A. (1962), J. Biol. Chem. 237, 580.

Boardman, N. K. (1968), Advances in Enzymology 30, 1.

Bulley, N. R., Nelson, C. D., and Tregunna, E. B. (1969), Plant Physiol. 44, 678.

Butler, W. L., Norris, K. H., Siegelman, H. W., and Hendrids, S. B. (1959), Proc. Natl. Acad. Sci. U. S. 45, 1703.

Castleden, J. A. (1969), J. Pharm. Sci. 58, 149.

Cherry, R. J., Hsu, K., and Chapman, D. (1971), Biochem. Biophys. Res. Comm. 43, 351.

Davson, H. and Danielli, J. F. (1935), J. Cell Comp. Physiol. 5, 495.

Doring, G., Stiehl, H. T., and Witt, H. T. (1967), cited by Rabinowitch and Bovindjee in "Photosynthesis" (1969), John Wiley & Sons, Inc., 192 and 216.

Doring, G., Bailey, J., Krentz, W., and Witt, H. T. (1968), cited by Rabinowitch and Govindjee in "Photosynthesis" (1969), John Wiley & Sons, Inc., 192 and 216.

Duysens, L. N. M. (1952), Ph. D. Thesis, Utrecht.

Duysens, L. N. M., Amesz, J., and Kamp, B. M. (1961), Nature 190, 510.

Eley, D. D. (1948), Nature 162, 819.

Emerson, R. and Lewis, C., (1943), Am. J. Botany 30, 165.

Forster, T. (1959), Discussions Faraday Soc. 27, 7.

French, C. S. (1959), "The Chlorophylls in vivo and in vitro", in "Encyclopedia of Plant Physiology" 5, W. Rubland, Ed., P. 232.

French, C. S. (1968), "The Absorption Spectra of chl a in Algae", Carnegie Inst. Wash. Year B 66, 177.

Goldup, A., Ohki, S., and Danielli, J. F. (1970), Recent Progress in Surface Science 3, 193.

Goodwin, T. W. (1965), Biochem. of Chloroplasts 1, Academic Press, London and New York.

Gorter, E. and Grendel, F. (1925), J. Med. 41, 439.

Govindjee, Cederstand, C., and Rabinowitch, E. (1961), Science 134, 391.

Govindjee and Bazzaz, M. (1967), Photochem. Photobiol. 6, 885.

Govindjee, Rabinowitch, E., and Govindjee (1968), Biochim. Biophys. Acta 162, 539.

Halldal, P. (1969), Photochem. Photobiol. 10, 23.

Hans, E. (1968), Physiol. Plant 21, 602.

Haxo, F. T. and Blinks, L. R. (1950), J. Gen. Physiol. 33, 389.

Hesketh, T. R. (1969), Nature 224, 1026.

Horio, R. and San Pietro, A. (1964), Proc. Natl. Acad. Sci. U. S. 51, 1226.

Ichimura, S. (1960), Biophys. J. 1, 99.

Izawa, S., Itoh, M., and Shibata, K. (1963), Biochim. Biophys. Acta 75, 349.

Izawa, W. and Good, N. E. (1965), Biochim. Biophys. Acta 102, 20.

Izawa, S. and Hind, G. (1967), Biochim. Biophys. Acta 143, 377.

Jacobs, E. E., Vatter, A. E., and Holt, A. S. (1953), J. Chem. Phys. 21, 2246.

Jacobs, E. E., Holt, A. S., and Rabinowitch, E. (1954), J. Chem. Phys. 22, 142.

Jagendorf, A. T., Hendricks, S. B., Avron, M., and Evans, M. B. (1958), Plant Physiol. 33, 72.

Katz, E. (1949), "Photosynthesis in Plants", Iowa State College Press, Ames, Iowa, p. 287.

Kobamoto, N. and Tien, H. T. (1969), Nature 224, 1107.

Kobamoto, N. (1970), Ph. D. Thesis, Michigan State University, East Lansing, Michigan.

Kobamoto, N. and Tien, H. T. (1971), Biochim. Biophys. Acta 241 129.

Kok, B. (1956), Biochim. Biophys. Acta 22, 399.

Kok, B. and Hoch, G. (1961), "Light and Life", McElroy, W. D., and Glass, B., Eds., Johns Hopkins Press, Baltimore, Maryland, p. 397.

Kok, B. (1965), "Plant Biochemistry" by Geza Doby, translated from the Hungarian by I. Finaly, revised by Scripta Technica, Inc., London and New York, p. 903.

Kok, B. and Cheniae, G. M. (1966), in Current Topics in Biochem. 1, Dorker and Ratterdam, Eds., p. 383.

Litvin, F. F. and I-Tan' Ho (1967), Fizol. Rust. 14, (2)219.

Ludlow, C. J. and Park, R. B. (1969), Plant Physiol. 44, 540.

Lundegardh, H. (1966), Physiol. Plant 19, 754 and 541.

Mitchell, P. (1966), Biol. Rev. 41, 445.

Moss, R. A. and Loomis, E. E. (1952), Plant Physiol. 27, 370.

Mueller, P., Rudin, D. O., Tien, H. T., and Wescott, W. C. (1962a), Nature 194, 979.

Mueller, P., Rudin, D. O., Tien, H. T., and Wescott, W. C. (1962b), Circulation 26, 1167.

Mueller, A., Rumberg, B., and Witt, H. T. (1963), Proc. Roy. Soc. (London) B. 157, 131.

Mueller, A., Fork, D. C., and Witt, H. T. (1963), Z. Naturforsch 18b, 142.

Mueller, P., Rudin, D. O., Tien, H. T., and Wescott, W. C. (1964), Recent Progr. Surface Science 1, 379.

Mueller, P. and Rudin, D. O. (1968), Nature 217, 713.

Mueller, P. and Rudin, D. O. (1969), "Translocators in BLM, Their Role in Dissipative and Conservative Bioenergy Transductions in Current Topics in Bioenergetics" 3, Sanadi, D. Ras., Ed., Acad. Press.

Muhlethaler, K. (1966), "Biochemistry of Chloroplasts", Goodwin, T. W., Ed., Acad. Press, p. 60.

Myers, J. and French, C. S. (1960), J. Gen. Physiol. 43, 732.

Myers, J. (1963), Natl. Acad. Sci. - Natl. Research Council Publ. 1145, 301

Nelson, R. C. (1957), J. Chem. Physics 27, 864.

Overbeek, J. Th. G. (1960), J. Phys. Chem. 64, 1178.

Rabinowitch, E. (1956), "Photosynthesis" 2, Part 1, Interscience Publishers, P. 1280-1310.

Rabinowitch, E., Govindjee, and Thomas, J. B. (1960), Science 132, 422.

Rabinowitch, E. (1968), "Photosynthesis", Gauthier-Villars, Paris.

Rabinowitch, E. and Govindjee (1969), "Photosynthesis", John Wiley & Sons, Inc.

Sauer, K. and Calvin, M. (1962), Biochim. Biophys. Acta 64, 324.

Schlögl, R. (1969), Quarterly Reviews of Biophysics 2, 3, 305.

Smith, I. H. C. and French, C. S. (1963), Ann. Review Plant Physiol. 14, 181.

Tanada, T. (1951), in "Photosynthesis", cited by Rabinowitch and Govindjee, (1969), p. 146.

Thompson, T. E. and Henn, F. A. (1969), Ann. Rev. Biochem. 38, 241

Tien, H. T. and Diana, A. L. (1967), J. of Colloid and Interface Science 24, 287.

Tien, H. T. and Diana, A. L. (1968), Chem. Phys. Lipids 2, 55.

Tien, H. T. (1968a), J. Phys. Chem. 72, 4512.

Tien, H. T. (1968b), Nature 219, 272.

Tien, H. T. and Verma, S. P. (1970), Nature 227, 1232.

Tien, H. T. (1971), in "The Chemistry of Biosurfaces" Hair, M., Ed., Marcel Dekker, Inc.

Ting, H. P. et al (1968), Biochim. Biophys. Acta 163, 439.

Trissl, H. W. and Lauger, P. (1970), Z. Naturforsch 25b, 1059.

Tweet, A. G., Gaines, G. L. Jr., and Bellamy, W. D. (1964), J. Chem. Physics 40, no. 9, 2596.

Van, N. T. and Tien, H. T. (1970), J. Physical Chem. 74, 3560.

Verwey, E. T. W. and Overbeek, J. Th. G., "Theory of the Stability of Lyophobic Colloids", Elsevier Publishing Co., Inc.

Warburg, O. and Krippahl, S. and Schroeder, W. (1955), Z. Naturforsch, 10b, 631.

Wettstein, D. Von., "Biochemistry of Chloroplasts", T. W. Goodwin, Ed., p. 19.

Zscheile, F. P. and Comar, C. L. (1941), cited by Kamen, M. D. (1963), in "Primary Processes in Photosynthesis", Acad. Press, London, New York, p. 95.